Mining the Roles of Wheat (Triticum Aestivum) SnRK Gene Family in Biotic and Abiotic Responses

Jinghan Song
Yangtze University
Yiqin He
Yangtze University
Junliang Yin
Yangtze University
Wendi Huang
Yangtze University
Zehao Hou
Yangtze University
Yike Liu
Hubei Academy of Agricultural Sciences
Zhengwu Fang
Yangtze University
dongfang ma (madf@yangtzeu.edu.cn)
Yangtzeu University https://orcid.org/0000-0002-0724-0870

Research

Keywords: Triticum aestivum, SnRK, Genome-wide analysis, biotic and abiotic stress, TaSnRK2.4-B

Posted Date: November 12th, 2020

DOI: https://doi.org/10.21203/rs.3.rs-104118/v1

Abstract

Background

Sucrose non-fermenting-1-related protein kinase (SnRK) is a class of Ser/Thr protein kinases and plays vital functions in the plant stress responses. However, little is known about the SnRK in *Triticum aestivum* (TaSnRK).

Results

In this study, 149 TaSnRKs were identified from wheat and divided into three subfamilies, which may be due to the polyploidization induced gene duplication and high rate of homologous retention. A combination of public microarray datasets and quantitative real-time quantitative PCR (qRT-PCR) have further revealed the distinct expression patterns of TaSnRKs under specific abiotic/biotic stress responses. *TaSnRK2.4-B*, a member of SnRK2 subfamily, was located in the nucleus, cytoplasm, and cell membrane and showed ubiquitous expression in wheat life cycle, suggesting the possible response to polyethylene glycol (PEG), NaCl, heat, and cold stress, as well as the high concentrations of abscisic acid (ABA) application. Besides, transient Agro-infiltration assays showed that *TaSnRK2.4-B* was also involved in the resistance to pathogen.

Conclusions

These results imply that *TaSnRK2.4-B* may act as a multifunctional regulatory factor involved in multiple stress response pathways. Overall, our study provides new insights into the roles of TaSnRKs in biotic and abiotic responses.

Background

Plants have evolved a set of defending mechanisms, such as protein phosphorylation and dephosphorylation, as a response to myriad stresses including hormonal, pathogenic, and environmental stresses [1–2]. Sucrose non-fermenting-1-related protein kinase (SnRK) is a class of Ser/Thr protein kinases, modulating target proteins through phosphorylation to regulate the interrelationship of multiple signaling pathways in plants and plays a vital role in the stress responses [3–4].

SnRKs are widely found in plant kingdom and are strongly conserved among species. Three subfamilies, SnRK1, SnRK2, and SnRK3 have been divided according to the structural characteristics of proteins [5–6]. All plant SnRK subfamilies share a common S_TKc domain (Serine/Threonine protein kinases, PF00069), linked with a C-terminal kinase associated domain 1 (KA1 domain, PF02149) in SnRK1 [7]. SnRK2 contains SnRK2-specific box (glutamine-303 to proline-318) [8], while NAF domain (Asn-Ala-Phe, PF03822) is presents in the SnRK3 subfamily [9]. SnRK1, a heterotrimeric complex composed by α, β, and γ subunits, is homologous to the yeast SNF1 gene, which was first discovered and well-known by its role in the global regulation of carbon metabolism including glucose repression, and lipid accumulation [10]. SnRK2 and SnRK3, also known as CIPK (calcineurin B-like calcium sensor-interacting protein kinases), are unique existence in the plant kingdom. There are compelling pieces of evidence indicating that the divergence of SnRK2 and SnRK3

subfamilies is evolved after the duplication of SnRK1, which has enabled plants to form networks connecting metabolic and genetic responses to stresses, hormone, and calcium signal [4].

In *Arabidopsis thaliana*, the SnRK family contains 38 members, including three genes in SnRK1 subfamily, 10 SnRK2 genes, and 25 SnRK3 genes [5]. SnRK1 is related to increasing carbon and/or nitrogen assimilation and sensing nutrient and energy [11–12]. Over-expressing of *MhSnRK1* in Pingyitiancha (*Malus hupehensis* Rehd. var. *pinyiensis Jiang*) could regulate fruit development and increase the assimilation rate of both the carbon and nitrogen [11]. To date, increasing evidence have shown that SnRK2 and SnRK3 members contribute particular regulatory roles in hyperosmotic stress responses and ABA signaling. Among the ten SnRK2 genes identified in *Arabidopsis*, nine of them (except *SnRK2.9*) can be activated by hyperosmotic and salinity stresses, and five of the nine (*SnRK2.2*, *SnRK2.3*, *SnRK2.6*, *SnRK2.7*, and *SnRK2.8*) can be activated by ABA [6, 13]. *AtSnRK2.6* is particularly activated by ABA and involved in the ABA-regulated gene expression [14–15]. Several SnRK3 members are well described. The best-studied member is SOS2 (salt overly sensitive 2), which is involved in responses to salt stress and ABA signaling and is required for Na^+ and K^+ homeostasis and abiotic stress tolerance [16–17].

Bread wheat (*Triticum aestivum*) is one of the world's most important food crops, accounting for more than half of the total human food consumption [18]. The function of SnRK in wheat is also reflected in many fields. Transcription of *TaSnRK1* increased wheat FHB (Fusarium Head Blight) resistance in coordination with the deoxynivalenol (DON) induced *TaFROG* (*Triticum aestivum Fusarium Resistance Orphan Gene*) expression [19]. Overexpression of *TaSnRK2.8* enhanced cell membrane stability and enhanced tolerance to drought, salt, and cold stresses in *Arabidopsis* [20]. The SnRK3/CIPK protein kinase WPK4 positively regulates the transcription factor *TabZIP2*, which regulates the rearrangement of carbon and nutrient flows when wheat suffers drought [21]. Although several research on SnRKs in wheat had been reported [22–23], this protein family was never elucidated. In this study, the gene members belonging to the SnRK family in wheat (TaSnRK) and their potential roles under specific stress responses were characterized. A combination of both the bioinformatic and molecular research methodologies have allowed the member identification of the TaSnRK family whilst uncovering their expression patterns under specific responses under ABA, NaCl, PEG, powdery mildew, and *Fusarium graminearum* stresses. Our results has presented useful information for the understanding of TaSnRK family and provided clues for the future genetic improvement in wheat stress resistance.

Results

Identification and phylogeny analysis of TaSnRK genes

After genomic retrieval by BLASTp with 38 AtSnRK and 47 OsSnRK proteins (Table S1), 1240 putative TaSnRK proteins (734 HC members and 506 LC members) were hunted [5, 24–25]. However, after validation by NCBI CDD and SMART online tools, only 186 protein sequences (transcribed from 149 genes), including splice variants (181 HC members and 5 LC members), were confirmed. The SnRK family which contained 21 SnRK1 proteins (20 HC members and 1 LC member), 38 SnRK2 proteins (38 HC members), and 127 SnRK3 proteins (123 HC members and 4 LC members) (Fig. 1; Table S2). Because the naming method of SnRK

genes in wheat was not consistent currently, with several genes having several synonymous names, we renamed all genes according to their subfamily (SnRK1, SnRK2, and SnRK3) and sub-genome location (A, B, or D) (Table S2). Gene's name started with an abbreviation for the acronym of species name *Triticum aestivum* (Ta), followed by subfamily (SnRK1, SnRK2, and SnRK3). Genes belonging to triads share the same gene number, but use suffixes A, B, and D to distinguish subgenomes they located. Consecutive minuscules separated by a semicolon distinguished splice variants (e.g., TaSnRK1.3-B;a and TaSnRK1.3-B;b) [26]. Phylogenetic trees generated by SnRK protein sequences of *Arabidopsis*, rice, and *T. aestivum* showed that TaSnRKs belong to well-defined subfamilies (Fig. 1). A previous study found that 94 proteins from 30 genes of the TaSnRK3 subfamily were identified [23]. This article matched all these genes except TaCIPK6 because we did not retrieve its gene or CDS (Coding Domain Sequence) sequence. The remaining 29 genes belonging to the SnRK3 subfamily were firstly identified in this paper (Fig. 1; Table S2).

Chromosomal localization, gene duplication, synteny and Ka/Ks analysis

TaSnRK genes are located on 21 chromosomes, except gene TaSnRK3.44-U in an unanchored contig (Fig. 2a; Table S2). And their chromosome distributions are uneven. There are eight, seven, and eight genes on the 1A, 1B, and 1D chromosomes, respectively, and three, one, and two genes on the 7A, 7B, and 7D chromosomes, respectively. That may be related to the different sizes and structure of the chromosomes. Overall, TaSnRK genes tended to located in the more central segments of the chromosomes (R2a, R2b, and C; 73.3% of genes) were more than genes in the distal telomeric parts of the chromosomes (R1 and R3; 26.7% of genes) (Fig. 2a) [26].

Compared with the number of SnRK genes in *Arabidopsis* (47) and rice (38), the number in wheat was much higher (149) (Fig. 3a-c). This partially due to the hexaploid nature of wheat. However, even when corrected for ploidy-level, the number of SnRK genes in bread wheat was significantly higher than in *Arabidopsis* and rice (1.71- and 1.38-fold higher, respectively). Specifically, genes in SnRK1 and SnRK3 subfamilies are largely more than expectation (Fig. 3a-d). To better understand why SnRK genes are so abundant in the wheat, we analyzed homoeologous groups in detail (Table 1). At the genome-wide level, 35.8% of wheat genes were present triads [26]. By contrast, the triad proportion of TaSnRK genes is as high as 84.86%. If only "HC" SnRK genes (HC defines genes with high confidence in the wheat genome) were considered, this ratio was even higher (85.42%, Table 1). Moreover, the loss of one homolog was less pronounced in SnRK genes (2.68% vs. 13.2%, Table 1). And only 19 genes were singletons (12.75%; 11.81% for HC only) because they could not be identified as groups. Therefore, the high homologous retention rate could partly explain the high number of TaSnRK genes. That is also evidence that genome-wide doubling events (WGD) contribute to the expansion of gene families.

Table 1
Groups of homoeologous SnRK genes in wheat.

Homoeoligous group (A:B:D)	HC-only[1]	all wheat genes[2]	wheat SnRK (excluding splice variants, HC and LC)			wheat SnRK (excluding splice variants, HC-only)		
			number of groups	number of genes	% genes	number of groups	number of genes	% genes
1:1:1	41.3%	35.8%	42[5]	126	84.6%	41	123	85.4%
n:1:1/1:n:1/1:1:n[3]		5.7%	/	/	/	/	/	/
1:1:0/1:0:1/0:1:1		13.2%	2[6]	4	2.7%	2	4	2.8%
orphans/singletons		37.2%	19	19	12.8%	17	17	11.8%
other ratios[4]		8.0%	/	/	/	/	/	/
total		99.9%		149	100.0%		144	100.0%

[1,2]according to IWGSC (2018); [3] n > 1; [4] either n:1:n or 0:1:n, n > 1; [5] Compare to HC-only, one triads (TaSnRK3.30-A, TaSnRK3.30-B, TaSnRK3.41-D) was added; [6] Compare to HC-only, one triads (TaSnRK3.30-A, TaSnRK3.30-B) was changed to another triads (TaSnRK3.31-A, TaSnRK3.43-D)

Furthermore, to investigate the gene duplication events in wheat, tandem and segmental duplication were also analyzed. Through screening sequence's similarity and matching rate, 49 paralogous pairs belonging to segmental copies were found, and there was no tandem repetition (triads were not considered) (Fig. 2b; Table S3). Combined with the phylogenetic tree (Fig. 1), we found that the segment duplications occurred within each subfamily (SnRK1, 17 pairs; SnRK2, three pairs; SnRK3, 29 pairs). Additionally, synteny analysis between wheat, *Arabidopsis*, and rice were also compared to explore the evolutionary constraints acting on the SnRK gene family (Fig. 3e). The results revealed that 15 (wheat-*Arabidopsis*; SnRK1, 0 pairs; SnRK2, two pairs; SnRK3, 13 pairs) and 159 (wheat-rice; SnRK1, nine pairs; SnRK2, 35 pairs; SnRK3, 115 pairs) orthologous pairs were detected, respectively (Fig. 3e; Table S4). That reflects the conservative evolution nature of the SnRK gene family in the plant.

Meanwhile, we calculated Ka (non-synonymous substitution rate), Ks (synonymous substitution rate), and the Ka/Ks ratio of each pair (triad pairs are taken into account) to estimate evolutionary rates and determine the relative divergence times [27–29]. Except that the Ka/Ks ratios of two gene pairs (TaSnRK3.27-B/OsSnRK3.26, TaSnRK3.27-D/OsSnRK3.26) were > 1, the remaining pairs were all less than 0.87, implying that the SnRK genes were under different natural selection during plant adaptation to terrestrial environments (Fig. 3f; Table S3-4). Also, these genes' duplication events were estimated to have occurred around ~ 10.05 MYA (million years ago; Ks values average at 0.13). In addition, the Ka/Ks ratios of the orthologous gene-pairs between wheat and other two model plants were also calculated (Fig. 3g; Table S3-4). The average Ka/Ks value was maximum between wheat and *Arabidopsis* (0.54), followed by rice (0.13), suggesting the genes pairs between wheat and those two species appeared to have undergone extensive, intense purifying selection. The divergence time was about 41.50 and 10 MYA for *Arabidopsis* and rice, respectively. On the

whole, the differentiation of gene pairs is concentrated in the α WGD period, which flowering plants experienced together (Fig. 3g) [27].

Motif composition, exon-intron structure, protein feature and structure analysis

The conserved domain and gene structure analysis provide information regarding gene duplication and their functional conservation during evolution [30]. We analyzed TaSnRKs according to the following criteria: (1) one gene of the triads was retained, (2) only the first variant was kept, the 65 representative TaSnRKs were chosen (Fig. 4). First, we found six of 20 conserved motifs related to the functional domains in plant SnRK proteins (Fig. 4b; Fig. S1-2, Table S5). Motif 2 and motif 4 contained Ser/Thr active site and ATP-binding region, respectively. Motif 17, motif 15, and motif 8 contained specific conserved domain of SnRK1 (KA1), SnRK2 (glutamine-303 to proline-318), and SnRK3 (NAF), respectively. Besides, ABA-specific box hid in motif 18 (Fig. 4b; Fig. S1-2, Table S5). Overall, the same subfamily members shared similar motif compositions, supporting the clustering of the phylogenetic tree. Second, we found that all genes of the SnRK1 and SnRK2 subfamily had introns. However, there were 40% of SnRK3 genes without the intron. Furthermore, there were 28.6%, 5.3%, and 18.9% genes from SnRK1, SnRK2, and SnRK3 had UTR (untranslated region), respectively (Fig. 4c). We also noted that the exon number of TaSnRKs varied from 1 to 13. In short, the difference of gene and protein structure within three subfamilies illustrates the possibility related to the existence of gene subfunctionalization or neofunctionalization in the TaSnRK family.

To further understand the features of TaSnRKs, protein properties of 186 TaSnRK proteins were analyzed (Table S2). The length of TaSnRKs ranged from 103 (TaSnRK1.10-B) to 885 (TaSnRK3.32-B;c) amino acids (aa). The average molecular weight (MW) of SnRK1, SnRK2, and SnRK3 subgroup proteins were 53, 40, and 51 kDa, respectively. Meanwhile, the theoretical isoelectric point (pI) were ranged from 4.38 (TaSnRK2.8-D;a) to 9.51 (TaSnRK3.12-B and TaSnRK3.21-B). Compared to the other two subfamilies, the members of SnRK2 have lower MW values, and pIs are all less than 7 (Fig. 5a). All the TaSnRKs belonged to hydrophilic proteins due to their grand average of hydropathicity (GRAVY) values are negative. The secondary and tertiary structure analyses revealed the prominence of helices and loops in TaSnRK proteins (> 73%) (Fig. 5b; Table S2). In addition, SnRK1 proteins matched models 6b1u.2 and 6c9h.1, while SnRK2s matched three different models (3zuu.1, 3ujg.1, and 5wax.1). Members of the SnRK3 were matched to five models, two of which were shared with SnRK1s, and the remaining three were 5iso.1, 4czt.2, and 6c9d.1, respectively. Generally, protein properties were similar between the SnRK1s and SnRK3s, and SnRK2s were significantly different from them, which supports the functional differentiation of this gene family.

Promoter analysis

After analyzing the 1.5 kb upstream region of TaSnRK genes, we found that most of them have been broadly categorized into growth and development relate *cis*-acting elements. CAAT-box, a common element in promoter and enhancer regions that plays an essential role in transcription, is predominant among these genes (98.5%) [31]. Other *cis*-acting elements, such as A-box, AT-rich sequence, CAT-box, CCAAT-box, GCN4_motif, and O2-site, were also found in various genes and known for participating in multiple growth regulation processes (Fig. 6a; Fig. S3, Table S5) [31–33]. Furthermore, many identified elements are related to

hormone signaling pathways, namely auxin (AuxRR-core and TGA-element), abscisic acid (ABRE), gibberellin (TATC-box, GARE-motif, and P-box), salicylic acid (TCA-element and SARE), and methyl jasmonate (CGTCA-motif and TGACG-motif) [31, 34]. In addition, a few elements were predicted to be involved in abiotic stresses, such as wounding (WUN-motif), cold (LTR), and light (Box 4, GATA-motif, G-Box, I-box, Sp1, and MRE) [31–34]. We also found that the number of *cis*-acting elements distributed in the TaSnRK genes varied from 2 (TaSnRK3.42-B and TaSnRK3.44-U) to 63 (TaSnRK3.11-A) (Fig. 6b). The different numbers and types of *cis*-elements presenting indicated the diversified regulatory networks that the TaSnRK genes may involve.

Expression patterns of tissue developmental stages and stress conditions

To determine TaSnRK genes' expression patterns, we analyzed 209 RNA-seq samples under nonstress conditions of 'Azhurnaya' (a hexaploid wheat variety) (Fig. 7a; Fig. S4, Table S7-8) [26]. About 80.65% (genes) TaSnRKs were expressed at least one developmental stage with a broad expression range from 1 to 285 TPM (Transcripts Per Kilobase of exon model per Million mapped reads). The remaining 18.81% (35 genes) showed a deficient expression with a TPM < 1 and were considered not expressed (SnRK1s, six genes; SnRK2s, three genes; SnRK2s, 26 genes). TaSnRK genes were expressed in multiple tissues, including leaves, roots, sheaths, spikelets, anthers, and grains (Fig. 7a; Table S8), which was consistent with previous reports in *Arabidopsis* [4–5, 35], tomato [11], potato [36], pea [37], and maize [38–39]. To verify the expression patterns in wheat, we made hierarchical clustering according to expression similarity, and then group the data into 15 different expression modules (Fig. 7b; Fig. S4). The result showed that only four expression patterns in SnRK1, while the SnRK3 contained the most types of expression patterns (up to 12). Moreover, the expression modules I and V were the most widely distributed, with multiple gene anastomoses in all three subfamilies (Fig. 7b-c). In general, the genes of TaSnRK1s and TaSnRK2s were both ubiquitously expressed during the plant life cycle (Fig. 7c). In addition to being generally expressed (39/127, 30.7%), the TaSnRK3 genes were also explicitly highly expressed in reproductive organ spikelets (modules XIII (66/127, 60.0%) and XIV (2/127, 1.6%)). Interestingly, not or low-expressed genes (module VIII) were also concentrated in the SnRK3 subfamily (20/127, 15.7%). That may be related to a large number of genes and functional redundancy in this subfamily. The multi-tissue and multi-stage expression suggest the TaSnRK gene family's critical role in wheat growth and development.

To verify the response pattern of TaSnRKs to abiotic and biotic stresses in wheat, nine genes belonging to different subfamilies with universally expression patterns were randomly selected. Their expression patterns under various stresses were further illustrated by heatmap and analyzed by qRT-PCR.

At low temperature, *TaSnRK2.4-B*' expression was decreased (Fig. 8a), which was similar to the expression pattern of *ZmSnRK2.10* in maize [40]. In the SnRK3 subfamily, two genes were responsive to cold stress. One is *TaSnRK3.35-A*, whose expression was notably increased, may form a complex with CBL1 to regulate cold stress like homologous gene *AtSnRK3.10* [41]. Another is *TaSnRK3.16-D*, which was drastically down-regulated than control, implying that TaSnRK3 genes participate in cold response in various ways. Also, *TaSnRK1.1-A*, *TaSnRK2.4-B*, and *TaSnRK2.7-A* responded to phosphorus deficiency only in the root. Under drought treatment (Fig. 8a), the expression of *TaSnRK2.4-B*, *TaSnRK2.7-A*, and *TaSnRK3.35-A* were increased

significantly. In heat stress, except for *TaSnRK3.37-D*, the remaining eight genes all reached a peak at six hours. When subjected dual stress of drought and heat, *TaSnRK2.7-A* and *TaSnRK3.37-D* showed a gradual increase, and the remaining seven genes were down-regulated first and then up-regulated. In the qRT-PCR result (Fig. 8b), these nine genes also respond to drought stress. Under osmotic stress, the expression levels of *TaSnRK1.2-A*, *TaSnRK2.4-B*, *TaSnRK2.10-A*, *TaSnRK3.16-D*, *TaSnRK3.35-A*, and *TaSnRK3.37-D* changed significantly. For ABA treatment, each gene notably responded to the ABA signal but reached its maximum expression value at different times.

For biotic treatment, the response patterns of the nine genes were also varied (Fig. 8a). In the infection of *Zymoseptoria triticipowdery* in leaf, all TaSnRK genes showed down-regulated expression after 14 days post inoculation (dpi), showing the rife response pattern. Moreover, three different modes of expression were observed when threatened by stripe rust. First, the expression of *TaSnRK1.2-A*, *TaSnRK3.35-A*, and *TaSnRK3.37-D* was increased over time. Second, *TaSnRK1.1-A*, *TaSnRK2.4-B*, *TaSnRK2.7-A*, *TaSnRK2.10-A*, and *TaSnRK3.16-A* were decreased first and then increased gradually. Finally, the expression of *TaSnRK1.9-A* was lower and lower. When inoculated with powdery mildew, *TaSnRK1.2-A*, *TaSnRK2.7-A*, *TaSnRK2.10-A*, and *TaSnRK3.16-A* had significant positive responses to stress. In contrast, the expression of *TaSnRK2.4-B* decreased with the infestation time. Interestingly, in our qRT-PCR results (Fig. 8c), the genes that maintain continuous response to powdery fungus are *TaSnRK1.1-A*, *TaSnRK3.16-A*, and *TaSnRK3.37-A*. Similarly, through the RNA-seq data, we only found two genes that significantly responded to *Fusarium graminearum*, namely *TaSnRK1.2-A* and *TaSnRK2.7-A*. However, in our study, all nine genes were responded to *Fusarium graminearum* infection. The inconsistencies in response patterns may be related to the difference between cultivars and stress treatment time. In conclusion, wheat SnRK genes are involved in varieties of abiotic and biotic stress regulation.

Gene Ontology (GO), Kyoto Encyclopedia of Gene and Genome (KEGG) and Protein-protein interaction(PPI)network Analysis

To understand the functions of the biological processes, all TaSnRKs were searched for GO and KEGG databases. In total, 86.5% (129/149) TaSnRKs were assigned to one or more GO terms in the biological process (129 genes), molecular function (129 genes), and cellular component (102 genes) categories (Fig. 9a-b; Fig. S5, Table S10). We also mapped the TaSnRKs in the KEGG pathway database (Fig. 9b). The result revealed that most genes were enriched in signal transduction of environmental information processing pathways, supporting the previous studies [1–2, 4–5]. By grouping comparison, we found that the members from the TaSnRK1 and the TaSnRK3 subfamilies may perform similar functions on plant physiological regulation (Fig. S6). The reason is they shared eight identical pathways, except the pathways of “Folding, sorting and degradation” and “Membrane transport”, which were only annotated with the SnRK3 subfamily. By contrast, the TaSnRK2 members were only enriched on the “signal transduction pathway” of environmental information processing. That signals functional differentiation among the TaSnRK subfamilies and supports the SnRK genes regulation network drawn by Cramer et al. [42].

Furthermore, we used the model plant *Arabidopsis* protein database as a reference to constructed the interaction network of the three TaSnRK subfamilies, respectively. At first, 26 protein pairs were predicted with confidence to interact (score > 0.47) between 21 TaSnRK1s and 12 other proteins in the SnRK1 subfamily (Fig. 9c; Table S11). Among these protein pairs, AT4G16360, AKINBETA1, SEX4, and SNF4 code subunit β, and SNF4 code subunit γ, together with subunits α to form TaSnRK1 heterotrimers (Table S11) [7, 10]. And, TaSnRK1s maybe regulate sugar signals and control plant energy transfer through interacting with B3-domain transcription factor FUSCA3 (FUS3), which have been verified by experiments in *Arabidopsis* [35, 43]. Simultaneously, TaSnRK1s also bind to a myristoylated 2C-type protein phosphatase ABI1, which contributes to balance carbon and nitrogen and ABA-free signaling pathways [44]. Another PP2C protein that binds TaSnRK1s is PP2C74, which involved the early development in the plant as one of the substrates of AtNMT1 in *Arabidopsis* [45]. Secondly, 52 protein pairs associated with TaSnRK2s were identified. Of these, four pairs occurred within the TaSnRK2 subfamily, and 48 pairs were associated with 38 TaSnRK2s and other five functional proteins (Fig. 9c; Table S11). TaSnRK2s and their interaction proteins are all concentrated in the PYR/PRL-PP2C-SNRK-ABF signaling pathway [8, 13–15, 22, 24–25, 35, 43–44]. When ABA content is low, the activities of SnRK2s were inhibited by clade A PP2C phosphatases (ABI1, ABI2, and HAB1) [46–48]. After the concentration increases, ABA is bound to receptor PYR/PRL and PP2C phosphatases to form regulating complexes and release the inhibition of SnRK2s and downstream stress signaling [46–48]. Meanwhile, uninhibited SnRK2s [49–51] activate downstream bZIP-like transcription factor (ABF), induces ABA response gene expression, and regulates plant growth and development [52]. Ultimately, the signal transduction process is inhibited by SnRK-Calcium-binging Sensor (OZS1) and scaffold protein ABA Terminator (Fig. 9c, 10a) [53–54]. Finally, the SnRK3 subfamily has been shown to participate in complex networks of interactions. We identified 135 protein pairs involving 24 SnRK3 proteins and ten other proteins. Among them, 18.52% (25/135) of interactions occurred within the subfamily, while the remaining protein pairs (81.48%, 110/135) were concentrated in the calcium-dependent CBL-SnRK3 signaling pathway (Fig. 9c; Table S11) [1, 3, 9, 16–17, 23, 25, 41–42, 55–58]. We speculate that the complex of TaSnRK3s and CBL can regulate *Arabidopsis* K^+ transporter (AKT1), which balances the absorption and release of K^+ in root cells under low K^+ concentration [55]. Meanwhile, TaSnRK3s may participate in the SOS (SOS1, SOS2, SOS3, SIP3, and SIP4) pathway to regulate the transport of Na^+/H^+ reverse transporters (NHX1) and NO_3^- (NRT1.1) to enhance tolerance to abiotic stress [16–17, 23, 56–60].

Path analysis, subcellular localization and transient Agro-Infiltration assays of *TaSnRK2.4-B*

In previous studies, *TaSnRK2.7* (renamed as *TaSnRK2.4-D* in this study) responded to polyethylene glycol and NaCl stress, but not to ABA application [59]. However, *TaSnRK2.4-B*, the triplet of *TaSnRK2.4-D*, showed significant change under ABA stress (100 uM) (at 2 h, 12 h, and 24 h), which was at odds with previous research (Fig. 9b) [59]. To investigate whether *TaSnRK2.4-B* indeed responds to ABA signaling, we quantified the expression levels of several key genes involved in the ABA pathways concerning to SnRK2 subfamily (Fig. 10a; Fig. S7) [8, 22, 24, 44, 60]. On the one hand, *TaPYR1* (homologous to *AtPYR1*) was weakly expressed after ABA treatment, and *TaPYR4* (homologous to *AtPYR4)* and *TaPP2C* (homologous to *AtPP2CA* and *AtABI2*) was continuously decreased with stress time. Moreover, *TaSnRK2.4-B* and *TaABF* (homologous

to *AtABF*) both increased and reached a peak at 12 h and then decreased continuously. On the other hand, in the SCS-SnRK2 signaling pathway [60], *TaSCS* (homologous to *AtSCS-A* and *AtSCS-B*) was highly expressed at all time points, especially at 12 h, whose expression level was 731 times compared to control. Furthermore, its expression trend is utterly consistent with *TaSnRK2.4-B*. That suggests that ABA signaling may cause an outbreak of ROS (Reactive Oxygen Species), which induce SCS overexpression in a calcium- or non-calcium-dependent manner [60]. After that, *TaSCS* may inhibit the expression of *TaSnRK2.4-B* by directly interacting with it, as similarly reported in *Arabidopsis* [60].

To validate the subcellular localization of *TaSnRK2.4-B*, we successfully constructed the part27-35S:*TaSnRK2.4-B*-GFP fusion expression vector into *Agrobacterium* GV3101 and transferred it to tobacco leaves. The results showed that *TaSnRK2.4-B* was located in the cell membrane, cytoplasm, and nucleus (Fig. 10b), which was consistent with the localization results of its homologous gene TaSnRKs [22, 60].

In this study, we have demonstrated that *TaSnRK2.4-B* responds to many biotic stresses, and we wanted to examine whether this response exists in *Phytophthora infestans* (*P. infestans*) challenge. Therefore, the mature protein-coding regions of *TaSnRK2.4-B* were cloned and transiently expressed in *N. benthamiana* using *Agrobacterium*-mediated expression followed by a *P. infestans* infection. After six days post inoculation (dpi), significantly smaller lesions were observed in areas expressing *TaSnRK2.4-B* compared to that of free GFP (Fig. 10c-d; $P < 0.05$), suggesting that the expression of *TaSnRK2.4-B* inhibited P. infestans invasion to the host. This inhibition is likely to enhance plants' ability to resist stress by responding to signal transduction pathways of hormones such as salicylic acid or gibberellin [61–62]. However, the specific mechanism of action still needs further experimental investigation.

Discussion

SnRK family was highly conserved in eukaryotes, working as a sensor in the cellular energy metabolism [10–12, 35, 43, 62–63]. *PKABA1*, the primary member of the wheat SnRK family, was discovered and cloned from ABA-induced wheat embryo cDNA [19]. After that, five PKABA1-like protein kinase genes (*TaPK3*, *W55a*, *W55b*, *W55c*, and *TaSRK2C1*), activated by multiple stresses related to ABA signals, were excavated from wheat [21, 64–66]. However, compared with *Arabidopsis* and rice, the research on SnRKs in wheat is limited. So far, there has been no genome-wide analysis of the SnRK family in wheat. We have thereby developed a comprehensively evolutionary analysis and functional classification of the three SnRK subfamilies in wheat.

Based on the BLAST and HMM algorithm, 149 non-redundant SnRK genes were identified at the whole genome level of wheat (Fig. 1; Table S2). The number of TaSnRKs was 3.92 and 3.17 times higher than in *Arabidopsis* and rice, which could generally be explained by its hexaploidy and fragment replication (Fig. 3a-d). The Ka/Ks ratio test explains that the wheat SnRK family has experienced positive selection, but displayed different evolutionary branch selection pressures (Fig. 3f; Table S2). Meanwhile, we calculated that 77.9% (116/149) SnRK members had collinear relationships with rice, and these pairs were all distributed in the three subfamilies (Fig. 3e; Table S4). More interestingly, the same TaSnRK gene co-linear with multiple rice genes and vice versa. However, only 10.1% (15/149) of the SnRK members had collinearity pairs with *Arabidopsis* (Fig. 3e; Table S4). In general, the rice SnRK genes showed a more intimate genetic relationship with wheat than *Arabidopsis*, consistent with the evolution tendency. Three branches of the SnRKs existent in

Arabidopsis and rice (Fig. 3f), reflecting that the evolution of SnRK2 and SnRK3 from SnRK1 has already been completed before the arose of monocot and eudicot plants.

The protein property and structure of the wheat SnRK family were analyzed concerning the interrelationship with the protein function. It was found in our study that the N-terminus of the SnRK protein was more conservative in each subfamily in the full-length sequence alignment (Fig. 4; Fig. S2). By contrast, TaSnRKs shared a lower similarity in C-terminal sequences among the three subfamilies. The C-terminal of SnRK sequences generally includes KA1, SnRK2-specific box, and NAF domain [7–9], which is common in *Arabidopsis* [6, 10, 24], *Oryza sativa* [24], *Zea mays* [40], and *Brachypodium distachyon* [25]. However in wheat, motif 17 with the KA1 domain is distributed only in the SnRK1 subfamily, and motif 8 containing the NAF domain is distributed in the SnRK3 subfamily (Fig. 4; Fig. S2, Table S5). Motif 15 containing the SnRK2-specific box is conserved in the TaSnRK2 family and distributed in each member sequence. This result indicated that the wheat SnRK protein sequences were conserved in each subfamily. The tertiary structure prediction result further revealed the same subfamily members share similar protein models, suggesting that members of the same subfamily may also share similar functions (Fig. 5b). Nevertheless, the differences between the TaSnRK subfamilies cannot be ignored, which may relate to one or more domains at the C-terminal end.

At present, most of the SnRK proteins reported are found to be located in the cell membrane, cytoplasm, and nucleus as the regulation of SnRK kinase activity at different levels of transcription, post-transcription, protein translation, and post-translational modification [3, 10, 19, 46, 48, 52, 55, 58, 64]. For example, wheat SnRK2 member *PKABA1* was not regulated by ABA in the protein level but was regulated by ABA in the mRNA leve1 [19]. This multilevel regulatory ability has determined that the SnRK family plays a vital role in the plant regulatory network as an essential protein kinase [4, 6–7, 43]. For a better understanding of the plant SnRK families, we drew a schematic diagram of the regulatory network of plant SnRK family (Fig. 10e) [1, 4, 6–7, 10–11, 24–25, 42, 46–47, 54, 60]. Not only the SnRKs has multiple roles in sugar signal transduction [10, 12, 43], ABA signal regulation [14–15, 37, 39, 43–44, 46], osmotic stress response [1, 6, 13, 16, 52], but also the stomatal closure [6, 13], abiotic stress [6, 67], growth and development regulation [11, 35–36] are involved.

In this research, we have identified multiple *cis*-acting elements that responded to wheat growth and development regulation, as well as the hormone and stress response in the promoter regions of the three TaSnRK subfamily members (Fig. 6). Simultaneously, TaSnRKs were annotated to the three types of GO items and enriched to multiple KEGG pathways (Fig. 9a-b). The nine genes focused on were ubiquitously expressed during the wheat life cycle, except for *TaSnRK3.16-D*, whose expression level was low in general, but relatively higher in the reproductive organs. Overall, the TaSnRKs may play a role in various aspects of vegetative growth and reproductive development, and is not just limited to regulating root development as previously reported [22, 59].

For biotic stress, all nine genes responded to the infection of *Zymoseptoria triticipowdery* and stripe rust, according to public microarray datasets. In the powdery mildew and *Fusarium graminearum treatment*, there were discrepancies showed between the public data and our qRT-PCR results, which may be possibly due to the difference in experimental materials. But generally, some members of the three TaSnRK subfamilies

responded to the invasion of powdery mildew and *Fusarium graminearum*, which was consistent with the former reports to a certain extent [21, 62]. Still, further studies are needed for the verification.

Under the abiotic stress, *TaSnRK2.4-B*, *TaSnRK3.16-D*, and *TaSnRK3.35-A* both demonstrated the responses to cold stress. Except for *TaSnRK3.37-D*, the remaining eight genes were induced to express after high temperature treatment for 1 hour (Fig. 8a). Besides, these nine genes all responded to PEG, NaCl, ABA (100 uM), and phosphorus deficiency variously. In previous studies, the SnRK2 family was divided into three groups mainly based on the gene responding pattern to ABA signals (Fig. S8) [22, 24, 48, 59, 67]. SnRK2s in Group I cannot activated by ABA treatment and Group II SnRK2s responded weakly to ABA, whereas SnRK2s in Group III were strongly induced by the ABA signal. In 2011, Zhang et al. [59] identified a Group I gene, *TaSnRK2.7* (renamed as *TaSnRK2.4-D*), that did not respond to ABA (5 uM). However, in our study, it was found the *TaSnRK2.4-B*, a triad gene of *TaSnRK2.7*, responded to ABA (100 uM) signal significantly (Fig. 8b). By adjusting the ABA application concentration in the experiment, we concluded that the Group I genes could be more sensitive to high concentration of ABA. Also, from the signaling pathway, TaSCS were significantly induced after the ABA application. We speculated that it might interact with and inhibit the expression of *TaSnRK2.4-B* through Ca^{2+} dependent or independent means (Fig. 10e) [60]. Furthermore, *TaSnRK2.4-B* was found to be located in both the cell nucleus, cytoplasm, and membrane, and its overexpression in tobacco has enhanced tolerance to P. infestans invasion (Fig. 10c-d). Consequently, it could be reasoned that *TaSnRK2.4-B* has the very potential to improve the crop tolerance to stresses, underlying a practical breeding utility in the wheat production.

Conclusions

Totally, we completed genome-wide identification and classification of the wheat SnRK family. Replication events analysis showed that both WGD and fragment duplication contributed to the expansion of the TaSnRK family. Ka/Ks value suggested that most TaSnRKs were undergoing positive selection and the pressure intensity varied among the subfamilies. The GO annotation, KEGG, PPI network, transcriptomic profiling, and qRT-PCR analyses indicated the TaSnRK family played the role of multifunctional regulators responding to diversified biotic and abiotic stresses. Subcellular localization showed the presence of *TaSnRK2.4-B* in the cell membrane, cytoplasm, and nucleus. Expression patterns revealed that *TaSnRK2.4-B* responds to PEG, NaCl, and high concentration ABA. Moreover, transient agro-infiltration assays showed that TaSnRK2.4-B was involved in the resistance to the pathogen. As a potential gene in crop tolerance, its function needs further study. Overall, our study brings new insight for transcriptional regulatory mechanisms of TaSnRKs and transgenic breeding in crop plants.

Methods

Identification and classification of TaSnRK protein sequences

The computer-based method was used to identify SnRK gene family members from the wheat reference genome IWGSC RefSeq v1.1 assembly (https://wheat-urgi.versailles.inra.fr/Seq-Repository/Assemblies) [30]. The known 38 AtSnRK proteins and 47 OsSnRK proteins sequences were collected and used as query sequences for BLASTp searching against the IWGSCv1.1 [5,24-25]. The first uncurated candidate hits were

further screened using SMART (http://smart.embl-heidelberg.de/) and NCBI CDD (https://www.ncbi.nlm.nih.gov/Structure/cdd/wrpsb.cgi) to predict domains which belong to SnRK gene family. All SnRK protein sequences contained the S_TKc domain (Serine/Threonine protein kinases, catalytic domain). Besides, SnRK1 subfamily contained KA1 (C-terminal kinase associated domain 1) [7], SnRK2 subfamily contained SnRK2-specific box (glutamine-303 to proline-318) [8], and SnRK3 subfamily contained NAF (Asn-Ala-Phe) [9]. According to these specific domains, TaSnRKs were identified and classified.

Phylogenetic analyses of the SnRK gene family

To further explore the evolutionary relationship of plant SnRKs, multiple sequence alignments and phylogenetic analysis of the SnRK proteins were performed with Clustalw [68]. And neighbor-Joining (NJ) was used to perform phylogenetic analyses of the SnRK proteins with 1000 replicated-bootstraps in MEGA 7.0 [69-70]. The midpoint rooted base tree was drawn and cleaned up via Interactive Tree of Life (ITOL, version 3.2.317, http://itol.embl.de).

Chromosomal location, gene duplication, and Ka/Ks analysis of TaSnRKs

The start and end location information of TaSnRKs extracting from the reference IWGSCv1.1 GFF3 file was used to draw the physical map via MapInspect software [31-32]. Tandem duplication events were identified using the following evaluation criteria: (1) length of the aligned sequence > 80% of the length of each sequence; (2) identity > 80%; (3) threshold $\leq 10^{-10}$; (4) only one duplication event could be admitted when genes were linked closely; (5) the intergenic distance was less than 25 kb. If genes satisfied criteria (1), (2), and (3) and located on different chromosomes, they were judged as segmental duplications [30-31]. The evolutionary rates (Ka, Ks, and Ka/Ksratio) were estimated by TBtools (https://github.com/CJ-Chen/TBtools) [71]. On the basis of the synonymous substitutions per year (λ) of 2.6×10^{-9} for wheat, the divergent time of the duplicated SnRK genes was estimated ($T = Ks/2\lambda \times 10^{-6}$ MYA) [72].

Protein sequences analysis

The characteristic features of TaSnRK proteins were predicted using ExPASy Server10 (SIB Bioinformatics Resource Portal, https://prosite.expasy.org/PS50011). Signal peptide lengths were predicted with SignalP 4.1 (http://www.cbs.dtu.dk/services/SignalP/), and Plant-mPLoc executed the prediction of subcellular localization (http://www.csbio.sjtu.edu.cn/bioinf/plant-multi/). The SOPMA (https://npsa-prabi.ibcp.fr/cgi-bin/npsa_automat.pl?page=npsa_sopma.html) was used to predicted the secondary and three-dimensionally structure by the intensive mode. Structure validation was performed using Ramachandran plots (http://www.mordred.bioc.cam.ac.uk/rapper/rampage.php/). The MEME v4.9.1 (http://meme-suite.org/index.html) and SMART motif search tool (http://smart.embl-heidelberg.de/) were used to identify conserved motifs of TaSnRK proteins. These motif patterns were drawn by TBtools software [71]. The GSDS2.0 (http://gsds.cbi.pku.edu.cn/index.php) was used to draw gene exon-intron structures.

Cis-elements analysis and expression Pattern Analyse

We are using PlantCARE (http://bioinformatics.psb.ugent.be/webtools/plantcare/html/) identify cis-acting elements in the upstream sequences (1-1.5 kb) of the 186 TaSnRKs. Then, the predicted results were

organized and displayed by the R package “pheatmap” [30]. RNA-seq data of wheat SnRK genes were downloaded from Wheat Expression Browser (http://www.wheat-expression.com/ and http://bar.utoronto.ca/efp_wheat/). The MORPHEUS (https://software.broadinstitute.org/morpheus/) was used to generate heatmaps of TaSnRKs fold change based on the log2 (TPM+1) values. Genes were clustered according to their expression using K-means (K-means = 15) [73].

GO annotation, KEGG annotation, and PPI network prediction

GO annotations of TaSnRK proteins was performed by Blast2GO [74]. KEGG pathways analysis of TaSnRKs was performed using the KEGG web server (http://www.kegg.jp/). The PPI network was constructed using the STRING database (https://string-db.org/), and the genes with confidence score ≥ 0.4 were reserved.

Plant materials, treatments, and qRT-PCR analysis

Seeds of Yangmai 20, a hexaploid common wheat cultivar, were surface-sterilized with 1% hydrogen peroxide, rinsed thoroughly with distilled water, and germinated in an incubator at 20 ℃ for two days then placed in 1/2 strength Hoagland nutrient solution [75]. When wheat grew to one heart and one leaf, the plants were treated with 150 mM sodium chloride (NaCl), 20% polyethylene glycol 6000 (PEG 6000), and 100 uM ABA. The plants grow at 26 ℃ and 16 h/8 h (day/night) environment during application. Roots were sampled at two, 12, 24, 48, and 72 h after treatments.

The Yangmai 20 plants were cultivated in soil in a growth chamber at 20 ℃ under a 16 h light/8 h dark photoperiod. When wheat seedlings’coleoptiles reached 0.5 cm, they were point inoculated with either water (control) or *Fusarium graminearum* (strain PH-1). Plant growth, inoculation and infection conditions were described in detail previously [76]. The *Blumeria graminis f. sp. Tritici* (Bgt strain E09) was maintained on susceptible wheat ‘MingXian 169’ [77]. The 7-day-old seedlings were inoculated with Bgt conidia from ‘MingXian 169’ seedlings infected 10 days previously. The inoculated leaves of Yangmai 20 were harvested at one, three and five dpi, frozen immediately in liquid nitrogen and stored at −80 °C. The test was carried out with three biological replications.

Total RNA was isolated from 100 mg tissues by using TRizol reagent (Invitrogen, U.S.A) and digested with DNaseI (TaKaRa, U.S.A) to eliminate DNA. RNA was reverse-transcribed to cDNA by using RevertAid Reverse Transcriptase (Vazyme, China). Quantitative expression was performed with a qRT-PCR system (BIO-RAD, U.S.A.). Gene-specific primers were designed using Primer 5.0. Primers that met the two conditions, (1) containing single and correct size segments in ordinary PCR products, (2) showing single melt peak of qRT-PCR, were chosen to be used in the further experiment. The qRT-PCR reaction system and protocol were carried out as manufacturer's instructions of 2× SYBR Green qPCR Master Mix (Us everbright, China). Three technical replicates were used for each cDNA. The relative gene expression level was calculated with the $2^{-\triangle\triangle Ct}$ method.

Subcellular localization and transient Agro-Infiltration analysis of *TaSnRK2.4-B*

The full-length open reading frame (ORF) of *TaSnRK2.4-B* were fused upstream of GFP in the PART27 expression vector driven by the CaMV35S promoter. The recombinant vector were transformed into

Agrobacterium tumefaciens strain GV3101 and then infected *Nicotiana benthamiana* leaves. After 48 hours, the injected leaves were placed on the glass slides and imaged by laser scanning confocal microscopy (OLYMPUS FV3000, Tokyo, Japan). The exciting light wavelength was 488 nm.

Agro-infiltration experiments were implemented on leaves of 6- to 8-week-old *N. benthamiana.* After 24 h, infiltrated *N. benthamiana* leaves were excised and transferred into sealed moist plastic trays and inoculated with 10 µl *P. infestans* strains (88069) zoospore suspension (100 zoospores/µl) at the infiltration range [78]. Photographing under ultraviolet light and recording lesion diameters of the inoculated leaves at six dpi. Assay consisted of three biological replications, and each biological replication contained ten technical duplications.

Abbreviations

SnRK: Sucrose non-fermenting-1-related protein kinase; Ta: *Triticum aestivum*; qRT-PCR: quantitative real-time quantitative PCR; PEG: polyethylene glycol; ABA: abscisic acid; S_TKc domain: Serine/Threonine protein kinases; KA1 domain: C-terminal kinase associated domain 1; CIPK: calcineurin B-like calcium sensor-interacting protein kinases; FHB: Fusarium Head Blight; DON: deoxynivalenol; *TaFROG*: *Triticum aestivum Fusarium Resistance Orphan Gene*; CDS: Coding Domain Sequence; WGD: genome-wide doubling events; Ka: non-synonymous substitution rate; Ks: synonymous substitution rate; aa: amino acids; MW: molecular weight; pI: theoretical isoelectric point; GRAVY: grand average of hydropathicity; TPM: Transcripts Per Kilobase of exon model per Million mapped reads; dpi: days post inoculation; GO: Gene Ontology; KEGG: Kyoto Encyclopedia of Genes and Genomes; PPI: Protein-protein interaction; ROS: Reactive Oxygen Species; *P. infestans*: *Phytophthora infestans*; ORF: full-length open reading frame.

Declarations

Acknowledgements

We thank the Instrument sharing platform of Yangtzeu University and lab members for their assistance in this study.

Authors' contributions

Conceptualization, Z.W. Fang and D.F. Ma; methodology, J.H. Song and Y.Q. He; validation, D.F. Ma and J.L. Yin; formal analysis and investigation, W.D. Huang and Z.H. Hou; resources, Z.W. Fang and D.F. Ma; data curation, J.H. Song; writing original draft preparation, Y.Q. He and J.H. Song; writing—review and editing, J.L. Yin and Y.K. Liu; visualization, J.H. Song; supervision, Z.W. Fang; funding acquisition, Z.W. Fang and D.F. Ma.

Funding

This research was funded by "National Key R&D Program of China (2017YFD0100800)", "The Major Program of Technological Innovation of Hubei Province (2018ABA085)", and "Open Program of Hubei Key Laboratory

of Food Crop Germplasm and Genetic Improvement ”(2018lzjj09).

Availability of data and materials

All data generated or analyzed during this study are included in this published article and its supplementary information files.

Ethics approval and consent to participate

Not applicable.

Consent for publication

Not applicable.

Competing interests

The authors declare that they have no competing interests.

Author details

[1] College of Agriculture, Yangtze University, Jingzhou 434025, Hubei, China. [2] Institute of Food Crops, Hubei Academy of Agricultural Sciences, Wuhan 430064, Hubei, China.

References

1. Yu Q, An L, Li W. The CBL-CIPK network mediates different signaling pathways in plants. Plant Cell Rep. 2014;33:203-214.
2. Cohen P. Review lecture: protein phosphorylation and hormone action. Proc R Soc Lond. 1988;2349(1275):115-44.
3. Yan J, Niu F, Liu W, Zhang H, Wang B, Yang B, Jiang Y. *Arabidopsis* CIPK14 positively regulates glucose response. Biochem Bioph Res Co. 2014;450(4):1679-1683.
4. Halford G, Hey S.J. Snf1-related protein kinases (SnRKs) act within an intricate network that links metabolic and stress signalling in plants. Biochem J. 2009;419(5):247-59.
5. Hrabak EM, Catherine W, Chan M, Gribskov M, Harper JF, Choi JH, Halford N, Kudla J, Luan S, Nimmo HG, Sussman MR. The *Arabidopsis* CDPK-SnRK superfamily of protein kinases. Plant Physiol. 2003;132(2):666-680.
6. Coello P, Hey SJ, Halford NG. The sucrose non-fermenting-1-related (SnRK) family of protein kinases: potential for manipulation to improve stress tolerance and increase yield. J Exp Bot. 2011;62(3):883-893.

7. Amodeo GA, Rudolph MJ, Tong L. Crystal structure of the heterotrimer core of saccharomyces cerevisiae ampk homologue snf1. N 2007;449(7161):492-495.
8. Christophe B, Pierre-Olivier DF, Clara B, Stephane C, Jean-Marie S, Alain V, Jerome G, Helene BB, Se ´bastien Thomine. Identification of features regulating OST1 kinase activity and OST1 function in guard cells. Plant P 2006;141(8):1316–1327.
9. Albrecht V, Ritz O, Linder S, Harter K, Kudla J. The NAF domain defines a novel protein-protein interaction module conserved in Ca^{2+}-regulated kinases. EMBO J. 2001;20(5):1051-63.
10. Dong X, Cui N, Wang L, Zhao X, Qu B, Li T, Zhang G. The SnRK protein kinase family and the function of SnRK1 protein kinase. Int. J. Agric. Biol. 2012;14(4):575-579.
11. Wang X, Peng F, Li M, Yang L, Li G. Expression of a heterologous SnRK1 in tomato increases carbon assimilation:nitrogen uptake and modifes fruit development. Plant Physiol. 2012;169:1173-1182.
12. Robaglia C, Tomas M, Meyer C. Sensing nutrient and energy status by SnRK1 and TOR kinases. Curr Opin Plant Biol. 2012;15(3):301-307.
13. Boudsocq M, Droillard MJ, Barbier-Brygoo H, Lauriere C. Different phosphorylation mechanisms are involved in the activation of sucrose non-fermenting 1 related protein kinases 2 by osmotic stresses and abscisic acid. Plant Molecular Biology. 2007;63(4):491-503.
14. Mustilli AC, Merlot S, Vavasseur A, Fenzi F, Giraudat J. *Arabidopsis* OST1 protein kinase mediates the regulation of stomatal aperture by abscisic acid and acts upstream of reactive oxygen species production. The Plant Cell. 2002;14:3089-3099.
15. Yoshida R, Hobo T, Ichimura K, Mizoguchi T, Takahashi F, Aronso J, Ecker JR, Shinozaki ABA-activated SnRK2 protein kinase is required for dehydration stress signaling in *Arabidopsis*. Plant and Cell Physiology. 2002;43(12):1473-1483.
16. Liu J, Ishitani M, Halfter U, Kim CS, Zhu J. The *Arabidopsis thaliana* SOS2 gene encodes a protein kinase that is required for salt tolerance. Proceedings of the National Academy of Sciences of the USA. 2000;97(7):3730-3734.
17. Guo Y, Halfter U, Ishitani M, Zhu J. Molecular characterization of functional domains in the protein kinase SOS2 that is required for plant salt tolerance. Plant Cell. 2001;13:1383-1400.
18. Yin JL, Fang ZW, Sun C, Zhang P, Zhang X, Lu C, Wang SP, Ma DF, Zhu Y Rapid identification of a stripe rust resistant gene in a space-induced wheat mutant using specific locus amplified fragment (SLAF) sequencing. Scientific Reports. 2018;8(1):3086.
19. Anderberg RJ, Walker-Simmons MK. Isolation of a wheat cDNA clone for an abscisic acid-inducible transcript with homology to protein kinases. Proc. Natl. Acad. Sci. U.S.A. 1992;89(21):10183-10187.
20. Luang S, Sornaraj P, Bazanova N, Jia W, Eili O, Hussain SS, Kovalchuk N, Agarwal PK, Hrmova M, Lopato:S. The wheat TabZIP2 transcription factor is activated by the nutrient starvation-responsive SnRK3/CIPK protein kinase. Plant Molecular Biology. 2018;96(21):543-561.
21. Han XY, Zhang L, Zhao LF, Xue PY, Qi T, Zhang CL, Yuan HB, Zhou LX, Wang DW, Qiu JL, Shen QH. SnRK1 Phosphorylates and Destabilizes WRKY3 to Enhance Barley Immunity to Powdery Mildew. Plant Communications. 2020;1(4):100083.

22. Zhang HY, Li WY, Mao XG, Jing RL, Jia HF. Differential activation of the wheat snrk2 family by abiotic stresses. Frontiers in Plant Science. 2016;7(106):420.
23. Sun T, Wang Y, Wang M, Li TT, Zhou Y, Wang XT, Wei SY, He GY, Yang GX. Identification and comprehensive analyses of the CBL and CIPK:gene families in wheat (*Triticum aestivum*). BMC Plant Biology. 2015;15(1):269.
24. Saha J, Chatterjee C, Sengupta A, Gupta K, Gupta B. Genome-wide analysis and evolutionary study of sucrose non-fermenting 1-related protein kinase 2 (SnRK2) gene family members in *Arabidopsis* and *Oryza*. Computational Biology and Chemistry. 2014;49(9):59-70.
25. Wang LZ, Hu W, Sun JT, Liang XY, Yang XY, Wei SY, Wang XT, Zhou Y, Xiao Q, Yang GX, He Genome-wide analysis of SnRK gene family in Brachypodium distachyon and functional characterization of BdSnRK2.9. Plant Science. 2015;237:33-45.
26. Ramírez-González RH, Borrill P, Lang D, Harrington SA, Brinton J, et al. The transcriptional landscape of polyploid wheat. Science. 2018;361(6403):662.
27. Liu S, Liu Y, Yang X, Tong C, Edwards D, Parkin IA, Zhao M, Ma J, Yu J, Huang S, et al. The Brassica oleracea genome reveals the asymmetrical evolution of polyploid genomes. Nat Commun. 2014;5(8):3930.
28. Jiao Y, Wickett NJ, Ayyampalayam S, Chanderbali AS, Landherr L, Ralph PE, Tomsho LP, Hu Y, Liang H, Soltis PS. Ancestral polyploidy in seed plants and angiosperms. Nature. 2011;473(7345):97-100.
29. Vanneste K, Baele G, Maere S, Yves VDP. Analysis of 41 plant genomes supports a wave of successful genome duplications in association with the Cretaceous-Paleogene boundary. Genome Res. 2014;24:1334-47.
30. Fang ZW, Jiang WQ, He YQ, Ma DF, Liu YK, Wang SP, Zhang YX, Yin JL. Genome-Wide Identification:Structure Characterization:and Expression Profiling of Dof Transcription Factor Gene Family in Wheat (*Triticum aestivum*). Agronomy. 2020;10(294):1-27.
31. Song JH, Ma DF, Yin JL, Yang L, He YQ, Zhu ZW, Tong HW, Chen L, Zhu G, Liu YK, Gao CB. Genome-Wide Characterization and Expression Profiling of Squamosa Promoter Binding Protein-Like (SBP) Transcription Factors in Wheat (*Triticum aestivum*). Agronomy. 2019;9(527):1-33.
32. Zhou XY, Zhu XG, Shao WN, Song JH, Jiang WQ, He YQ, Yin JL, Ma DF, Qiao Genome-Wide Mining of Wheat DUF966 Gene Family Provides New Insights Into Salt Stress Responses. Frontiers in Plant science. 2020;28(11).
33. Jiang WQ, Geng YP, Liu YK, Chen SH; Cao SL, Li W, Chen HG, Ma DF, Yin JL. Genome-wide identification and characterization of SRO gene family in wheat: Molecular evolution and expression profiles during different stresses. Plant Physiology and Biochemistry. 2020;154:590-611.
34. He YQ, Huang WD, Yang L, Li YT, Lu C, Zhu YX, Ma DF, Yin JL. Genome-wide analysis of ethylene-insensitive3 (EIN3/EIL) in *Triticum aestivum*. Crop Science. 2020;60:2019-2037.
35. Tsai AY, Gazzarrini S. AKIN10 and FUSCA3 interact to control lateral organ development and phase transitions in *Arabidopsis*. Plant J. 2012;69(5):809-821.
36. Lovas A, Bimbo A,. Szabo L; Banfalvi Z. Antisense repression of StubGAL83 affects root and tuber development in potato. Plant J. 2003;33(1):139-147.

37. Radchuk R, Radchuk V, Weschke W, Borisjuk L, Weber Repressing the expression of the SUCROSE NONFERMENTING-1-RELATED PROTEIN KINASE gene in pea embryo causes pleiotropic defects of maturation similar to an abscisic acid-insensitive phenotype. Plant Physiology Preview. 2005;12(2):1-16.
38. Zou HW, Zhang XH, Zhao JR, Yang Q, Wu ZY, Wang FG, Huang CL. Cloning and characterization of maize ZmSPK1:a homologue to nonfermenting 1-related protein kinase2. J. Biotechnol. 2006;5(6):490-496.
39. Fan WQ, Zhao MY, Li SX, Bai X, Li J, Meng HW, Mu ZX. Contrasting transcriptional responses of PYR1/PYL/RCAR ABA receptors to ABA or dehydration stress between maize seedling leaves and roots. Bmc Plant Biology. 2016;16(1):99.
40. Huai JL, Wang M, He J.G, Zheng J, Dong ZG, Lv HK, Zhao JF, Wang GY. Cloning and characterization of the SnRK2 gene family from Zea mays. Plant Cell Reports. 2008;27(17):1861-1868.
41. Huang CL, Ding S, Zhang H, Zhang H, Du H, An LZ. CIPK7 is involved in cold response by interacting with CBL1 in *Arabidopsis thaliana*. Plant science. 2011;181(1):57-64.
42. Cramer GR, Urano K, Delrot S, Pezzotti M, Shinozaki K. Effects of abiotic stress on plants: a systems biology perspective. BMC Plant Biol. 2011;11(1):163.
43. Tsai YL, Gazzarrini S. Overlapping and distinct roles of AKIN10 and FUSCA3 in ABA and sugar signaling during seed germination. Plant Signaling and Behavior. 2012;7(10):1238-1242.
44. Yu L, Yuki S, Li XW, Mori IC, Takakazu M, Takashi H, Takeo S. ABI1 regulates carbon/nitrogen-nutrient signal transduction independent of ABA biosynthesis and canonical ABA signalling pathways in *Arabidopsis*. Journal of Experimental Botany. 2015;66(15):4851.
45. Tsugama D, Liu S, Takano T. A putative myristoylated 2C-type protein phosphatase:PP2C74:interacts with SnRK1 in *Arabidopsis*. Febs Letters. 2012;586(6):693-698.
46. Klimecka M, Bucholc M, Maszkowska J, Ewa K, Grażyna G, Małgorzata L, Jadwiga S, Grażyna D. Regulation of ABA-Non-Activated SNF1-Related Protein Kinase 2 Signaling Pathways by Phosphatidic Acid. Int. J. Mol. Sci. 2020;21(14):
47. Sang-Youl P, Pauline F, Noriyuki N, Jensen DR, Hiroaki F. Abscisic Acid Inhibits Type 2C Protein Phosphatases via the PYR/PYL Family of START Proteins. Science. 2009;324(5930):1068-1071.
48. Kulik A, Wawer I, Krzywińska E, Bucholc M, Dobro wolska G. SnRK2 Protein Kinases-Key Regulators of Plant Response to Abiotic Stresses. Omics: a journal of integrative biology. 2011;15(12):859-872.
49. Zhen L,. Yuan L; Zhang ZJ, Liu XL, Hu CC, Du YY, Sang T, Zhu C, Wang YB, Satheesh V, Pratibha P, Zhao Y, Song CP, Tao WA, Zhu JK, Wang PC. Wang P A RAF-SnRK2 kinase cascade mediates early osmotic stress signaling in higher plants. Nature Communications. 2020;11(1):613.
50. Soma F, Takahashi F, Suzuki F, Shinozaki K, Yamaguchi-Shinozaki K. Plant Raf-like kinases regulate the mRNA population upstream of ABA-unresponsive SnRK2 kinases under drought stress. Nature communications. 2020;11(1):1373.
51. Takahashi Y, Jingbo Z, Po-Kai H, Ceciliato HO, Julian SI. MAP3Kinase-dependent SnRK2-kinase activation is required for abscisic acid signal transduction and rapid osmotic stress response. Nature communications. 2020;11(1):112.

52. Fujita Y, Yoshida T, Yamaguchi-Shinozaki Pivotal role of the AREB/ABF-SnRK2 pathway in ABRE-mediated transcription in response to osmotic stress in plants. Physiologia Plantarum. 2013;147(1):15-27.
53. Shoko S, Srinivas B, Akihiro K, Masanori T, Machi K, Mitsuko A, Nobuyoshi N, Tatsuro N. ; Tomomi T, Munehiko A, Hikaru S. Disruption of a gene encoding C4-dicarboxylate transporter-like protein increases ozone sensitivity through deregulation of the stomatal response in *Arabidopsis thaliana*. Plant and Cell Physiology. 2008;49(1):2-10.
54. Wang J, Ren:Z.Y, Cheng C.H, Wang T, Ji H.T, Zhao Y, Deng Z.P, Zhi L.Y, Lu J.J, Wu X.Y, Xu S.M, Cao M.M, Zhao H.T, Liu L, Zhu J.K, Li X. Counteraction of ABA-Mediated Inhibition of Seed Germination and Seedling Establishment by ABA Signaling Terminator in *Arabidopsis*. Molecular Plant. 2020;13(9):1284-1297.
55. Wang XP, Chen LM, Liu WX, Shen L, Wang FL, Zhou Y, Zhang Z, Wu WH, Wang AtKC1 and CIPK23 synergistically modulate AKT1-mediated low potassium stress responses in *Arabidopsis*. Plant Physiol. 2016;170(4):1493-1508.
56. Halfter U, Ishitani M, Zhu JK. The Arabidopsis SOS2 protein kinase physically interacts with and is activated by the calcium binding protein SOS3. Proc. Acad. Sci. USA. 2000;97(7):3735-3740.
57. Batelli G, Verslues PE, Agius F, Qiu QS, Fujii H, Pan SQ, Schumaker KS, Grillo S, Zhu JK. SOS2 promotes salt tolerance in part by interacting with the vacuolar H^+-ATPase and upregulating its transport activity. Cell. Biol. 2007;27(22):7781-7790.
58. Cui XY, Du YT, Fu JD, Yu TF, Wang CT, Chen M, Chen J, Ma YZ, Xu ZS. Wheat CBL-interacting protein kinase 23 positively regulates drought stress and ABA responses. BMC Plant Biology, 2018;18(1):93.
59. Zhang HY, Mao X, Jing RL, Chang XP, Xie HM. Characterization of a common wheat (*Triticum aestivum*) TaSnRK2.7 gene involved in abiotic stress responses. Journal of Experimental Botany. 2011;62(3):975-988.
60. Julkowska Tale of Two Isoforms: Calcium-Dependent Inhibition of SnRK2 by SnRK-Calcium-Binding Sensor. Plant Physiology 2020;182(2):683-684.
61. Kim CY, Vo KTX, An G, Jeon JS. A rice sucrose non-fermenting-1 related protein kinase 1:OSK35:plays an important role in fungal and bacterial disease resistance. Applied Biological Chemistry. 2015;58(5):669-675.
62. Perochon A, Jia JG, Kahla A, Arunachalam C, Scofield SR, Bowden S; Wallington E, Doohan FM. TaFROG Encodes a Pooideae Orphan Protein That Interacts with SnRK1 and Enhances Resistance to the Mycotoxigenic Fungus *Fusarium graminearum*. Plant Physiology. 2015;169(4):2895-2906.
63. Nukarinen E, Nagele T, Pedrotti L. Quantitative phosphoproteomics reveals the role of the ampk plant ortholog SnRK1 as a metabolic master regulator under energy deprivation. SCI REP. 2016;6(1):31697.
64. Holappa LD, Walker-Simmons MK. The wheat protein kinase gene:TaPK3:of the PKABA1 subfamily is differentially regulated in greening wheat seedlings. Plant Mol. Biol. 1997;33(5):935-941.
65. Xu ZS, Liu L, Ni ZY, Liu P, Chen M, Li LC. W55a encodes a novel protein kinase that Is involved in multiple stress responses. Integr. Plant Biol. 2009;51(001):58-66.

66. Du XM, Zhao XL, Li XJ, Guo CJ, Lu WJ, Gu JT. Overexpression of TaSRK2C1:a wheat SNF1-related protein kinase 2 gene:increases tolerance to dehydration:salt:and low temperature in transgenic tobacco. Plant Mol. Biol. Rep. 2013;31(4):810-821.
67. Zhang HY, Mao X, Wang C. Overexpression of a Common Wheat Gene TaSnRK2.8 Enhances Tolerance to Drought:Salt and Low Temperature in *Arabidopsis*. PLoS ONE. 2010;5(12):e16041.
68. Thompson JD, Higgins DG, Gibson TJ. CLUSTALW: improving the sensitivity of progressive multiple sequence alignment through sequence weighting:position-specific gap penalties and weight matrix choice. Nucleic Acids Research. 1994;22(22):4673-4680.
69. Kumar S, Stecher G, Tamura K. MEGA7: Molecular evolutionary genetics analysis version 7.0 for bigger datasets. Molecular Biology Evolution. 2016;33(7):1870.
70. Chattha WS, Atif RM, Iqba M, Shafqat W, Farooq MA, Shakeel A. Genome-wide identification and evolution of Dof transcription factor family in cultivated and ancestral cotton species. Genomics 2020;6(112):4155-4170.
71. Chen CJ, Chen H, Zhang Y, Thomas H, Frank HM, Frank M, He YH, Xia: TBtools: An Integrative Toolkit Developed for Interactive Analyses of Big Biological Data. Molecular Plant. 2020;13(8).
72. Cheng XR, Xiong R, Yan HW, Gao YM, Liu HL, Wu Min, Xiang Y. The trihelix family of transcription factors: functional and evolutionary analysis in Moso bamboo (*Phyllostachys edulis*). BMC Plant Biology, 2019;19(1):154.
73. Jain Data clustering: 50 years beyond K-means. Pattern Recognition Letters. 2010;31(8):651-666.
74. Conesa A, Gotz S, Garcia-Gomez JM, Terol J, Talon MM. Robles:Blast2GO: a universal tool for annotation:visualization and analysis in functional genomics research. Bioinformatics. 2005;21(18):3674-3676.
75. Zhu Y, Jia J, Yang L; Xia Y, Zhang H, Jia J, Zhou R, Nie P, Yin JL; Ma D, Liu L. Identification of cucumber circular RNAs responsive to salt stress. BMC Plant Biology. 2019;19(1):164.
76. Yang XM, Ma J, Li HB, Ma HX, Yao JB, Liu CJ. Different genes can be responsible for crown rot resistance at different developmental stages of wheat and barley. J. Plant Pathol. 2010;128(4):495-502.
77. Hu YT, Liang YP, Zhang M, Tan FQ, Zhong SF. Comparative transcriptome profiling of Blumeria graminis f. sp. tritici during compatible and incompatible interactions with sister wheat lines carrying and lacking Pm40. PLoS ONE. 2018;13(7):1-19.
78. Tian YE, Yin JL, Sun JP, Ma YF, Wang QH, Quan JL. Population genetic analysis of *Phytophthora infestans* in northwestern China. Plant Pathol. 2016;65(1):17-25.

Figures

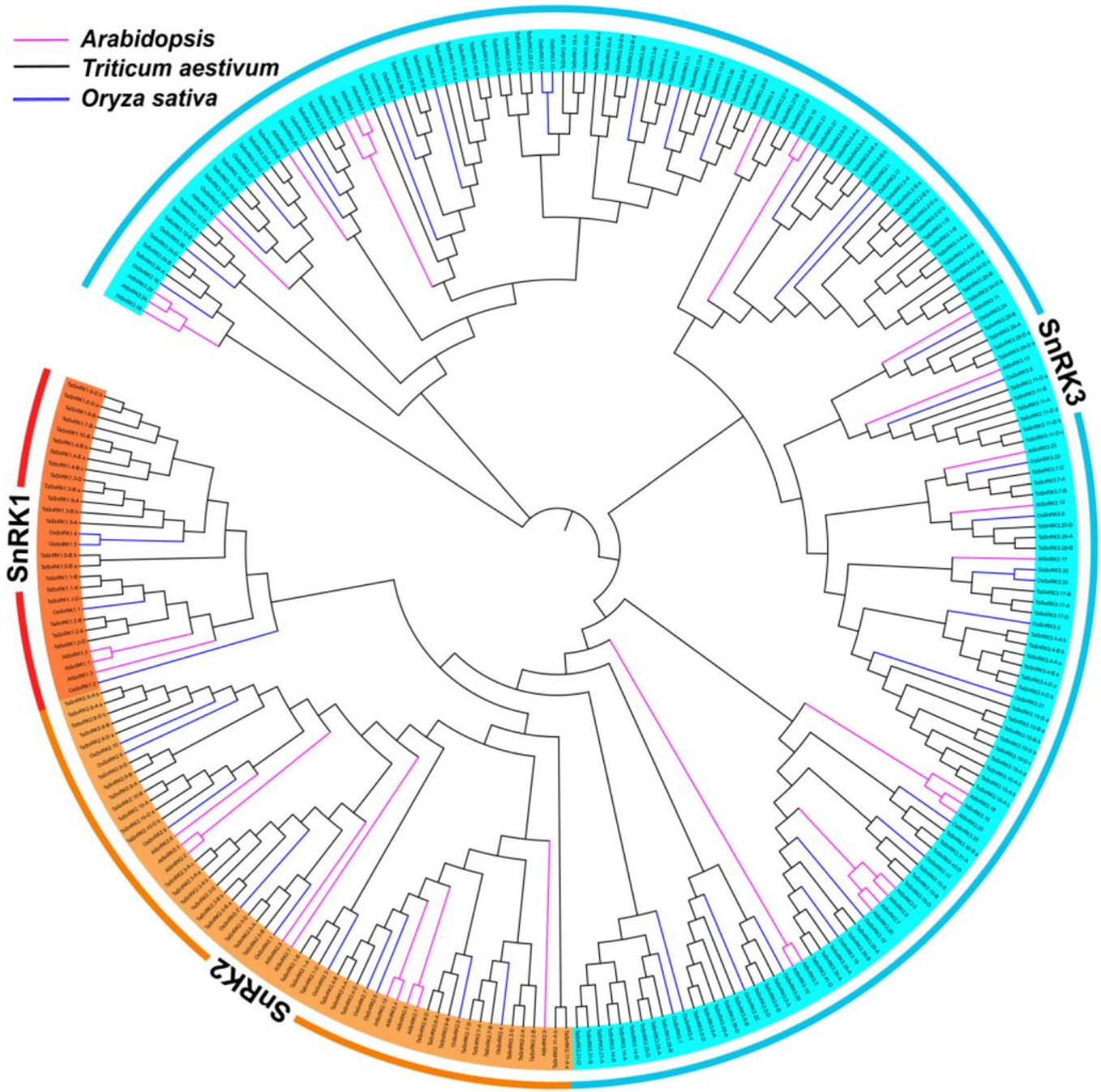

Figure 1

Phylogenetic tree of non-fermenting-1-related protein kinase (SnRK) predicted in wheat and those previously identified in Arabidopsis and Oryza sativa. All amino acid sequences, including 186 TaSnRKs, 47 OsSnRKs and 38 AtSnRKs, were aligned using ClustalW2, and the phylogenetic tree was constructed using the bootstrap neighbor-joining method (NJ) tree (1000 replicates) method and MEGA7.0 software. Different color ribbons mark different sub-families. SnRKs from wheat, rice, and Arabidopsis are distinguished with different color lines.

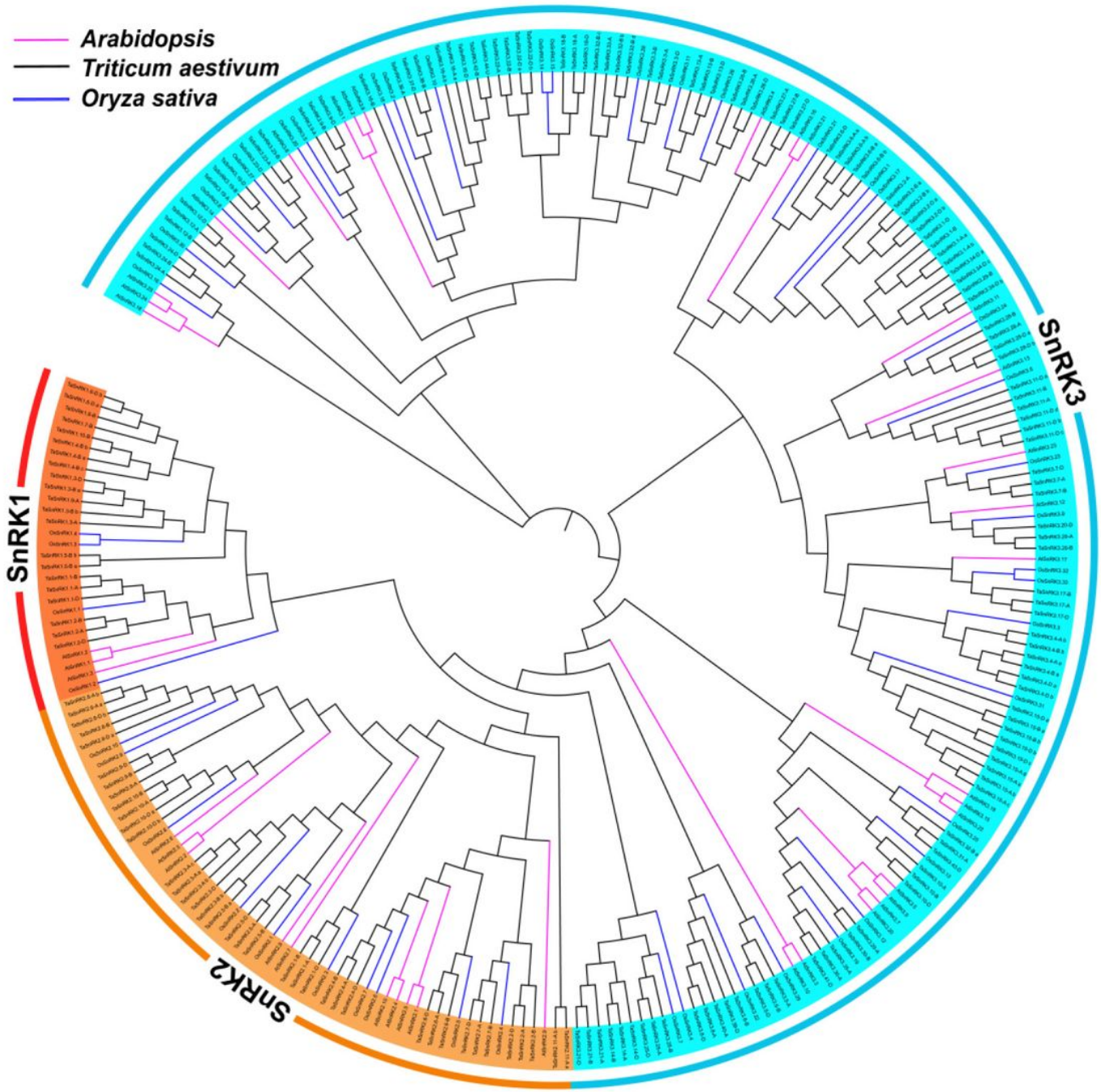

Figure 1

Phylogenetic tree of non-fermenting-1-related protein kinase (SnRK) predicted in wheat and those previously identified in Arabidopsis and Oryza sativa. All amino acid sequences, including 186 TaSnRKs, 47 OsSnRKs and 38 AtSnRKs, were aligned using ClustalW2, and the phylogenetic tree was constructed using the bootstrap neighbor-joining method (NJ) tree (1000 replicates) method and MEGA7.0 software. Different color ribbons mark different sub-families. SnRKs from wheat, rice, and Arabidopsis are distinguished with different color lines.

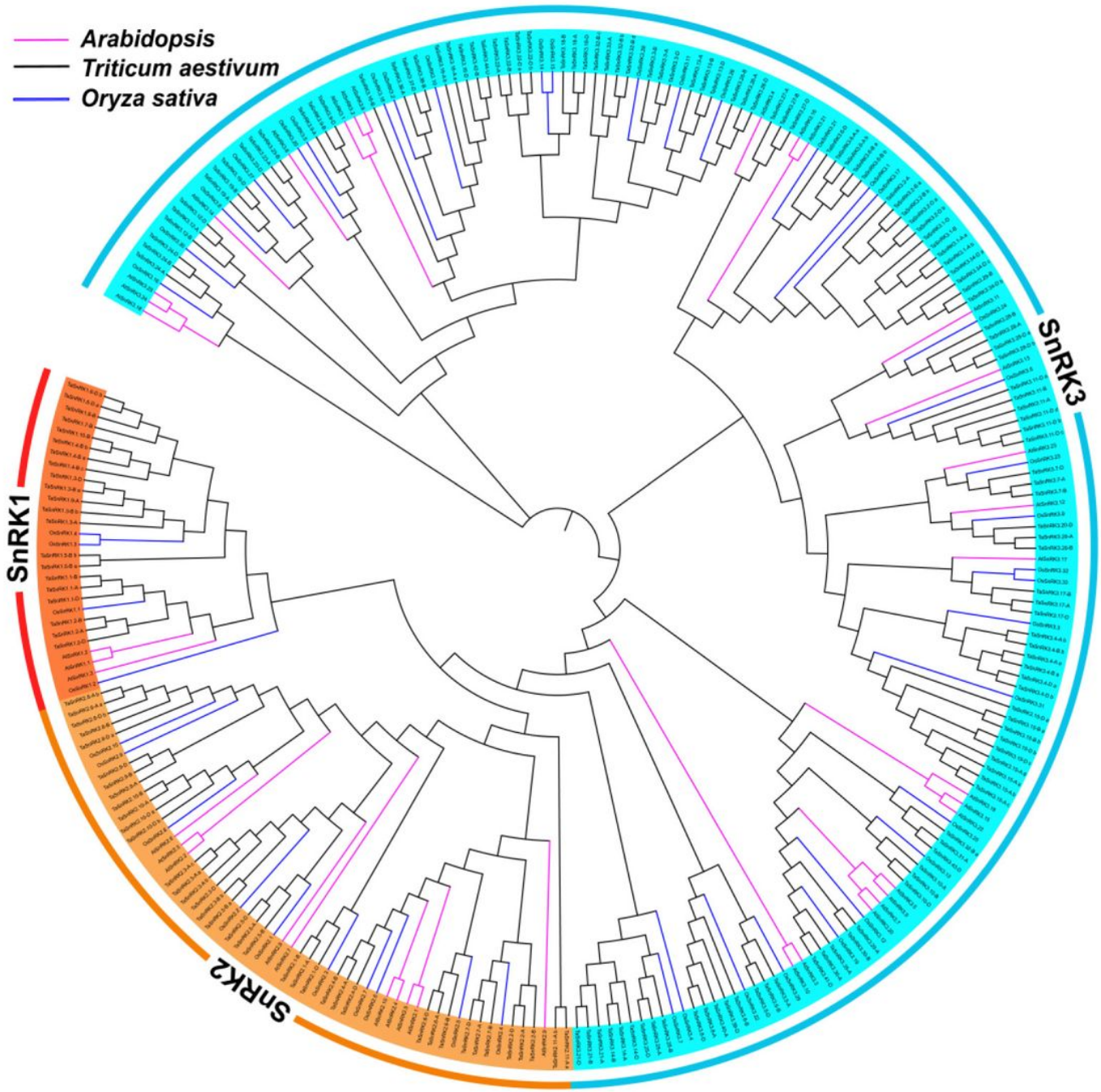

Figure 1

Phylogenetic tree of non-fermenting-1-related protein kinase (SnRK) predicted in wheat and those previously identified in Arabidopsis and Oryza sativa. All amino acid sequences, including 186 TaSnRKs, 47 OsSnRKs and 38 AtSnRKs, were aligned using ClustalW2, and the phylogenetic tree was constructed using the bootstrap neighbor-joining method (NJ) tree (1000 replicates) method and MEGA7.0 software. Different color ribbons mark different sub-families. SnRKs from wheat, rice, and Arabidopsis are distinguished with different color lines.

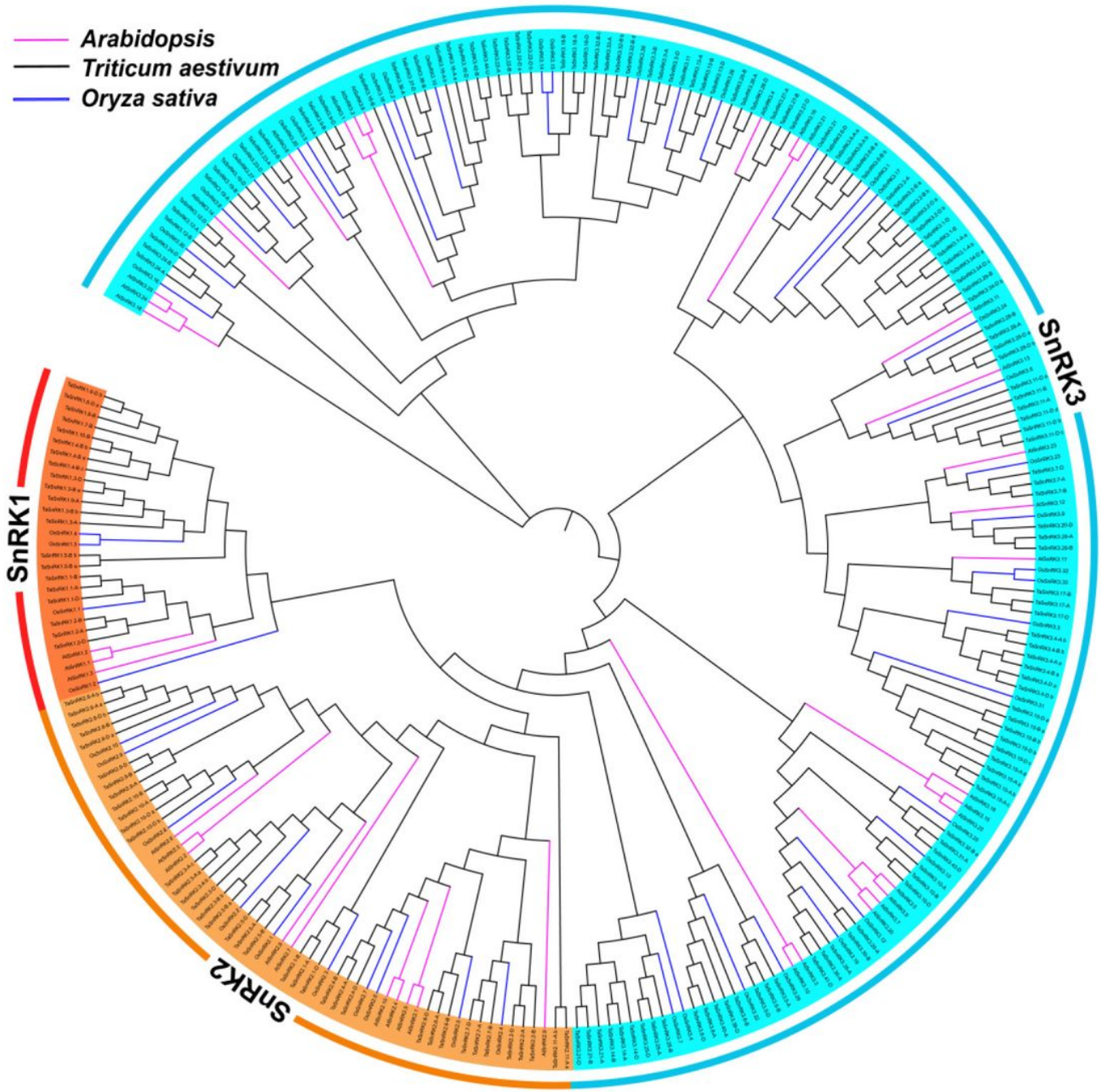

Figure 1

Phylogenetic tree of non-fermenting-1-related protein kinase (SnRK) predicted in wheat and those previously identified in Arabidopsis and Oryza sativa. All amino acid sequences, including 186 TaSnRKs, 47 OsSnRKs and 38 AtSnRKs, were aligned using ClustalW2, and the phylogenetic tree was constructed using the bootstrap neighbor-joining method (NJ) tree (1000 replicates) method and MEGA7.0 software. Different color ribbons mark different sub-families. SnRKs from wheat, rice, and Arabidopsis are distinguished with different color lines.

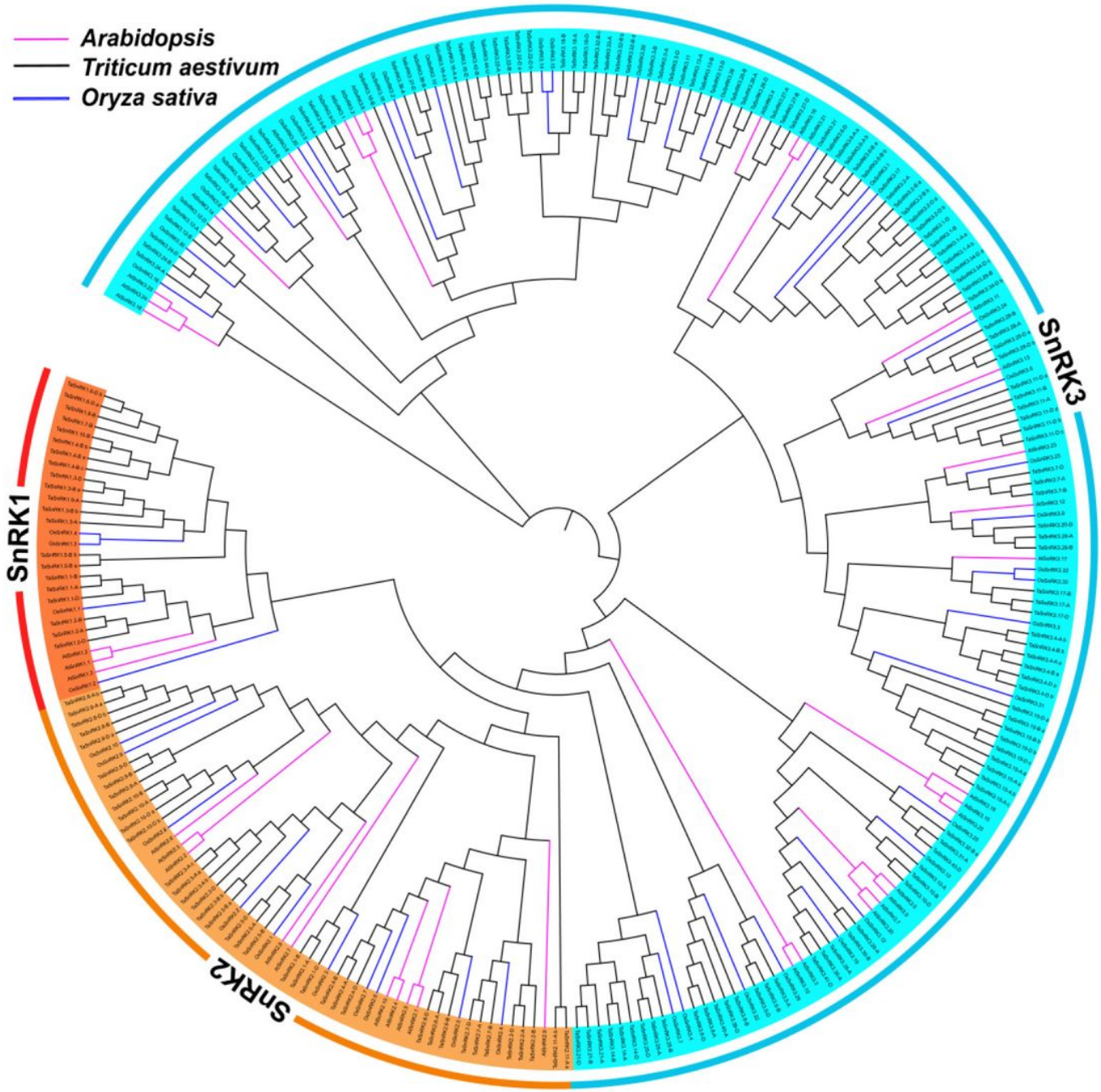

Figure 1

Phylogenetic tree of non-fermenting-1-related protein kinase (SnRK) predicted in wheat and those previously identified in Arabidopsis and Oryza sativa. All amino acid sequences, including 186 TaSnRKs, 47 OsSnRKs and 38 AtSnRKs, were aligned using ClustalW2, and the phylogenetic tree was constructed using the bootstrap neighbor-joining method (NJ) tree (1000 replicates) method and MEGA7.0 software. Different color ribbons mark different sub-families. SnRKs from wheat, rice, and Arabidopsis are distinguished with different color lines.

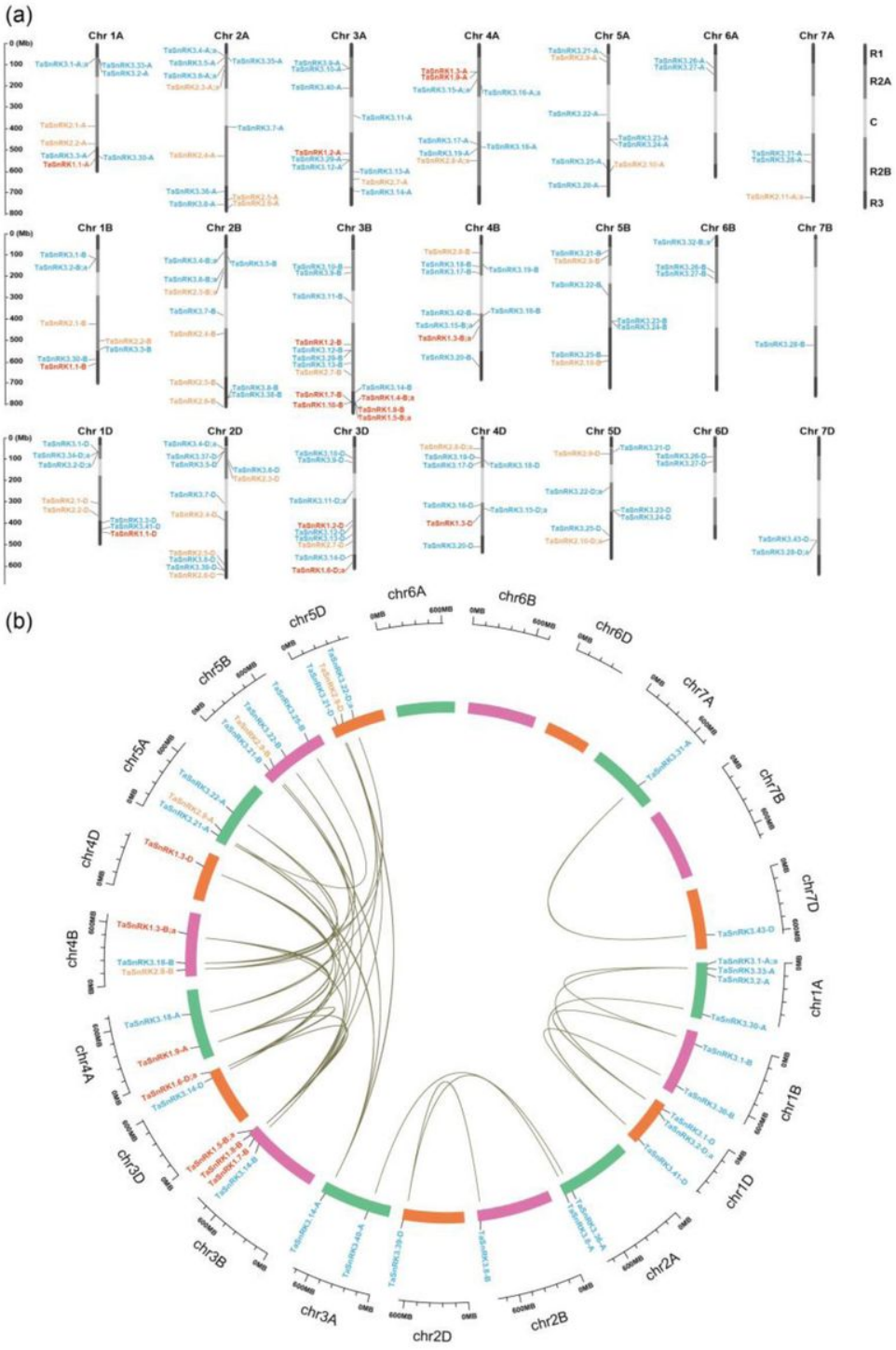

Figure 2

Chromosomal locations and gene duplication events of TaSnRKs. (a): Chromosomal locations of the 148 SnRKs genes of Triticum aestivum L. (TaSnRK). The rule on the left indicates the physical map distance among genes (Mbp). Dark black represents R1 and R3 (distal telomeric parts of the chromosomes), light gray represents R2A and R2B (sub-central segments of the chromosomes), and white represents C (central segments of the chromosomes). Gene members of SnRK1 (red), SnRK2 (orange), and SnRK3 (blue) were mapped to corresponding chromosomes. TaSnRK3.44-U gene was not mapped in chromosomes because it

was not predicted in any chromosomes. The specific location information of each gene on the chromosomes is shown in Table S2. (b): Gene duplication events of TaSnRKs. The detailed information of 49 segmental duplication pairs is listed in Table S3. There are no tandem duplication pairs predicted in TaSnRKs.

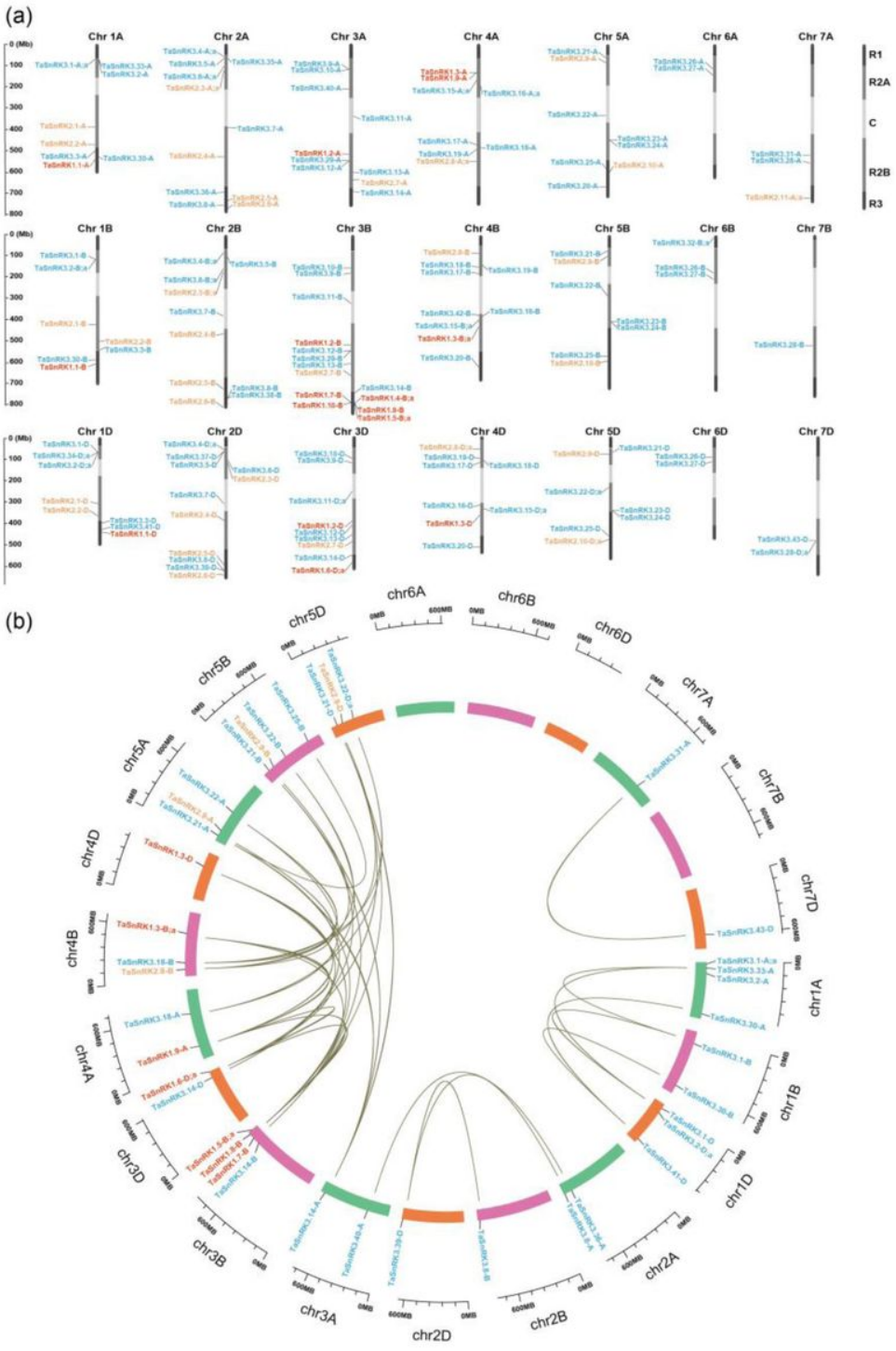

Figure 2

Chromosomal locations and gene duplication events of TaSnRKs. (a): Chromosomal locations of the 148 SnRKs genes of Triticum aestivum L. (TaSnRK). The rule on the left indicates the physical map distance among genes (Mbp). Dark black represents R1 and R3 (distal telomeric parts of the chromosomes), light gray

represents R2A and R2B (sub-central segments of the chromosomes), and white represents C (central segments of the chromosomes). Gene members of SnRK1 (red), SnRK2 (orange), and SnRK3 (blue) were mapped to corresponding chromosomes. TaSnRK3.44-U gene was not mapped in chromosomes because it was not predicted in any chromosomes. The specific location information of each gene on the chromosomes is shown in Table S2. (b): Gene duplication events of TaSnRKs. The detailed information of 49 segmental duplication pairs is listed in Table S3. There are no tandem duplication pairs predicted in TaSnRKs.

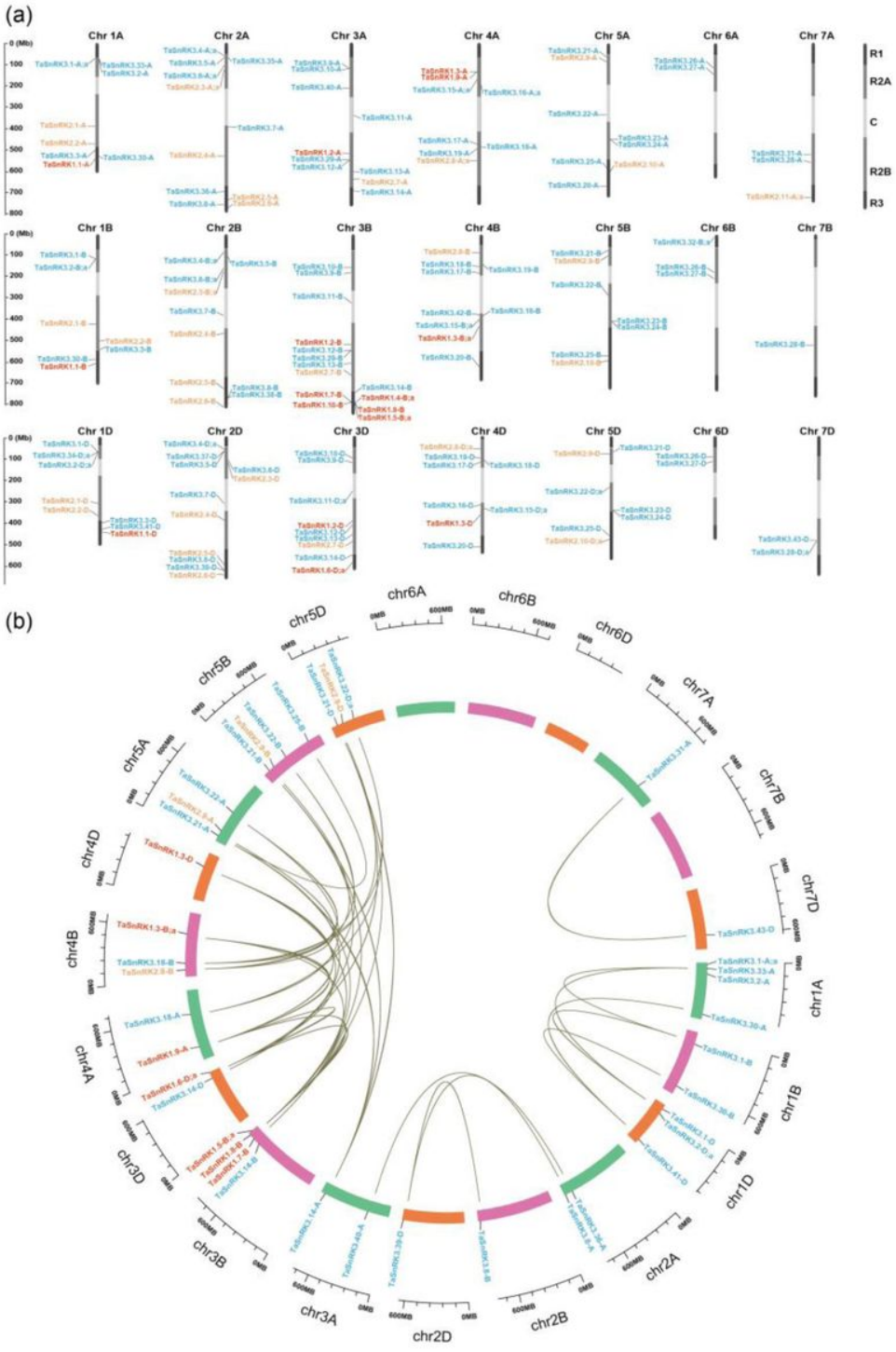

Figure 2

Chromosomal locations and gene duplication events of TaSnRKs. (a): Chromosomal locations of the 148 SnRKs genes of Triticum aestivum L. (TaSnRK). The rule on the left indicates the physical map distance among genes (Mbp). Dark black represents R1 and R3 (distal telomeric parts of the chromosomes), light gray represents R2A and R2B (sub-central segments of the chromosomes), and white represents C (central segments of the chromosomes). Gene members of SnRK1 (red), SnRK2 (orange), and SnRK3 (blue) were mapped to corresponding chromosomes. TaSnRK3.44-U gene was not mapped in chromosomes because it was not predicted in any chromosomes. The specific location information of each gene on the chromosomes is shown in Table S2. (b): Gene duplication events of TaSnRKs. The detailed information of 49 segmental duplication pairs is listed in Table S3. There are no tandem duplication pairs predicted in TaSnRKs.

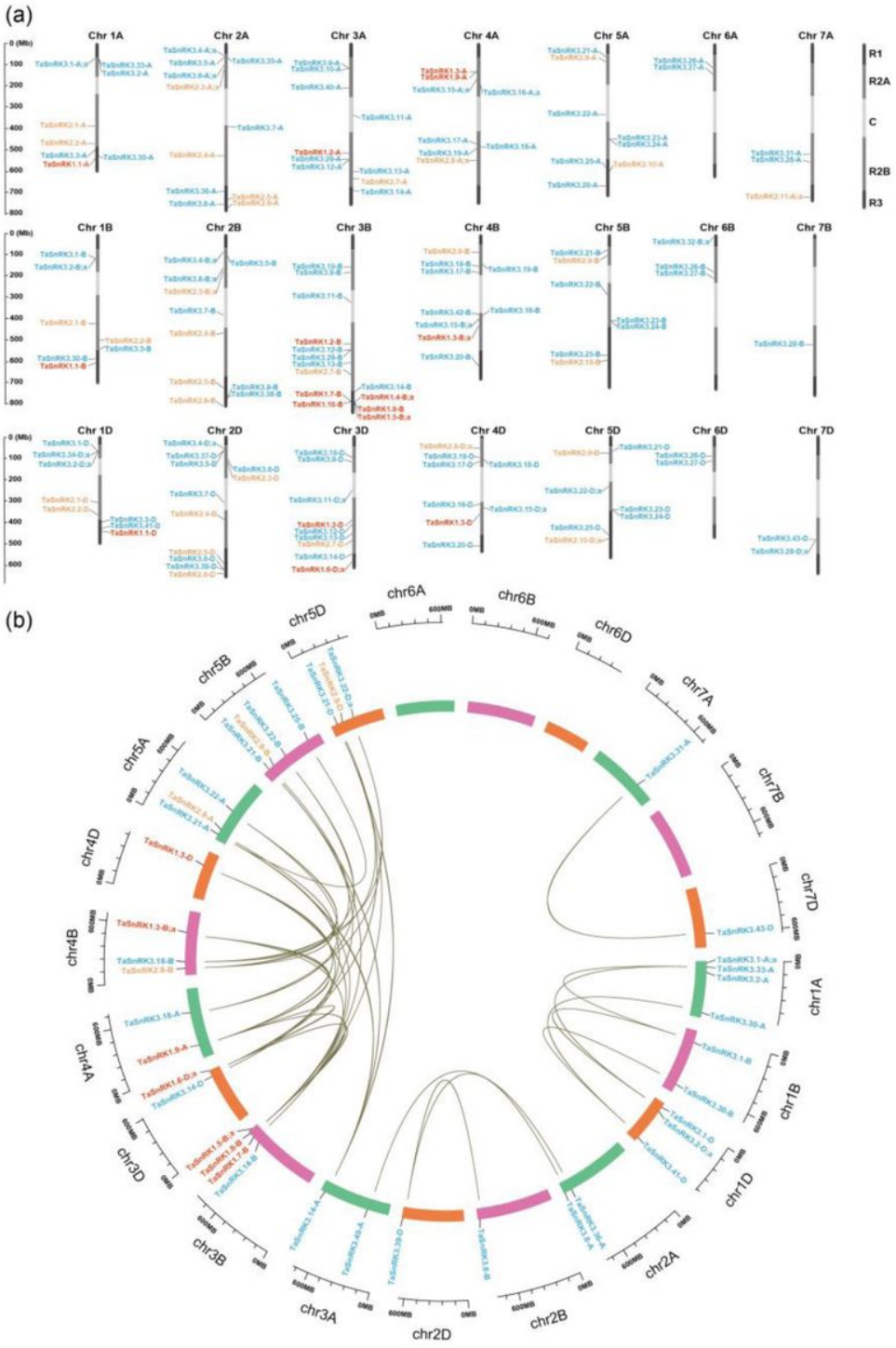

Figure 2

Chromosomal locations and gene duplication events of TaSnRKs. (a): Chromosomal locations of the 148 SnRKs genes of Triticum aestivum L. (TaSnRK). The rule on the left indicates the physical map distance among genes (Mbp). Dark black represents R1 and R3 (distal telomeric parts of the chromosomes), light gray represents R2A and R2B (sub-central segments of the chromosomes), and white represents C (central segments of the chromosomes). Gene members of SnRK1 (red), SnRK2 (orange), and SnRK3 (blue) were mapped to corresponding chromosomes. TaSnRK3.44-U gene was not mapped in chromosomes because it was not predicted in any chromosomes. The specific location information of each gene on the chromosomes is shown in Table S2. (b): Gene duplication events of TaSnRKs. The detailed information of 49 segmental duplication pairs is listed in Table S3. There are no tandem duplication pairs predicted in TaSnRKs.

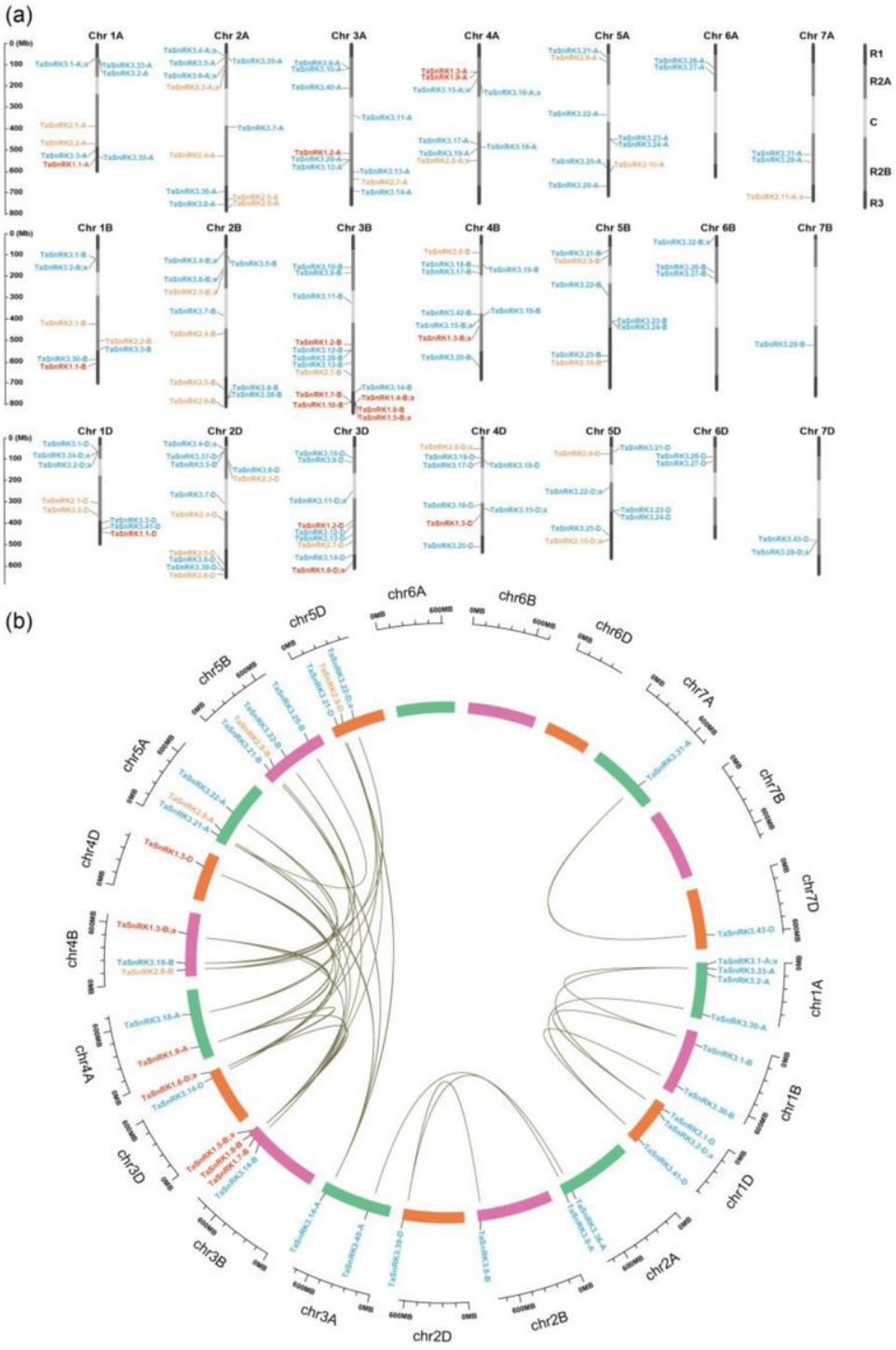

Figure 2

Chromosomal locations and gene duplication events of TaSnRKs. (a): Chromosomal locations of the 148 SnRKs genes of Triticum aestivum L. (TaSnRK). The rule on the left indicates the physical map distance among genes (Mbp). Dark black represents R1 and R3 (distal telomeric parts of the chromosomes), light gray represents R2A and R2B (sub-central segments of the chromosomes), and white represents C (central segments of the chromosomes). Gene members of SnRK1 (red), SnRK2 (orange), and SnRK3 (blue) were mapped to corresponding chromosomes. TaSnRK3.44-U gene was not mapped in chromosomes because it

was not predicted in any chromosomes. The specific location information of each gene on the chromosomes is shown in Table S2. (b): Gene duplication events of TaSnRKs. The detailed information of 49 segmental duplication pairs is listed in Table S3. There are no tandem duplication pairs predicted in TaSnRKs.

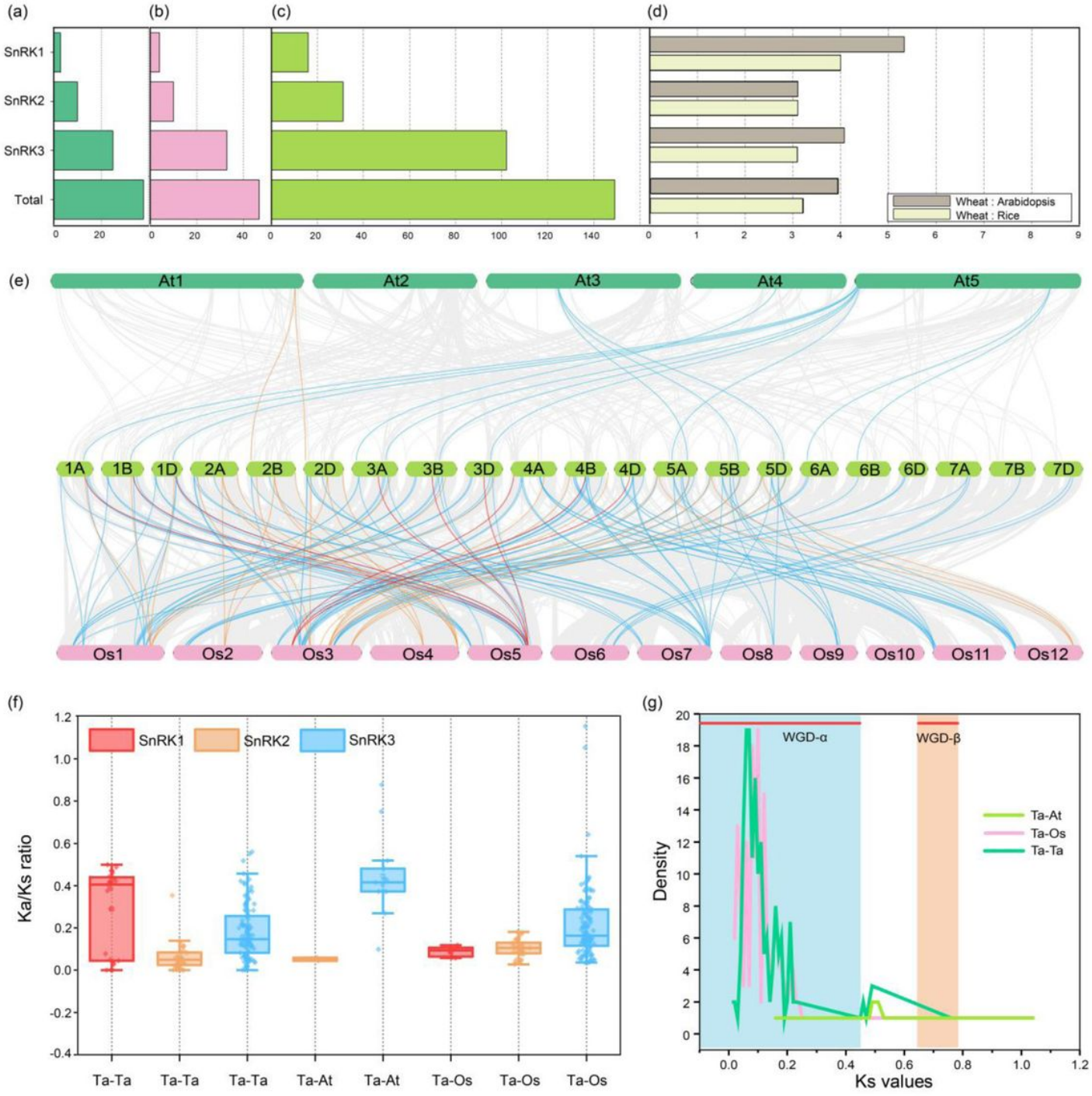

Figure 3

Chromosomal locations and gene duplication events of TaSnRKs. (a): Chromosomal locations of the 148 SnRKs genes of Triticum aestivum L. (TaSnRK). The rule on the left indicates the physical map distance among genes (Mbp). Dark black represents R1 and R3 (distal telomeric parts of the chromosomes), light gray represents R2A and R2B (sub-central segments of the chromosomes), and white represents C (central

segments of the chromosomes). Gene members of SnRK1 (red), SnRK2 (orange), and SnRK3 (blue) were mapped to corresponding chromosomes. TaSnRK3.44-U gene was not mapped in chromosomes because it was not predicted in any chromosomes. The specific location information of each gene on the chromosomes is shown in Table S2. (b): Gene duplication events of TaSnRKs. The detailed information of 49 segmental duplication pairs is listed in Table S3

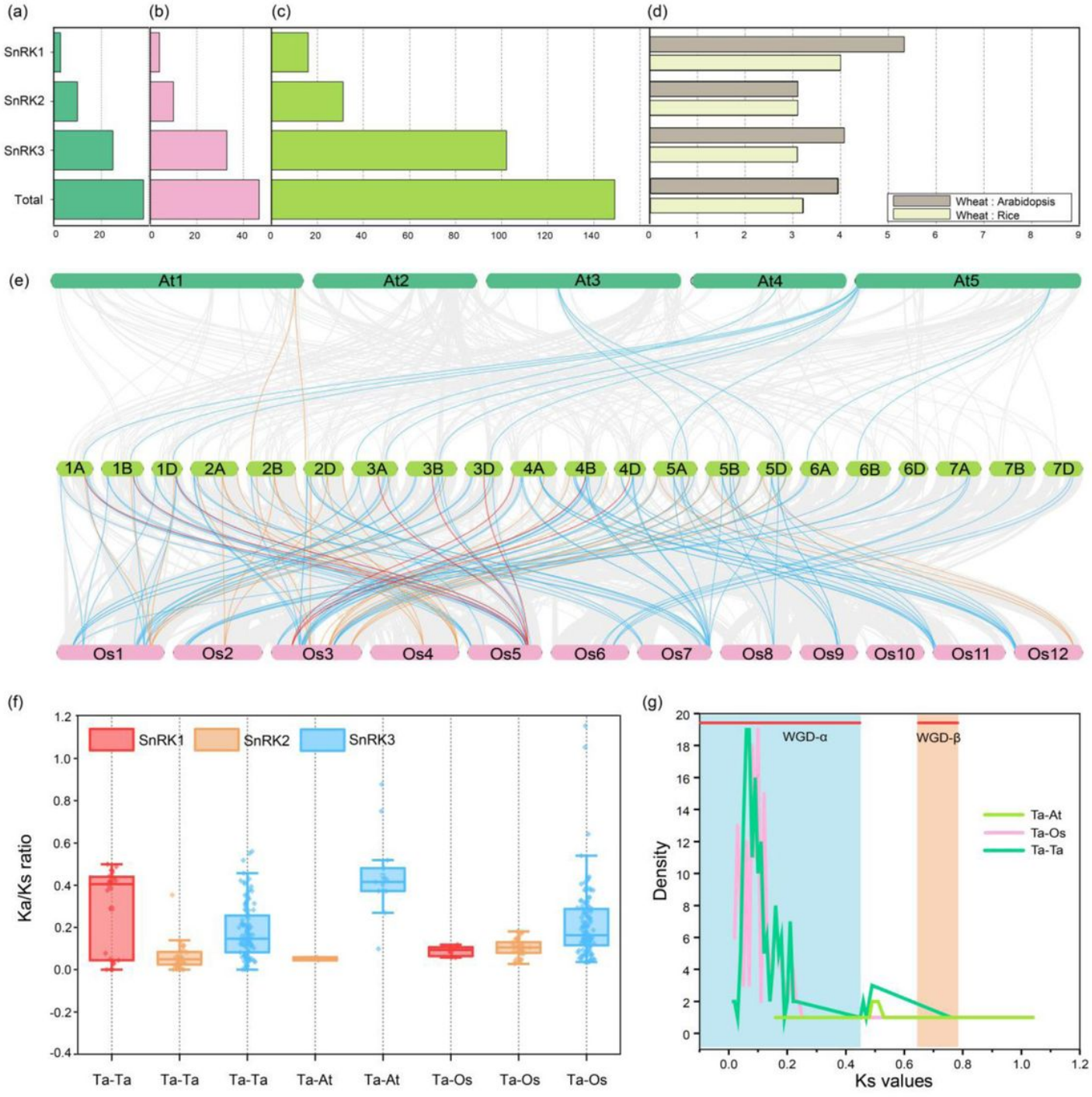

Figure 3

Chromosomal locations and gene duplication events of TaSnRKs. (a): Chromosomal locations of the 148 SnRKs genes of Triticum aestivum L. (TaSnRK). The rule on the left indicates the physical map distance

among genes (Mbp). Dark black represents R1 and R3 (distal telomeric parts of the chromosomes), light gray represents R2A and R2B (sub-central segments of the chromosomes), and white represents C (central segments of the chromosomes). Gene members of SnRK1 (red), SnRK2 (orange), and SnRK3 (blue) were mapped to corresponding chromosomes. TaSnRK3.44-U gene was not mapped in chromosomes because it was not predicted in any chromosomes. The specific location information of each gene on the chromosomes is shown in Table S2. (b): Gene duplication events of TaSnRKs. The detailed information of 49 segmental duplication pairs is listed in Table S3

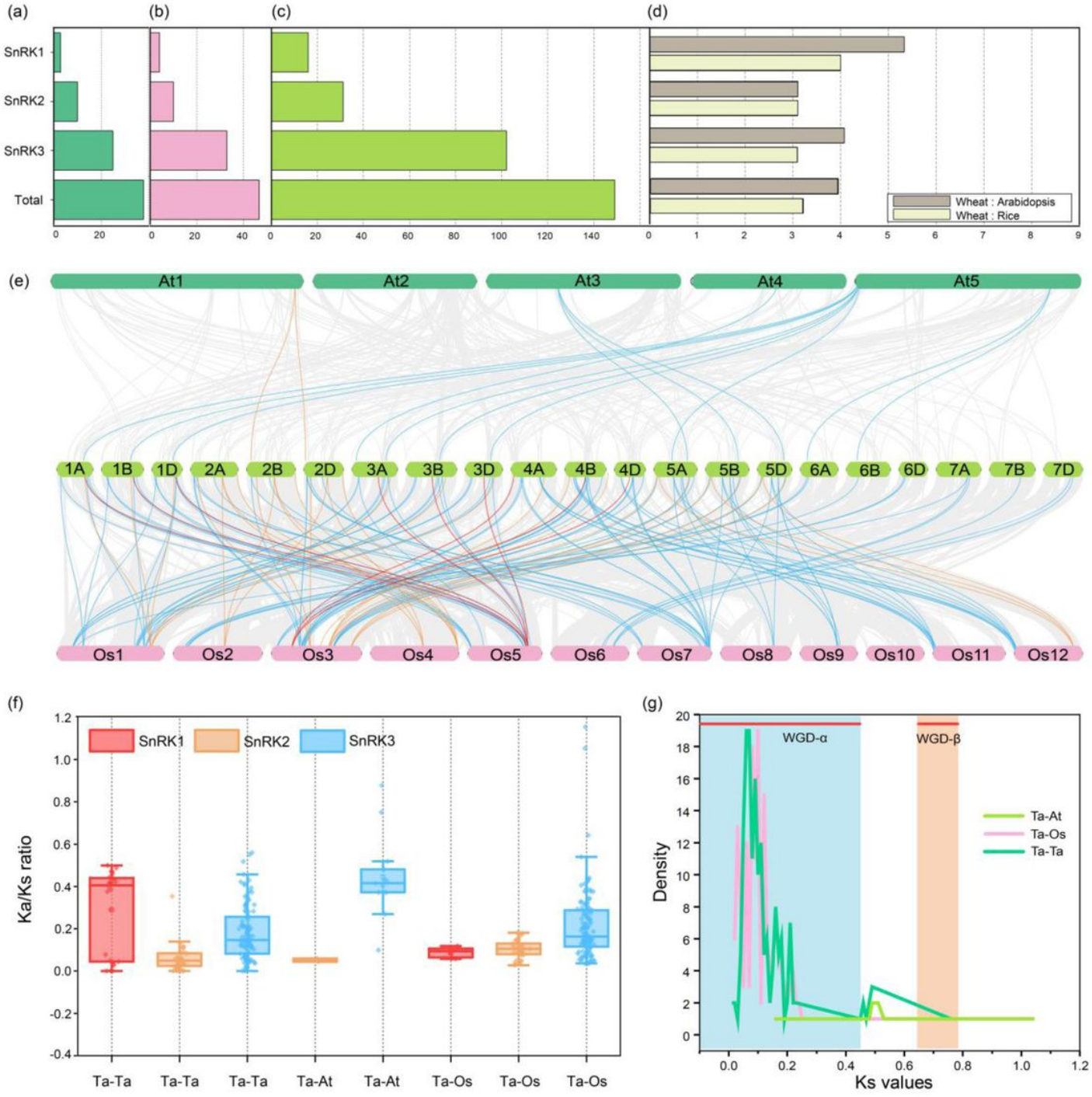

Figure 3

Chromosomal locations and gene duplication events of TaSnRKs. (a): Chromosomal locations of the 148 SnRKs genes of Triticum aestivum L. (TaSnRK). The rule on the left indicates the physical map distance among genes (Mbp). Dark black represents R1 and R3 (distal telomeric parts of the chromosomes), light gray represents R2A and R2B (sub-central segments of the chromosomes), and white represents C (central segments of the chromosomes). Gene members of SnRK1 (red), SnRK2 (orange), and SnRK3 (blue) were mapped to corresponding chromosomes. TaSnRK3.44-U gene was not mapped in chromosomes because it was not predicted in any chromosomes. The specific location information of each gene on the chromosomes is shown in Table S2. (b): Gene duplication events of TaSnRKs. The detailed information of 49 segmental duplication pairs is listed in Table S3

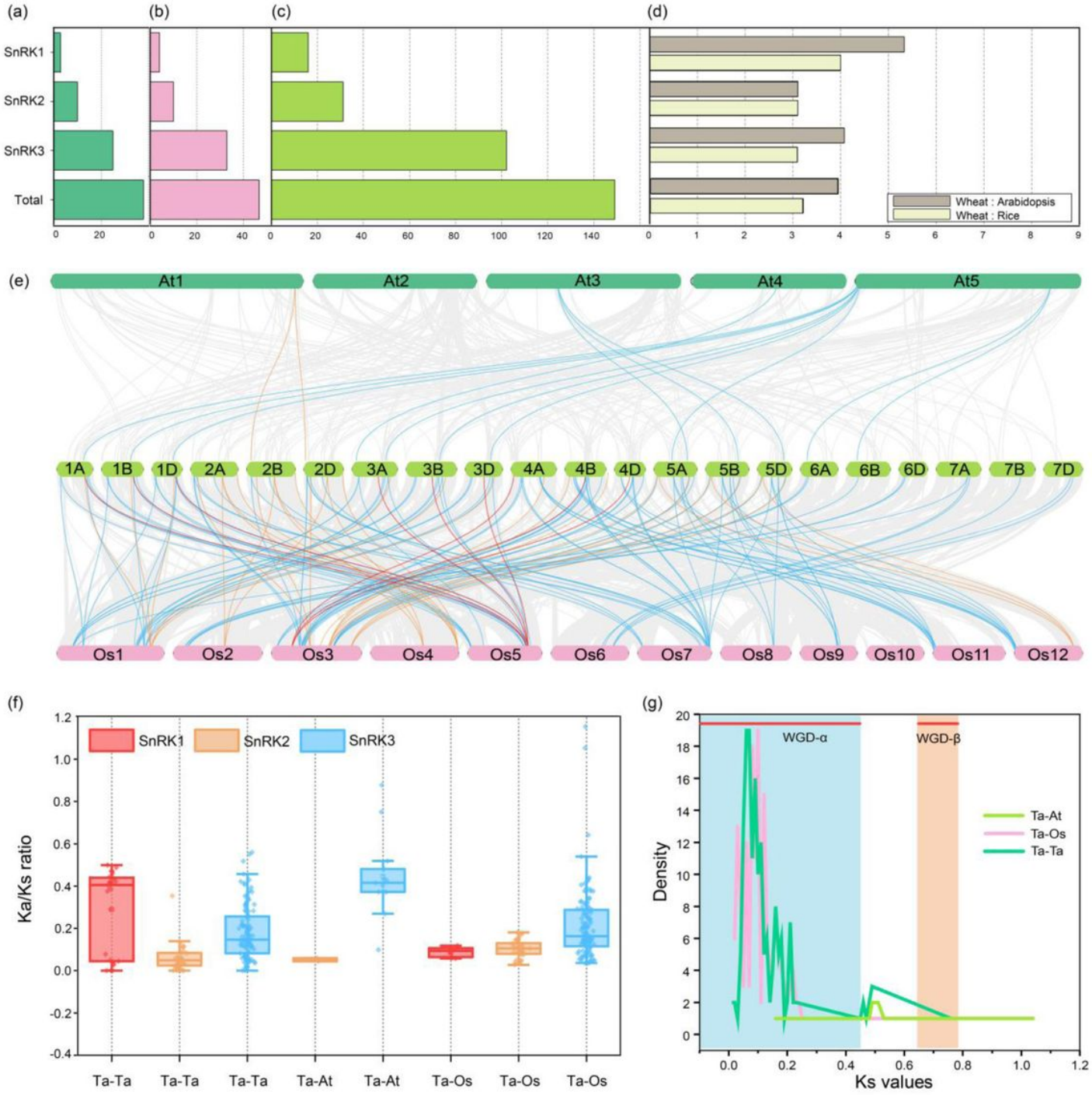

Figure 3

Chromosomal locations and gene duplication events of TaSnRKs. (a): Chromosomal locations of the 148 SnRKs genes of Triticum aestivum L. (TaSnRK). The rule on the left indicates the physical map distance among genes (Mbp). Dark black represents R1 and R3 (distal telomeric parts of the chromosomes), light gray represents R2A and R2B (sub-central segments of the chromosomes), and white represents C (central segments of the chromosomes). Gene members of SnRK1 (red), SnRK2 (orange), and SnRK3 (blue) were mapped to corresponding chromosomes. TaSnRK3.44-U gene was not mapped in chromosomes because it was not predicted in any chromosomes. The specific location information of each gene on the chromosomes is shown in Table S2. (b): Gene duplication events of TaSnRKs. The detailed information of 49 segmental duplication pairs is listed in Table S3

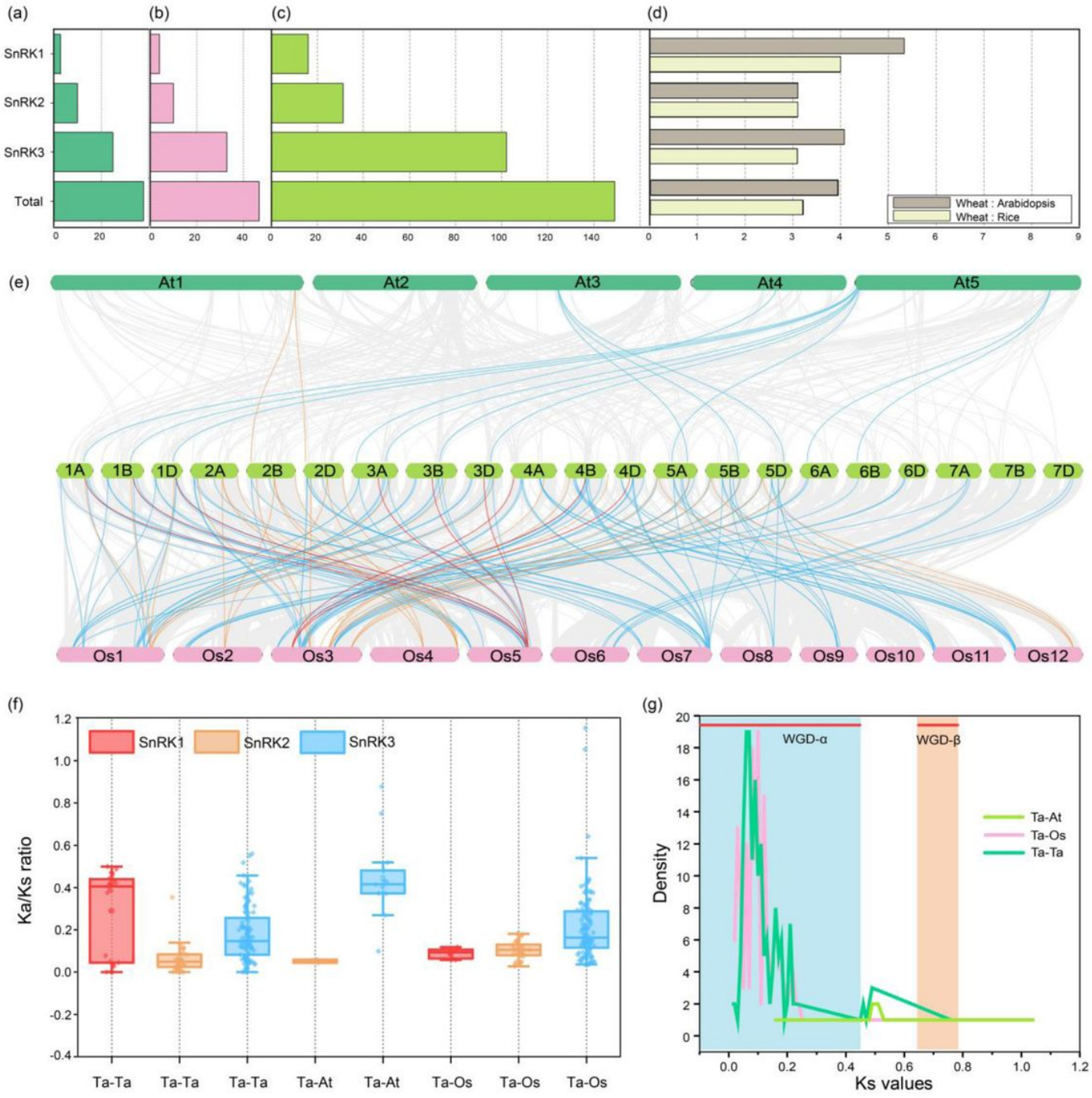

Figure 3

Chromosomal locations and gene duplication events of TaSnRKs. (a): Chromosomal locations of the 148 SnRKs genes of Triticum aestivum L. (TaSnRK). The rule on the left indicates the physical map distance among genes (Mbp). Dark black represents R1 and R3 (distal telomeric parts of the chromosomes), light gray represents R2A and R2B (sub-central segments of the chromosomes), and white represents C (central segments of the chromosomes). Gene members of SnRK1 (red), SnRK2 (orange), and SnRK3 (blue) were mapped to corresponding chromosomes. TaSnRK3.44-U gene was not mapped in chromosomes because it was not predicted in any chromosomes. The specific location information of each gene on the chromosomes

is shown in Table S2. (b): Gene duplication events of TaSnRKs. The detailed information of 49 segmental duplication pairs is listed in Table S3

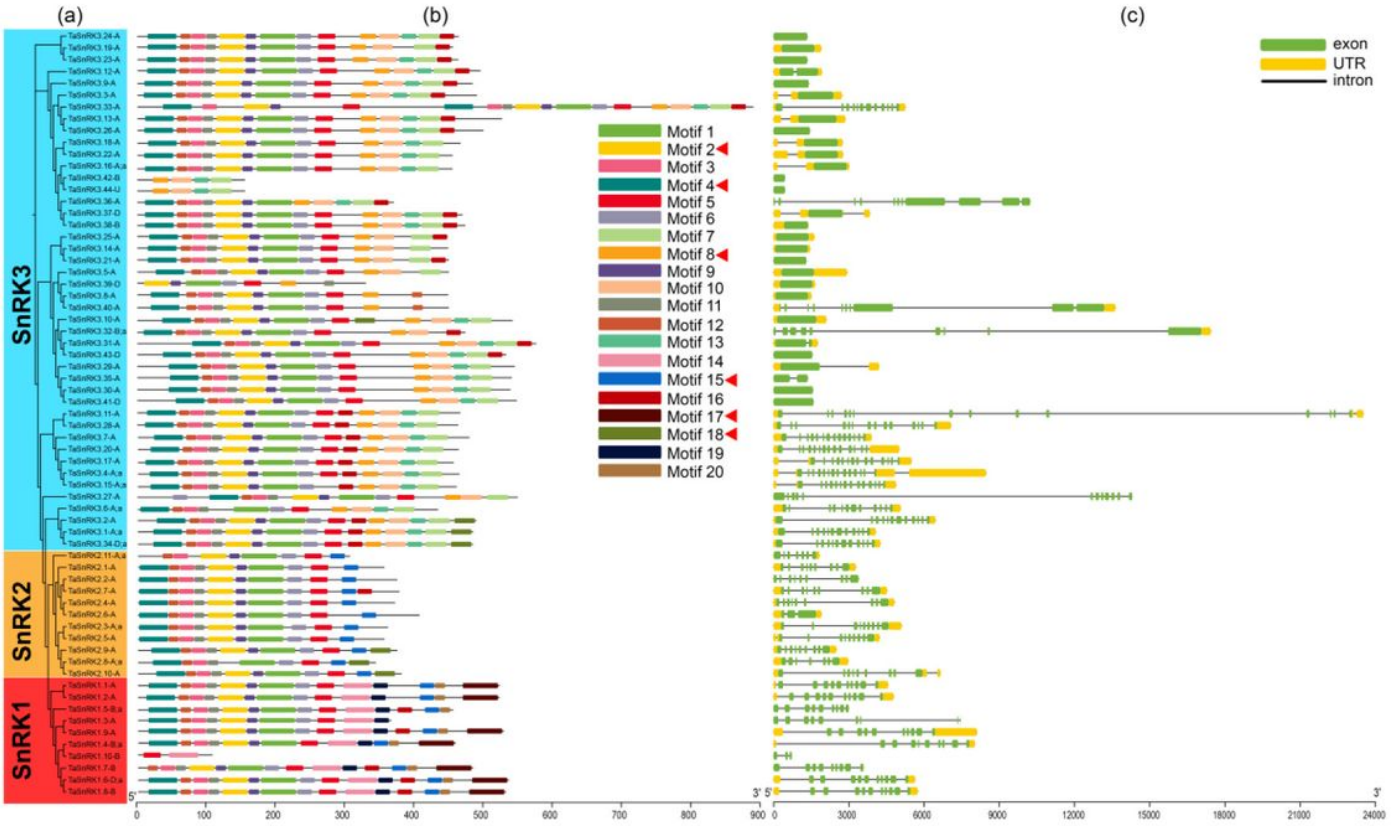

Figure 4

Gene structure and motif analyses of 65 representative TaSnRKs. (a): The phylogenetic tree of TaSnRKs. The tree was created with 1000 bootstraps by Neighbor-Joining (NJ) method in MEGA7. (b): The motifs of TaSnRKs were identified by MEME. MAST was used to exhibit the motif patterns. The red triangles indicate motifs associated with the functional domains. (c): The exon-intron structure of TaSnRKs. Exon-intron structure analyses were conducted using the GSDS. Lengths of exons and introns are displayed proportionally. Yellow boxes indicate the untranslated regions (UTRs). Green boxes indicate the exons. And black lines indicate the introns. Gene structure and motif analyses of 186 TaSnRKs can be found in Figure S1.

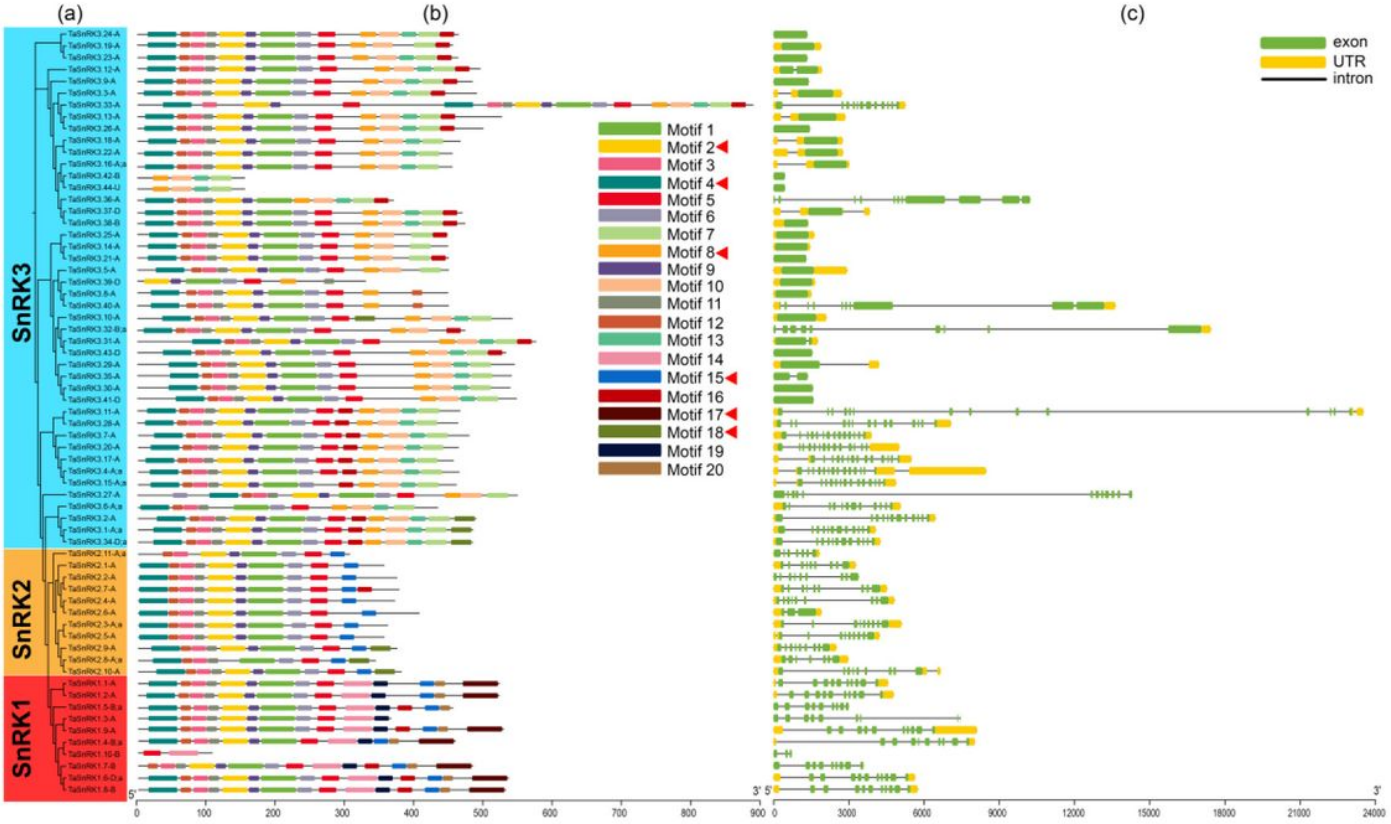

Figure 4

Gene structure and motif analyses of 65 representative TaSnRKs. (a): The phylogenetic tree of TaSnRKs. The tree was created with 1000 bootstraps by Neighbor-Joining (NJ) method in MEGA7. (b): The motifs of TaSnRKs were identified by MEME. MAST was used to exhibit the motif patterns. The red triangles indicate motifs associated with the functional domains. (c): The exon-intron structure of TaSnRKs. Exon-intron structure analyses were conducted using the GSDS. Lengths of exons and introns are displayed proportionally. Yellow boxes indicate the untranslated regions (UTRs). Green boxes indicate the exons. And black lines indicate the introns. Gene structure and motif analyses of 186 TaSnRKs can be found in Figure S1.

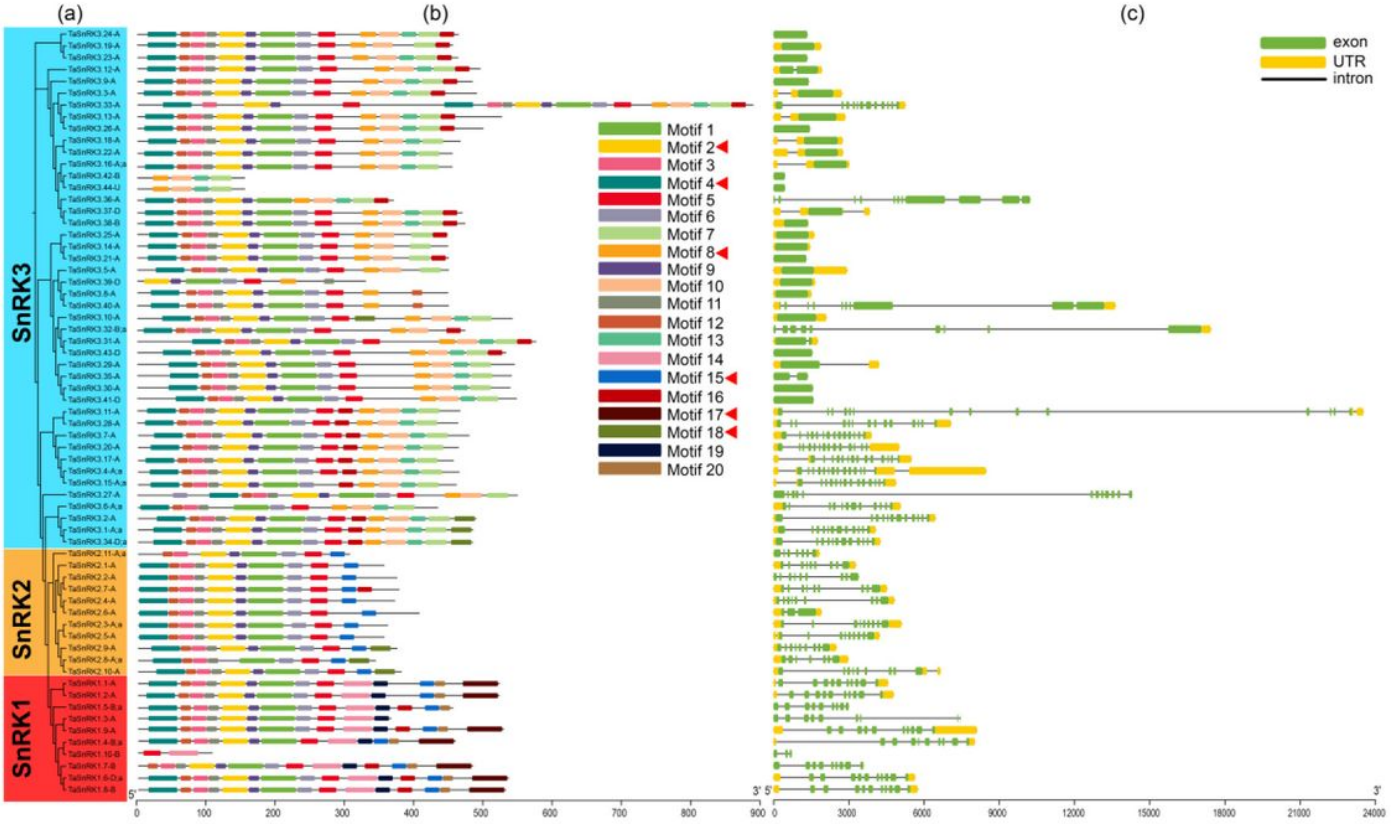

Figure 4

Gene structure and motif analyses of 65 representative TaSnRKs. (a): The phylogenetic tree of TaSnRKs. The tree was created with 1000 bootstraps by Neighbor-Joining (NJ) method in MEGA7. (b): The motifs of TaSnRKs were identified by MEME. MAST was used to exhibit the motif patterns. The red triangles indicate motifs associated with the functional domains. (c): The exon-intron structure of TaSnRKs. Exon-intron structure analyses were conducted using the GSDS. Lengths of exons and introns are displayed proportionally. Yellow boxes indicate the untranslated regions (UTRs). Green boxes indicate the exons. And black lines indicate the introns. Gene structure and motif analyses of 186 TaSnRKs can be found in Figure S1.

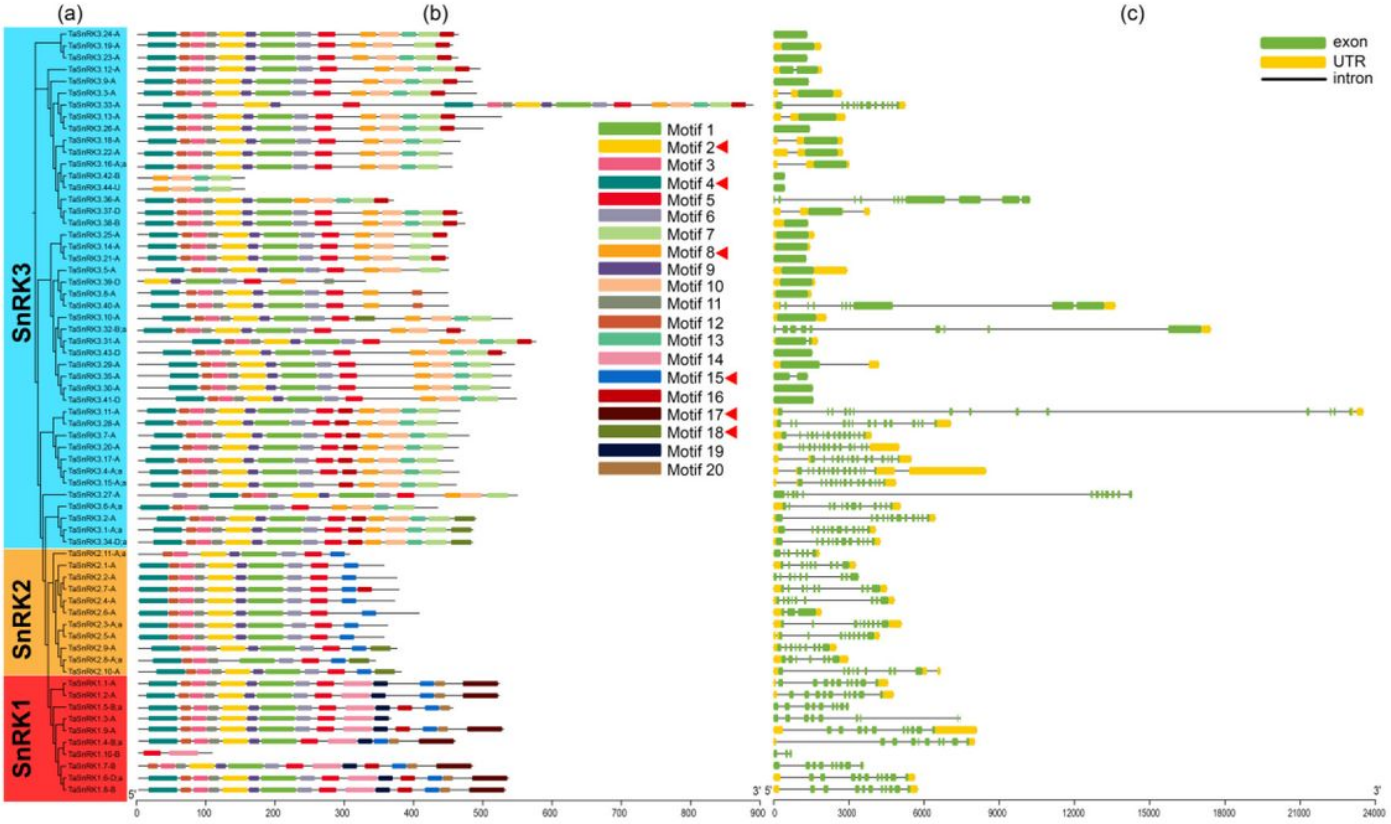

Figure 4

Gene structure and motif analyses of 65 representative TaSnRKs. (a): The phylogenetic tree of TaSnRKs. The tree was created with 1000 bootstraps by Neighbor-Joining (NJ) method in MEGA7. (b): The motifs of TaSnRKs were identified by MEME. MAST was used to exhibit the motif patterns. The red triangles indicate motifs associated with the functional domains. (c): The exon-intron structure of TaSnRKs. Exon-intron structure analyses were conducted using the GSDS. Lengths of exons and introns are displayed proportionally. Yellow boxes indicate the untranslated regions (UTRs). Green boxes indicate the exons. And black lines indicate the introns. Gene structure and motif analyses of 186 TaSnRKs can be found in Figure S1.

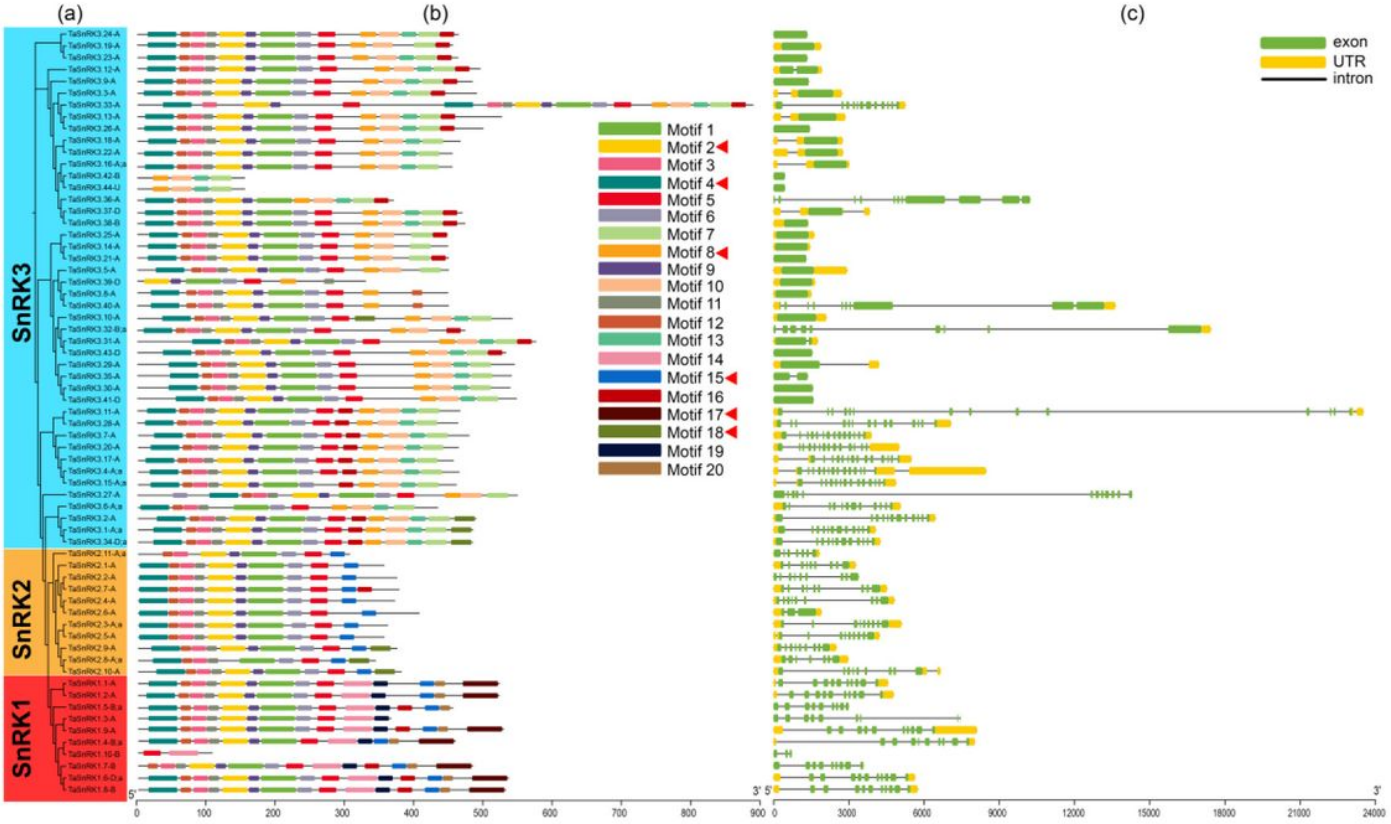

Figure 4

Gene structure and motif analyses of 65 representative TaSnRKs. (a): The phylogenetic tree of TaSnRKs. The tree was created with 1000 bootstraps by Neighbor-Joining (NJ) method in MEGA7. (b): The motifs of TaSnRKs were identified by MEME. MAST was used to exhibit the motif patterns. The red triangles indicate motifs associated with the functional domains. (c): The exon-intron structure of TaSnRKs. Exon-intron structure analyses were conducted using the GSDS. Lengths of exons and introns are displayed proportionally. Yellow boxes indicate the untranslated regions (UTRs). Green boxes indicate the exons. And black lines indicate the introns. Gene structure and motif analyses of 186 TaSnRKs can be found in Figure S1.

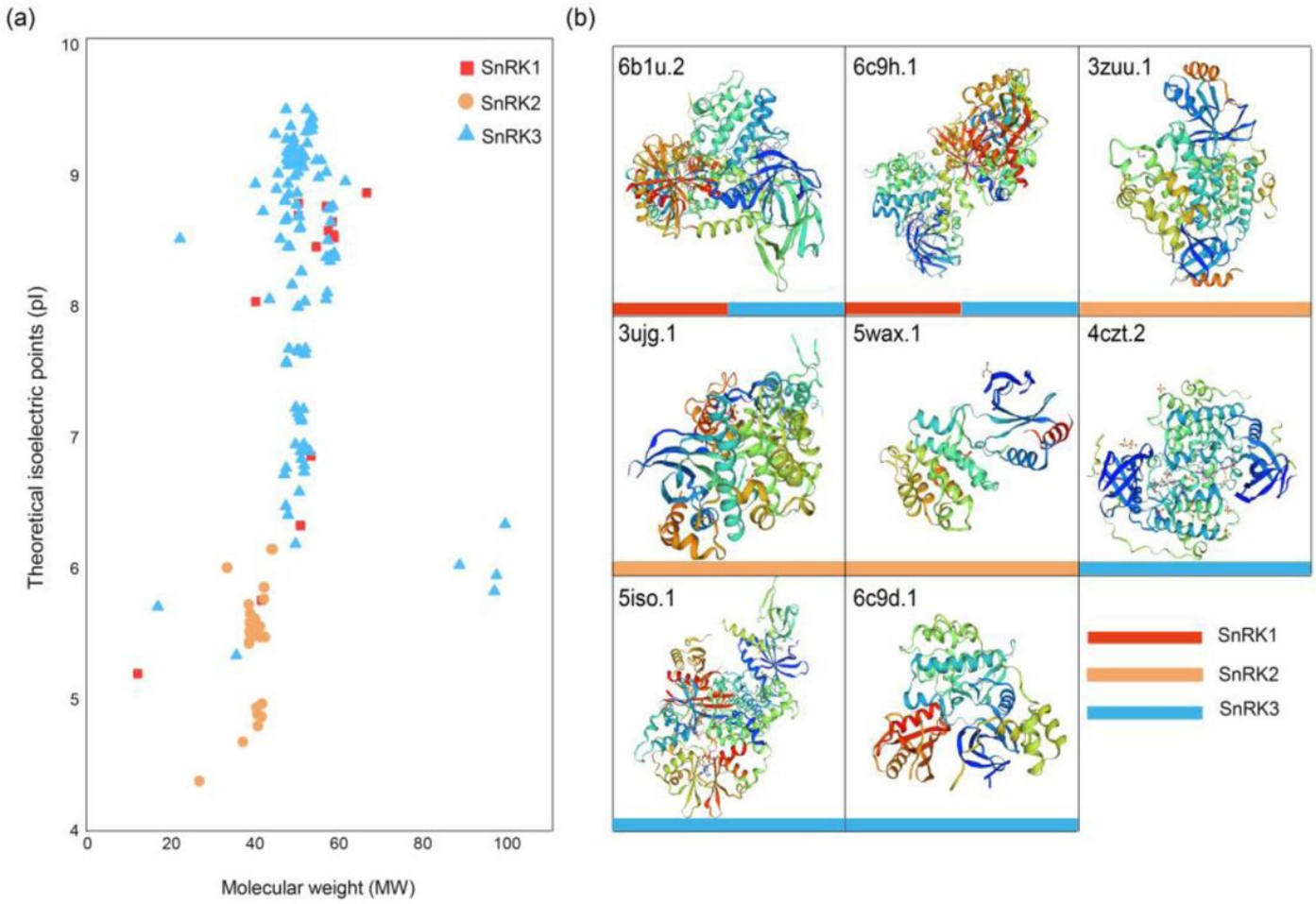

Figure 5

Distributions of MW and pI, and three-dimensional structure of TaSnRK proteins. (a): The distributions of MW and pI for the three subfamilies of wheat SnRKs. (b): Three-dimensional structure of TaSnRK proteins. The templates of 65 representative TaSnRK proteins are shown in Table S2.

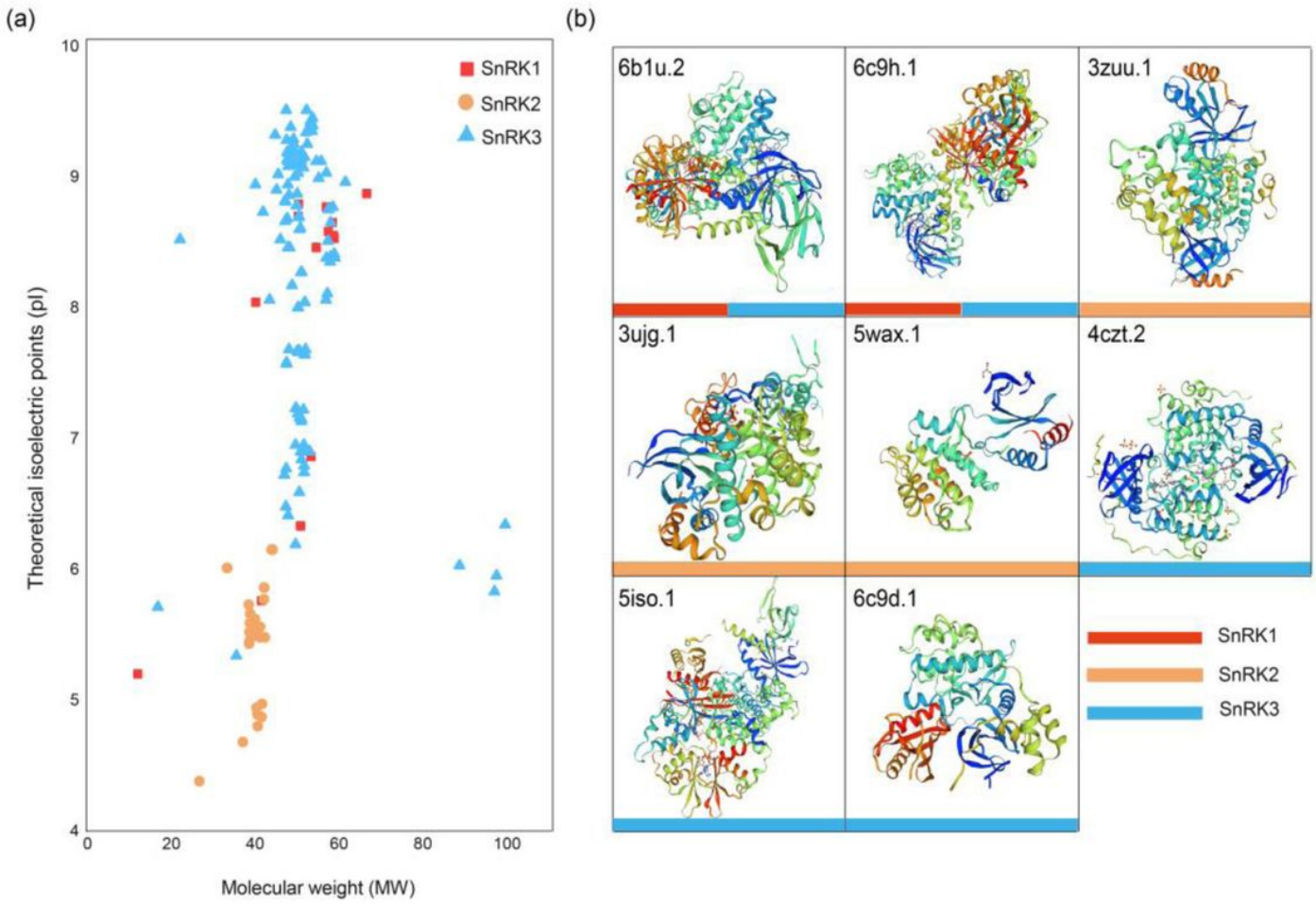

Figure 5

Distributions of MW and pI, and three-dimensional structure of TaSnRK proteins. (a): The distributions of MW and pI for the three subfamilies of wheat SnRKs. (b): Three-dimensional structure of TaSnRK proteins. The templates of 65 representative TaSnRK proteins are shown in Table S2.

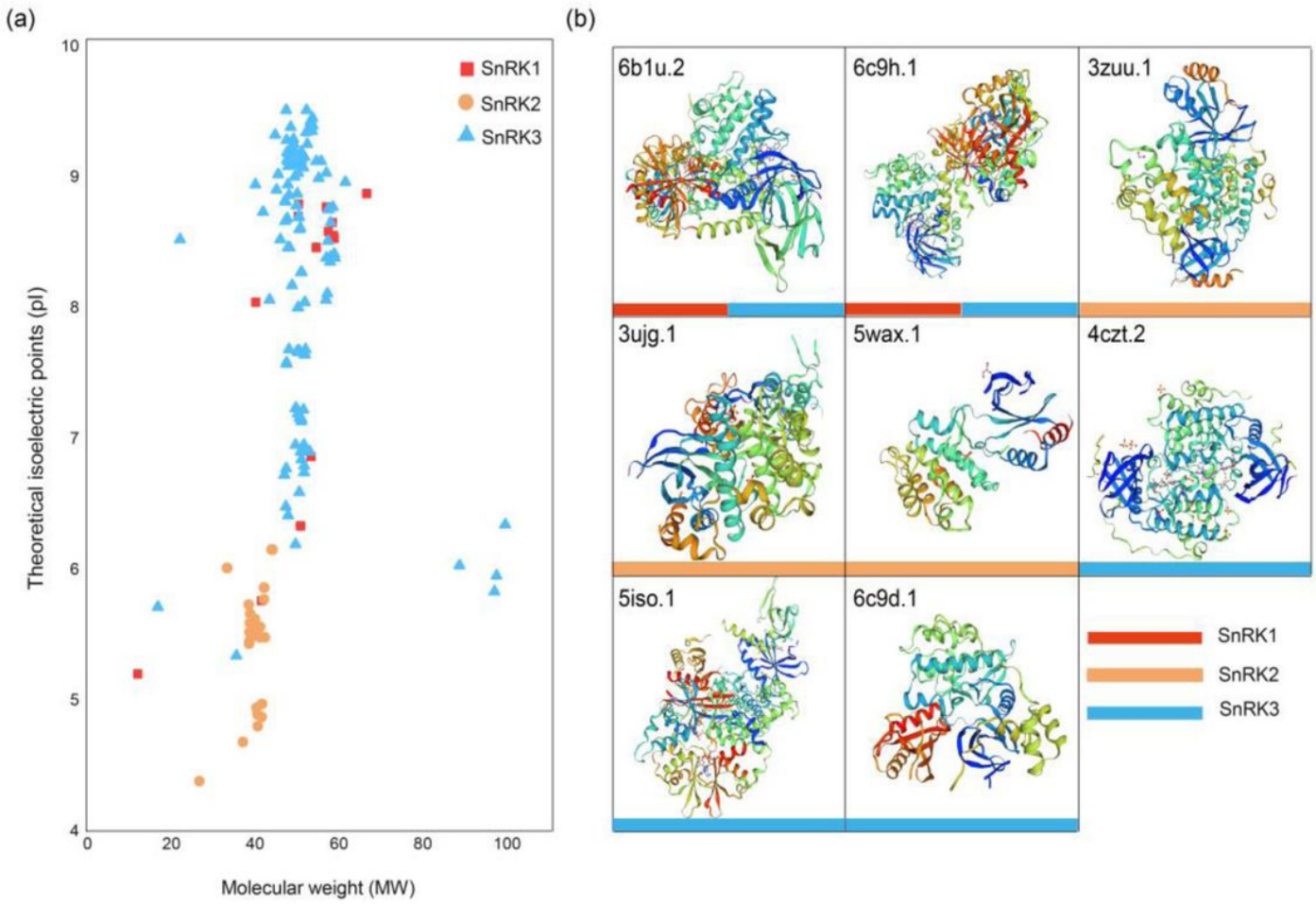

Figure 5

Distributions of MW and pI, and three-dimensional structure of TaSnRK proteins. (a): The distributions of MW and pI for the three subfamilies of wheat SnRKs. (b): Three-dimensional structure of TaSnRK proteins. The templates of 65 representative TaSnRK proteins are shown in Table S2.

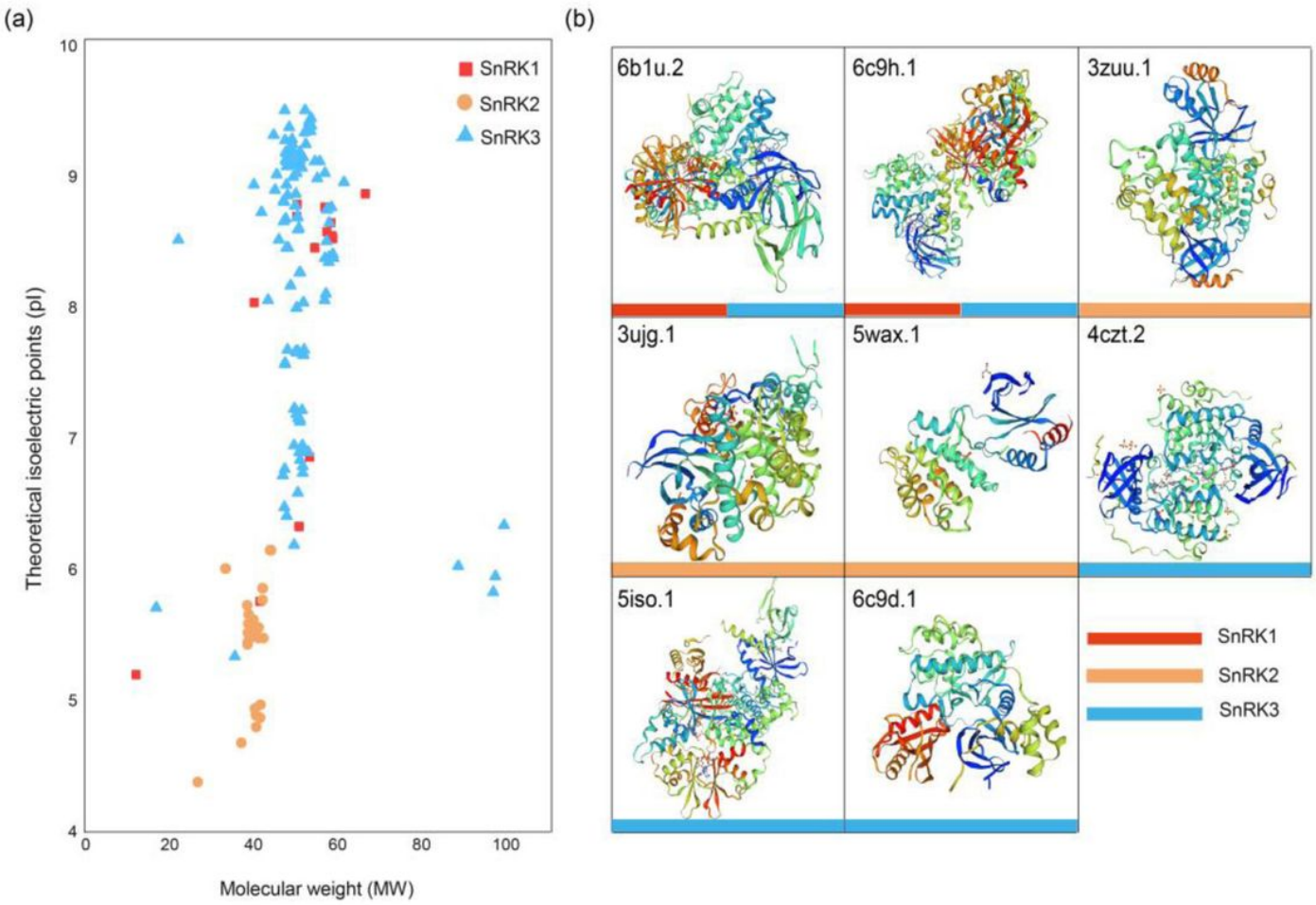

Figure 5

Distributions of MW and pI, and three-dimensional structure of TaSnRK proteins. (a): The distributions of MW and pI for the three subfamilies of wheat SnRKs. (b): Three-dimensional structure of TaSnRK proteins. The templates of 65 representative TaSnRK proteins are shown in Table S2.

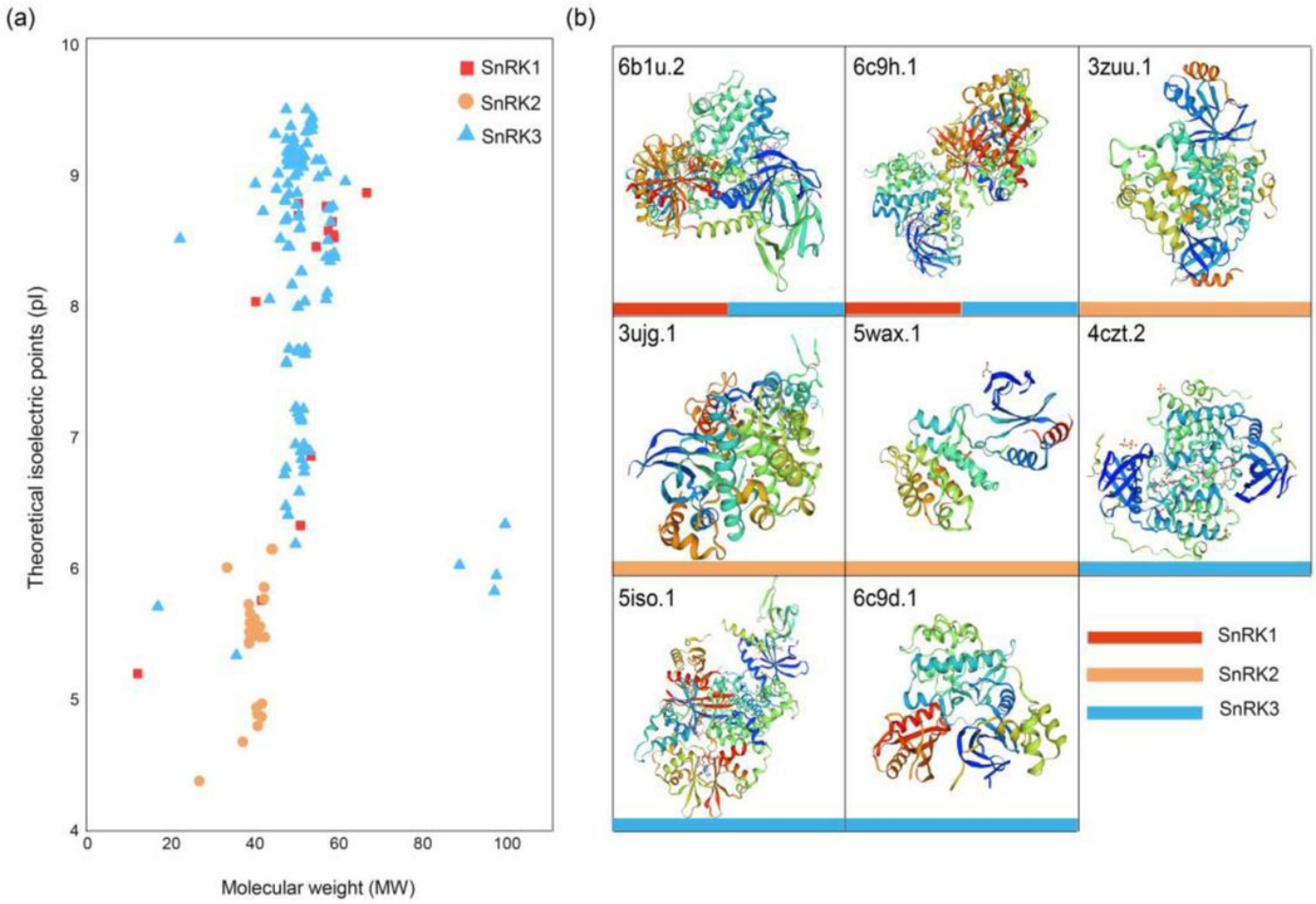

Figure 5

Distributions of MW and pI, and three-dimensional structure of TaSnRK proteins. (a): The distributions of MW and pI for the three subfamilies of wheat SnRKs. (b): Three-dimensional structure of TaSnRK proteins. The templates of 65 representative TaSnRK proteins are shown in Table S2.

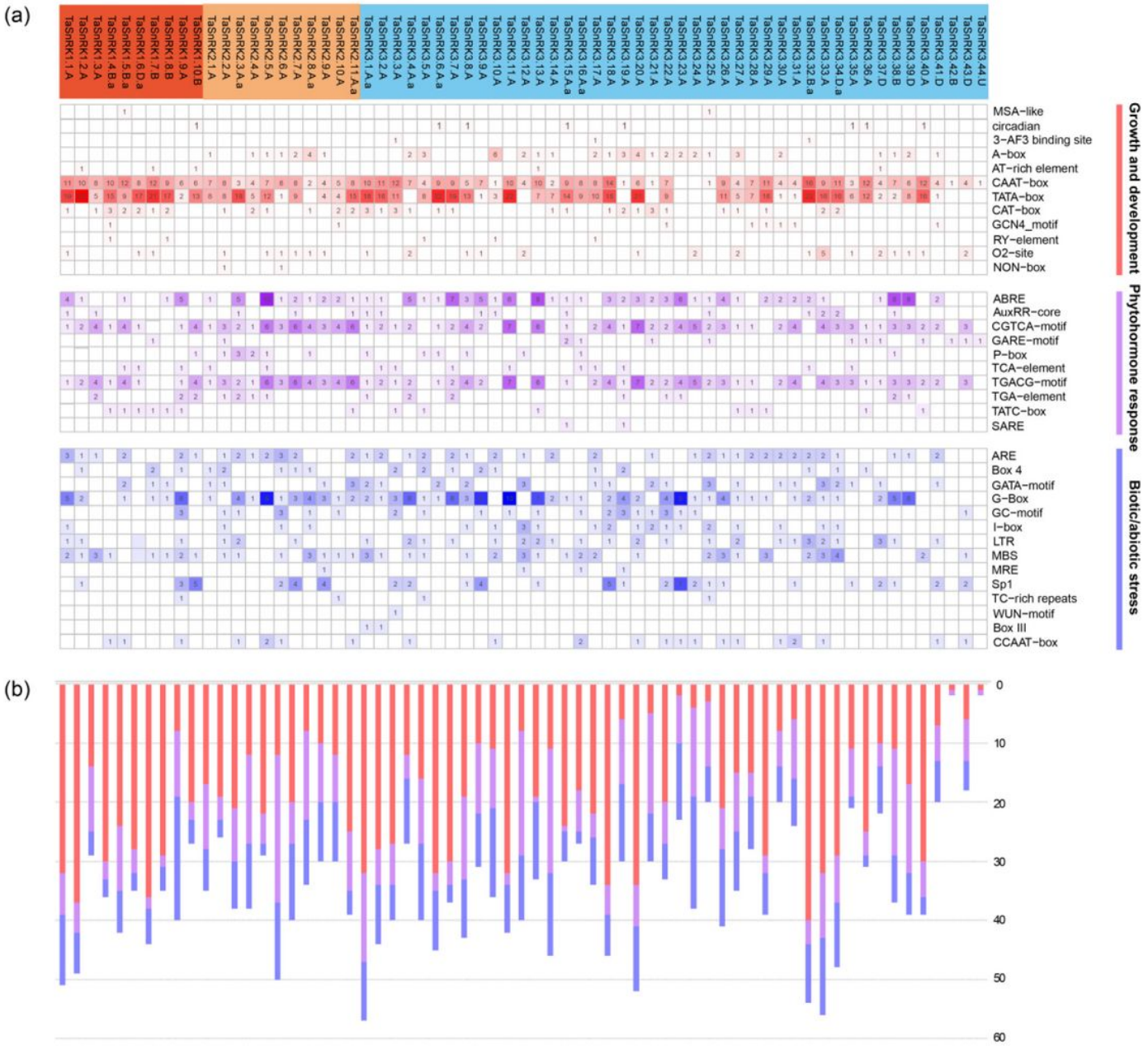

Figure 6

Distribution and summarizing of predicted cis-acting elements in the promoter of 65 representative TaSnRK genes. (a): Distribution of cis-acting elements involved in growth and development (red), phytohormone response (purple), and biotic/abiotic stresses(blue) in the promoter of the 65 TaSnRK genes. All elements in the promoter of 186 TaSnRK genes are shown in Figure S3 and Table S6. (b): Summarizing of promoter elements of three categories. Red, purple, and blue histograms indicates the sum of the cis-acting elements in three categories growth and development, phytohormone response, and biotic/abiotic stresses, respectively.

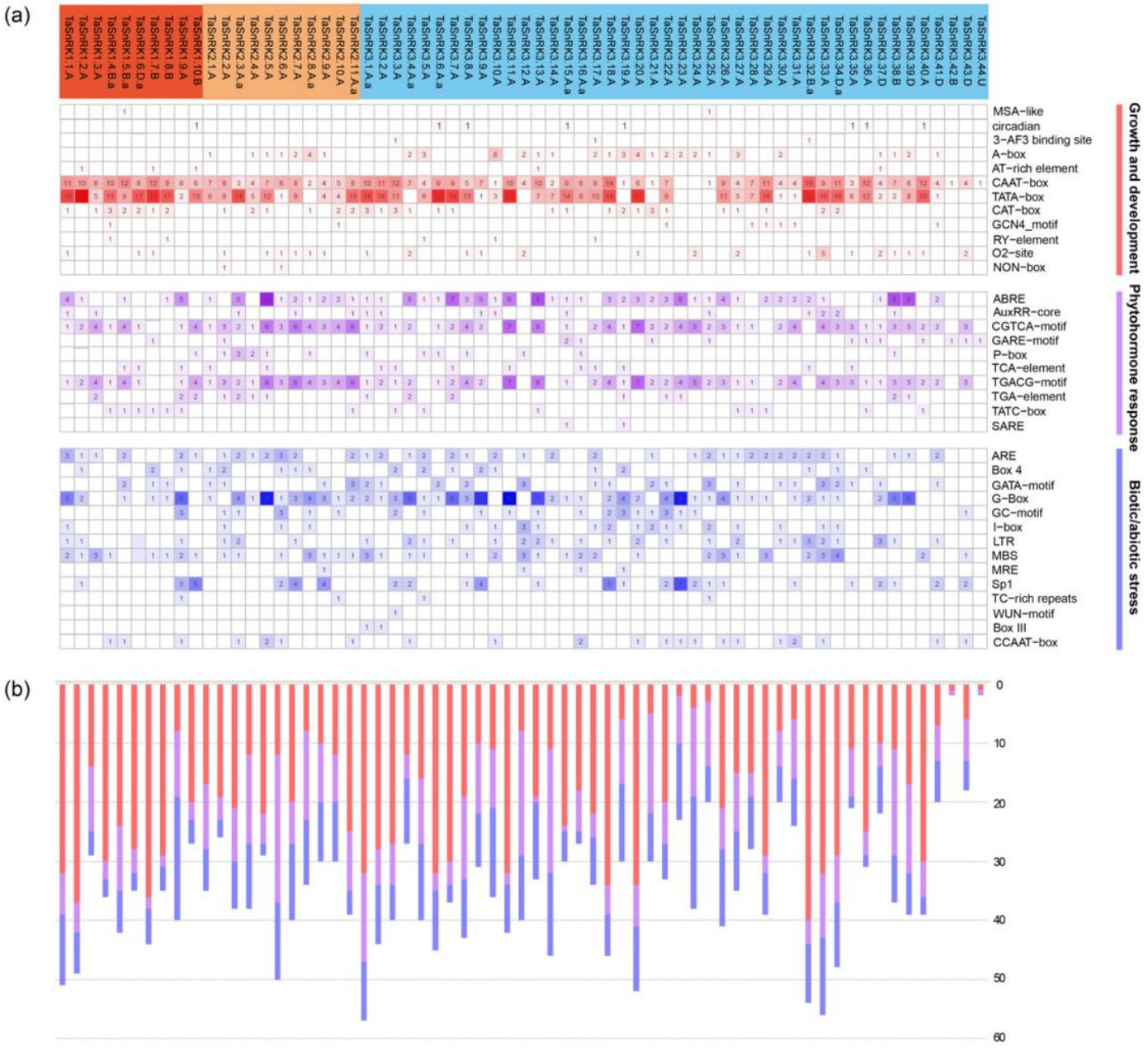

Figure 6

Distribution and summarizing of predicted cis-acting elements in the promoter of 65 representative TaSnRK genes. (a): Distribution of cis-acting elements involved in growth and development (red), phytohormone response (purple), and biotic/abiotic stresses(blue) in the promoter of the 65 TaSnRK genes. All elements in the promoter of 186 TaSnRK genes are shown in Figure S3 and Table S6. (b): Summarizing of promoter elements of three categories. Red, purple, and blue histograms indicates the sum of the cis-acting elements in three categories growth and development, phytohormone response, and biotic/abiotic stresses, respectively.

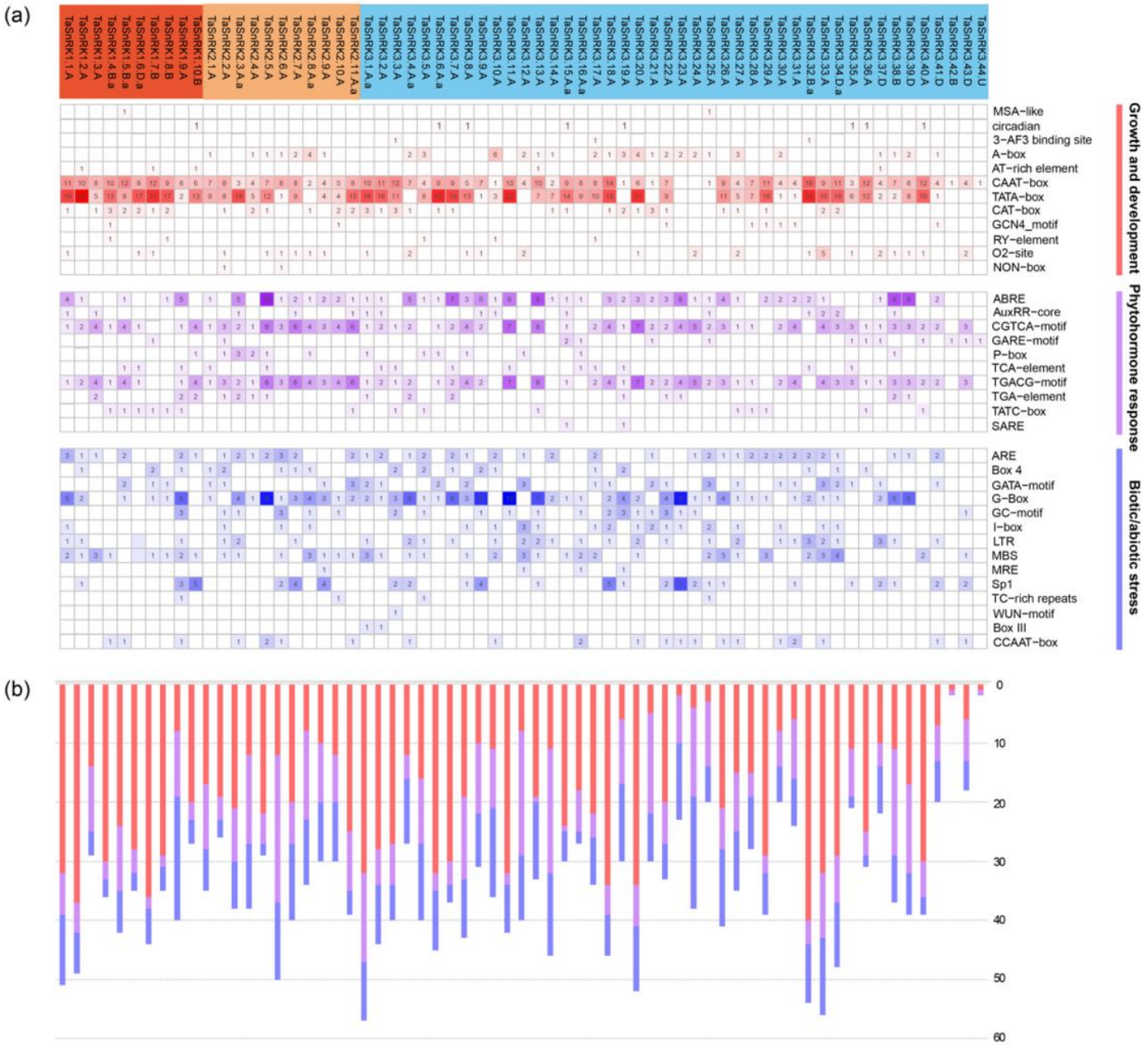

Figure 6

Distribution and summarizing of predicted cis-acting elements in the promoter of 65 representative TaSnRK genes. (a): Distribution of cis-acting elements involved in growth and development (red), phytohormone response (purple), and biotic/abiotic stresses(blue) in the promoter of the 65 TaSnRK genes. All elements in the promoter of 186 TaSnRK genes are shown in Figure S3 and Table S6. (b): Summarizing of promoter elements of three categories. Red, purple, and blue histograms indicates the sum of the cis-acting elements in three categories growth and development, phytohormone response, and biotic/abiotic stresses, respectively.

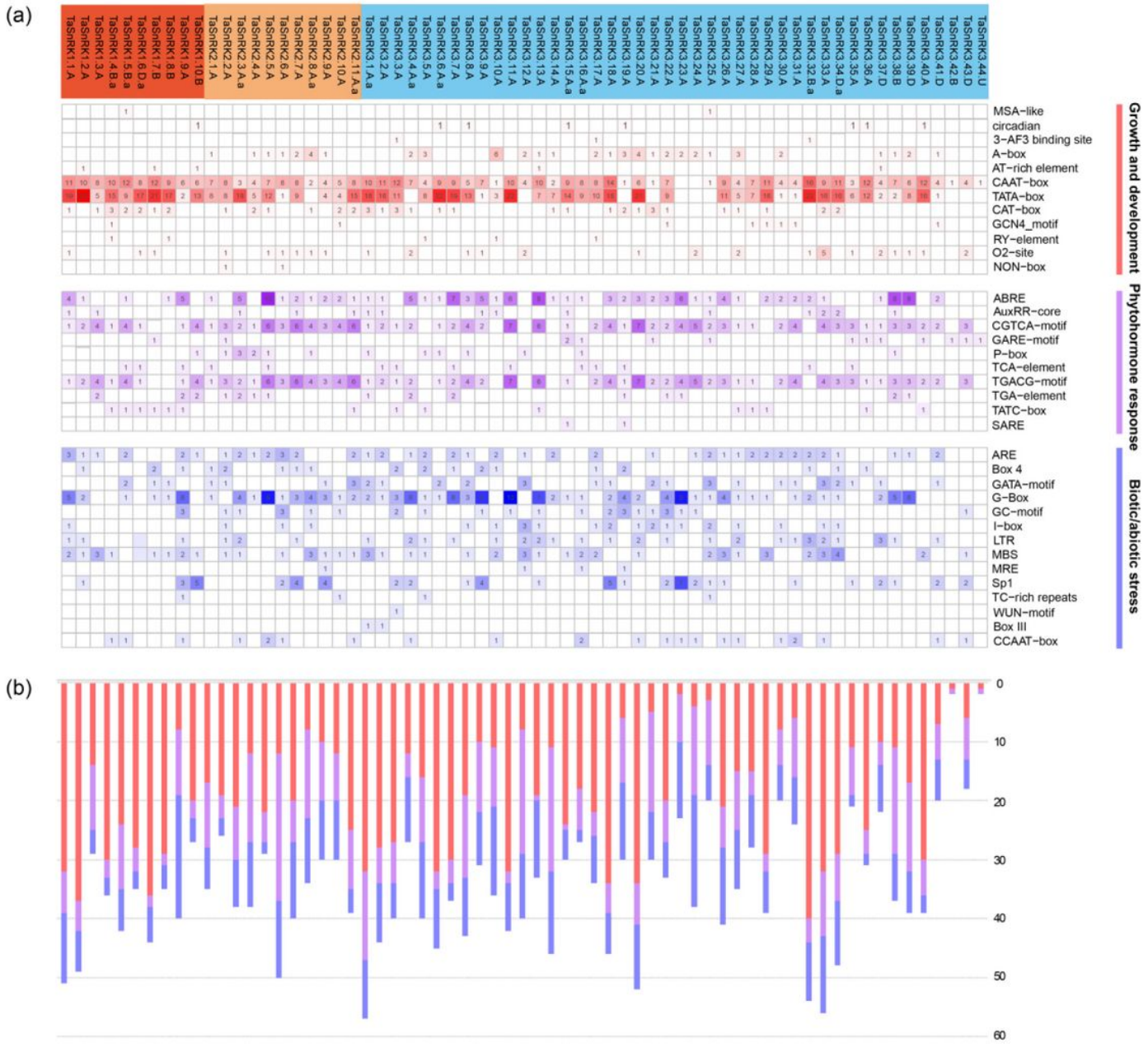

Figure 6

Distribution and summarizing of predicted cis-acting elements in the promoter of 65 representative TaSnRK genes. (a): Distribution of cis-acting elements involved in growth and development (red), phytohormone response (purple), and biotic/abiotic stresses(blue) in the promoter of the 65 TaSnRK genes. All elements in the promoter of 186 TaSnRK genes are shown in Figure S3 and Table S6. (b): Summarizing of promoter elements of three categories. Red, purple, and blue histograms indicates the sum of the cis-acting elements in three categories growth and development, phytohormone response, and biotic/abiotic stresses, respectively.

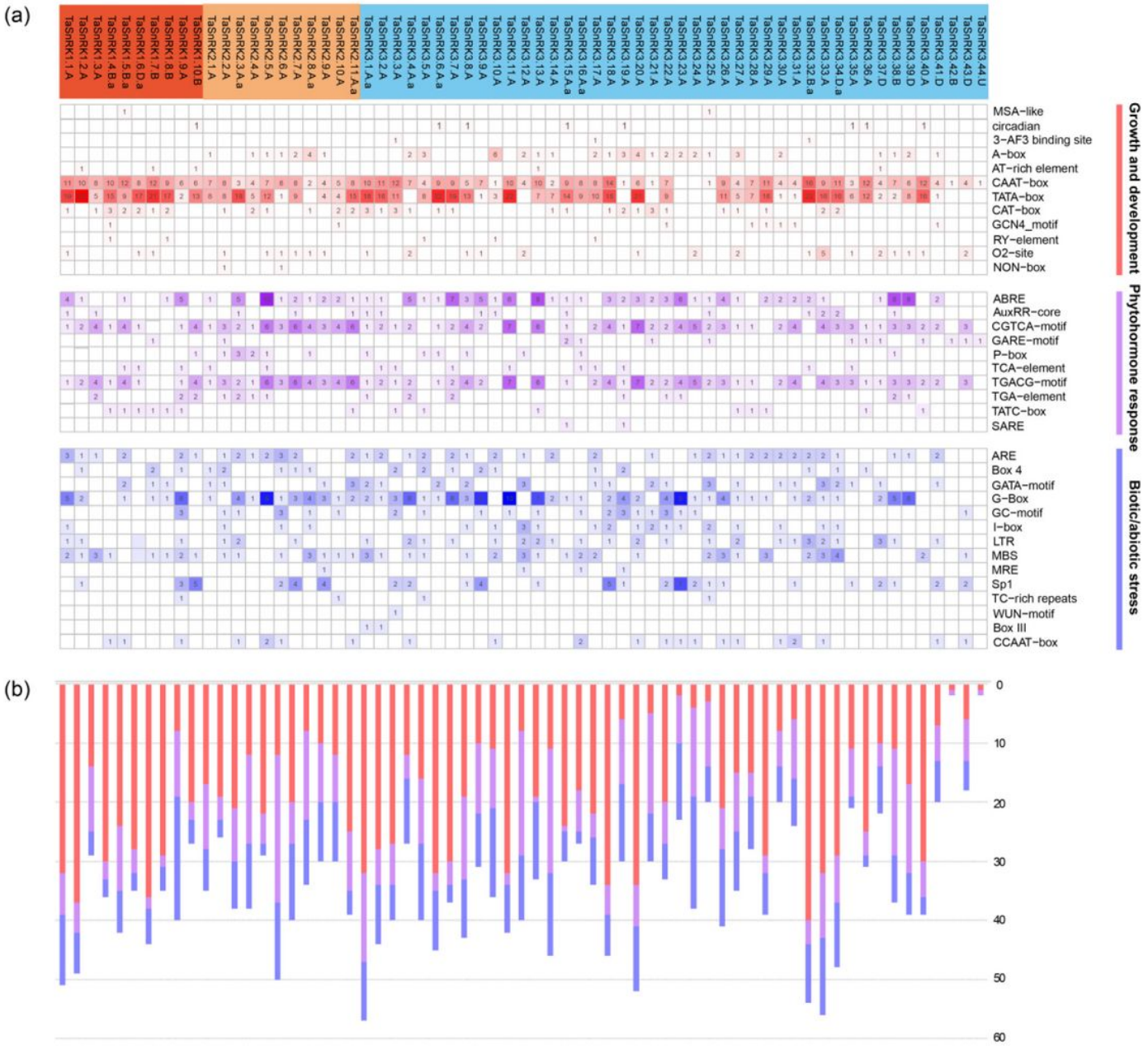

Figure 6

Distribution and summarizing of predicted cis-acting elements in the promoter of 65 representative TaSnRK genes. (a): Distribution of cis-acting elements involved in growth and development (red), phytohormone response (purple), and biotic/abiotic stresses(blue) in the promoter of the 65 TaSnRK genes. All elements in the promoter of 186 TaSnRK genes are shown in Figure S3 and Table S6. (b): Summarizing of promoter elements of three categories. Red, purple, and blue histograms indicates the sum of the cis-acting elements in three categories growth and development, phytohormone response, and biotic/abiotic stresses, respectively.

Figure 7

Transcriptome analyses of 186 TaSnRKs during wheat development (SRA number: PRJEB25639). (a): The expression level of 186 TaSnRK genes in three subfamilies (rows) and wheat developmental stages/tissues (columns) is shown as a heatmap. The gradual change of the color indicates different levels of gene fold change, detailed information is listed in Table S7-8. (b): Genes were clustered into 15 different types indicated by roman numbers according to their expression and mapped to three subfamilies. Larger circles indicate that more genes of this subfamily belong to this type (gene numbers for a particular circle size are

suggested). (c): A pheatmap shows mean expression values for the 15 different types. Colors in sectors indicate three subfamilies as part (a) and (b): SnRK1 (red), SnRK2 (orange), and SnRK3 (blue). The clustering heatmap with all genes and modules can be found in Table S9.

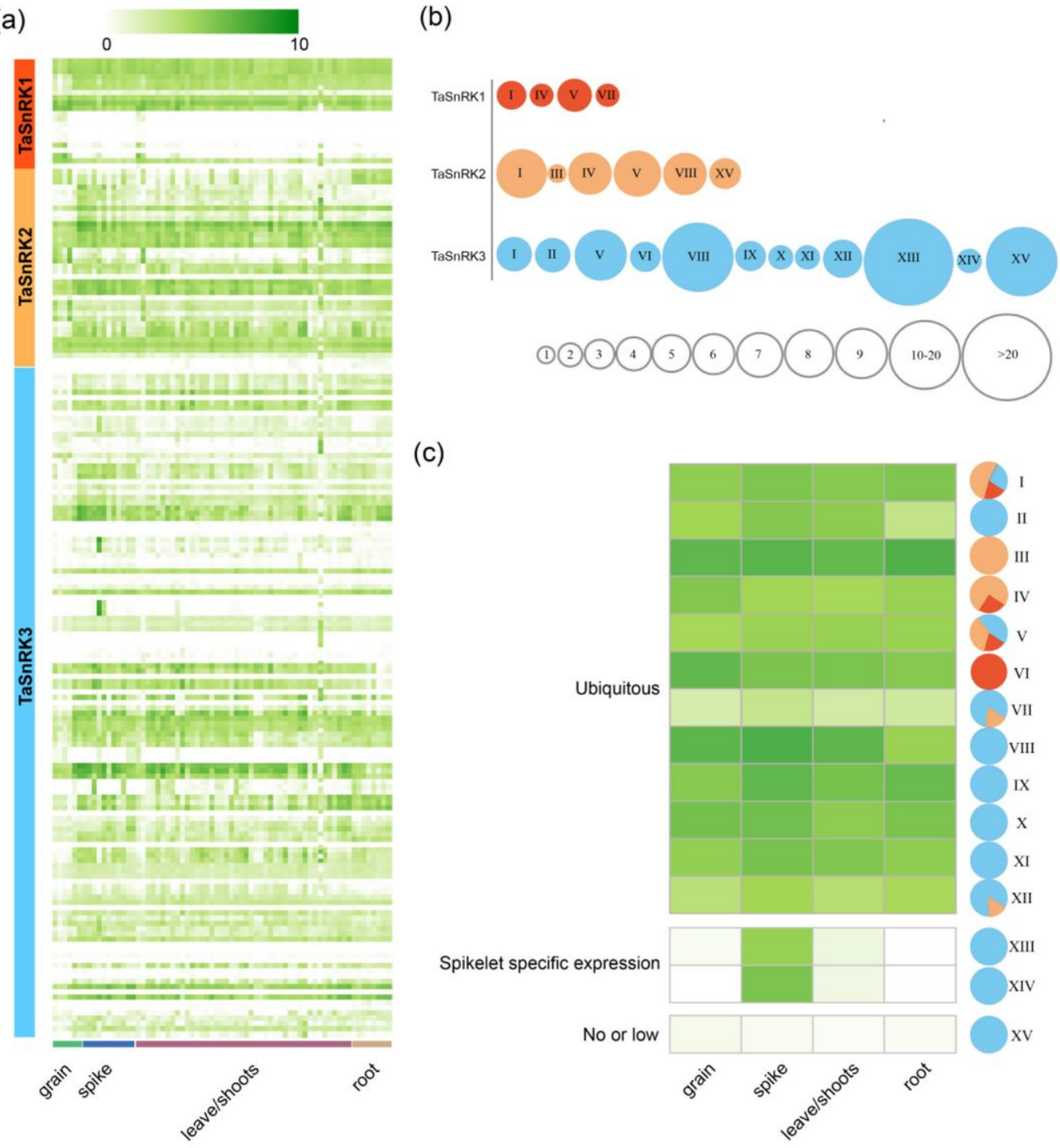

Figure 7

Transcriptome analyses of 186 TaSnRKs during wheat development (SRA number: PRJEB25639). (a): The expression level of 186 TaSnRK genes in three subfamilies (rows) and wheat developmental stages/tissues (columns) is shown as a heatmap. The gradual change of the color indicates different levels of gene fold

change, detailed information is listed in Table S7-8. (b): Genes were clustered into 15 different types indicated by roman numbers according to their expression and mapped to three subfamilies. Larger circles indicate that more genes of this subfamily belong to this type (gene numbers for a particular circle size are suggested). (c): A pheatmap shows mean expression values for the 15 different types. Colors in sectors indicate three subfamilies as part (a) and (b): SnRK1 (red), SnRK2 (orange), and SnRK3 (blue). The clustering heatmap with all genes and modules can be found in Table S9.

Figure 7

Transcriptome analyses of 186 TaSnRKs during wheat development (SRA number: PRJEB25639). (a): The expression level of 186 TaSnRK genes in three subfamilies (rows) and wheat developmental stages/tissues (columns) is shown as a heatmap. The gradual change of the color indicates different levels of gene fold change, detailed information is listed in Table S7-8. (b): Genes were clustered into 15 different types indicated by roman numbers according to their expression and mapped to three subfamilies. Larger circles indicate that more genes of this subfamily belong to this type (gene numbers for a particular circle size are suggested). (c): A pheatmap shows mean expression values for the 15 different types. Colors in sectors indicate three subfamilies as part (a) and (b): SnRK1 (red), SnRK2 (orange), and SnRK3 (blue). The clustering heatmap with all genes and modules can be found in Table S9.

Figure 7

Transcriptome analyses of 186 TaSnRKs during wheat development (SRA number: PRJEB25639). (a): The expression level of 186 TaSnRK genes in three subfamilies (rows) and wheat developmental stages/tissues (columns) is shown as a heatmap. The gradual change of the color indicates different levels of gene fold change, detailed information is listed in Table S7-8. (b): Genes were clustered into 15 different types indicated by roman numbers according to their expression and mapped to three subfamilies. Larger circles indicate that more genes of this subfamily belong to this type (gene numbers for a particular circle size are suggested). (c): A pheatmap shows mean expression values for the 15 different types. Colors in sectors indicate three subfamilies as part (a) and (b): SnRK1 (red), SnRK2 (orange), and SnRK3 (blue). The clustering heatmap with all genes and modules can be found in Table S9.

Figure 7

Transcriptome analyses of 186 TaSnRKs during wheat development (SRA number: PRJEB25639). (a): The expression level of 186 TaSnRK genes in three subfamilies (rows) and wheat developmental stages/tissues (columns) is shown as a heatmap. The gradual change of the color indicates different levels of gene fold change, detailed information is listed in Table S7-8. (b): Genes were clustered into 15 different types indicated by roman numbers according to their expression and mapped to three subfamilies. Larger circles indicate that more genes of this subfamily belong to this type (gene numbers for a particular circle size are

suggested). (c): A pheatmap shows mean expression values for the 15 different types. Colors in sectors indicate three subfamilies as part (a) and (b): SnRK1 (red), SnRK2 (orange), and SnRK3 (blue). The clustering heatmap with all genes and modules can be found in Table S9.

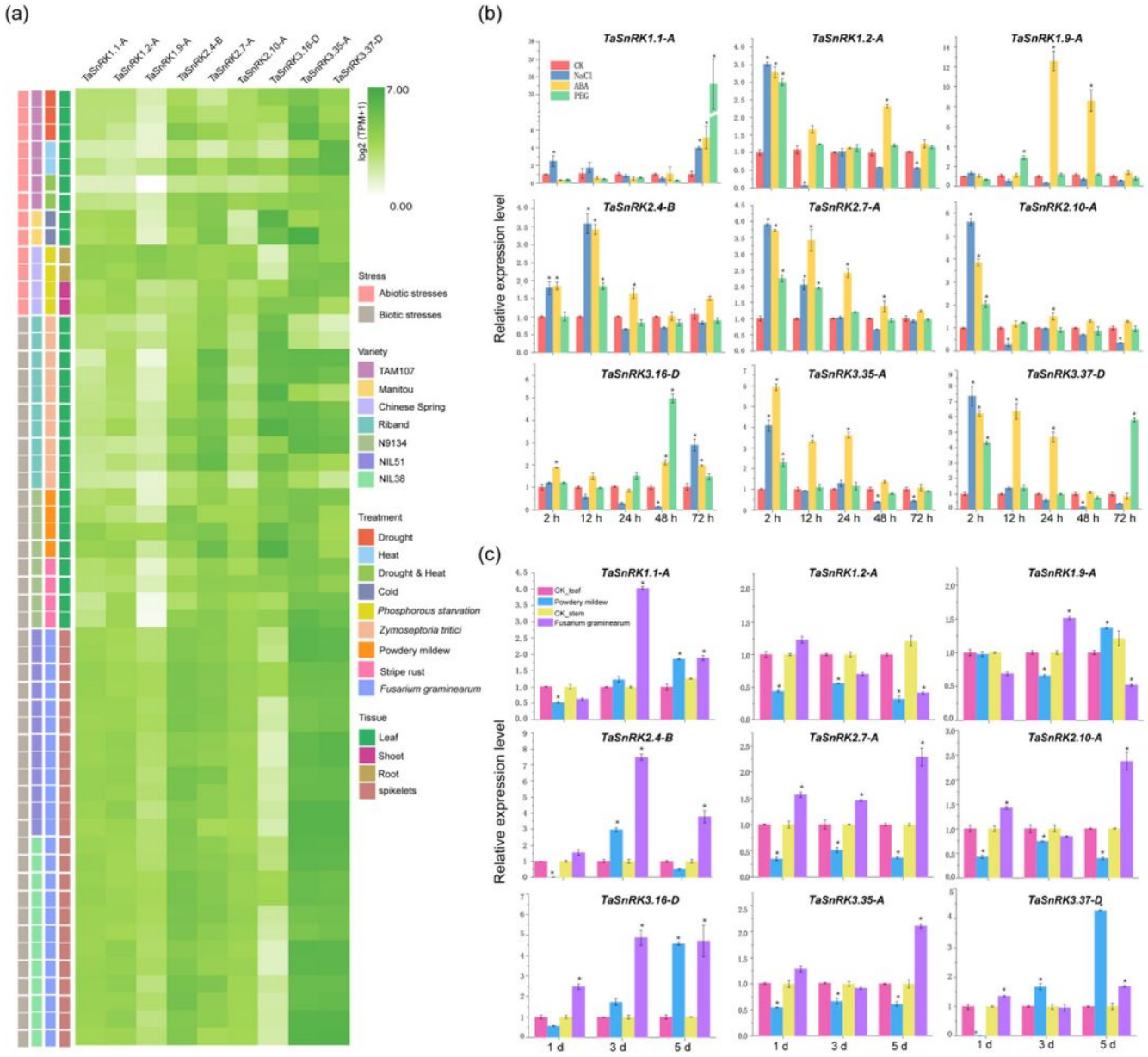

Figure 8

Expression patterns of nine selected TaSnRK genes under abiotic and biotic stresses. (a): Expression of the nine TaSnRK genes under multiple abiotic stresses involving PEG-6000 stress, cold stress, drought stress, heat stress, drought and heat combined stress, and phosphorous starvation (SRA numbers: PRJNA257938, PRJNA253535, PRJNA306536, and PRJDB2496), and biotic stress involving Zymoseptoria tritici, powdery mildew, stripe rust, and Fusarium graminearum (SRA numbers: PRJEB8798, PRJNA243835, and PRJEB12358). Detailed information is listed in Table S8 and S10. (b): Expression of the nine TaSnRK genes

under abiotic stresses including NaCl, ABA, and PEG. (c): Expression of the nine TaSnRK genes under powdery mildew and Fusarium graminearum. The relative expressions are shown in part (b), and (c) were determined by qRT-PCR with 2-△△ct method. Values are mean ± SD of three replications, and each replication included two technical replications. “*” indicates significant differences in comparison with the control at P < 0.05.

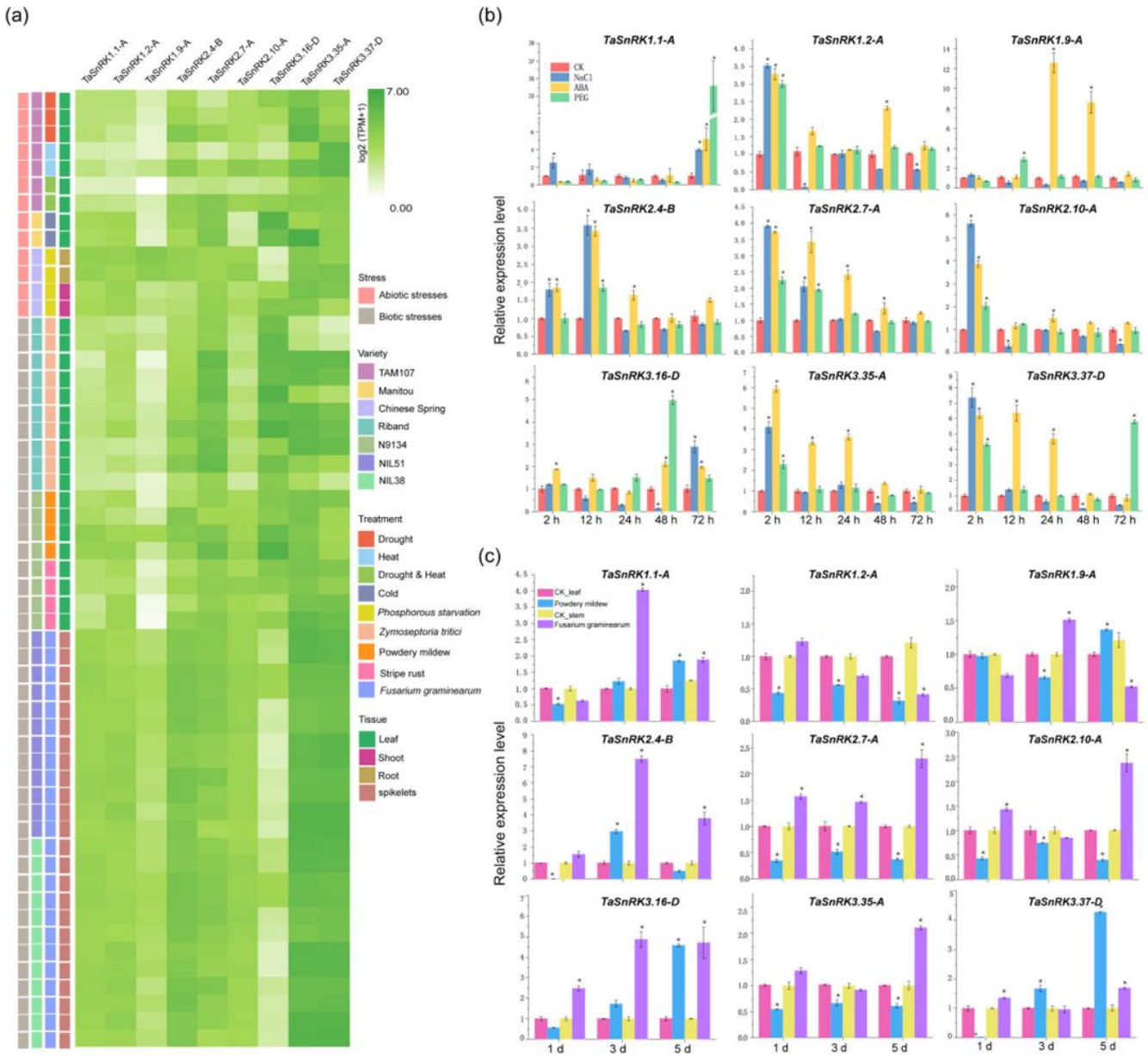

Figure 8

Expression patterns of nine selected TaSnRK genes under abiotic and biotic stresses. (a): Expression of the nine TaSnRK genes under multiple abiotic stresses involving PEG-6000 stress, cold stress, drought stress, heat stress, drought and heat combined stress, and phosphorous starvation (SRA numbers: PRJNA257938, PRJNA253535, PRJNA306536, and PRJDB2496), and biotic stress involving Zymoseptoria tritici, powdery

mildew, stripe rust, and Fusarium graminearum (SRA numbers: PRJEB8798, PRJNA243835, and PRJEB12358). Detailed information is listed in Table S8 and S10. (b): Expression of the nine TaSnRK genes under abiotic stresses including NaCl, ABA, and PEG. (c): Expression of the nine TaSnRK genes under powdery mildew and Fusarium graminearum. The relative expressions are shown in part (b), and (c) were determined by qRT-PCR with 2-△△ct method. Values are mean ± SD of three replications, and each replication included two technical replications. “*” indicates significant differences in comparison with the control at P < 0.05.

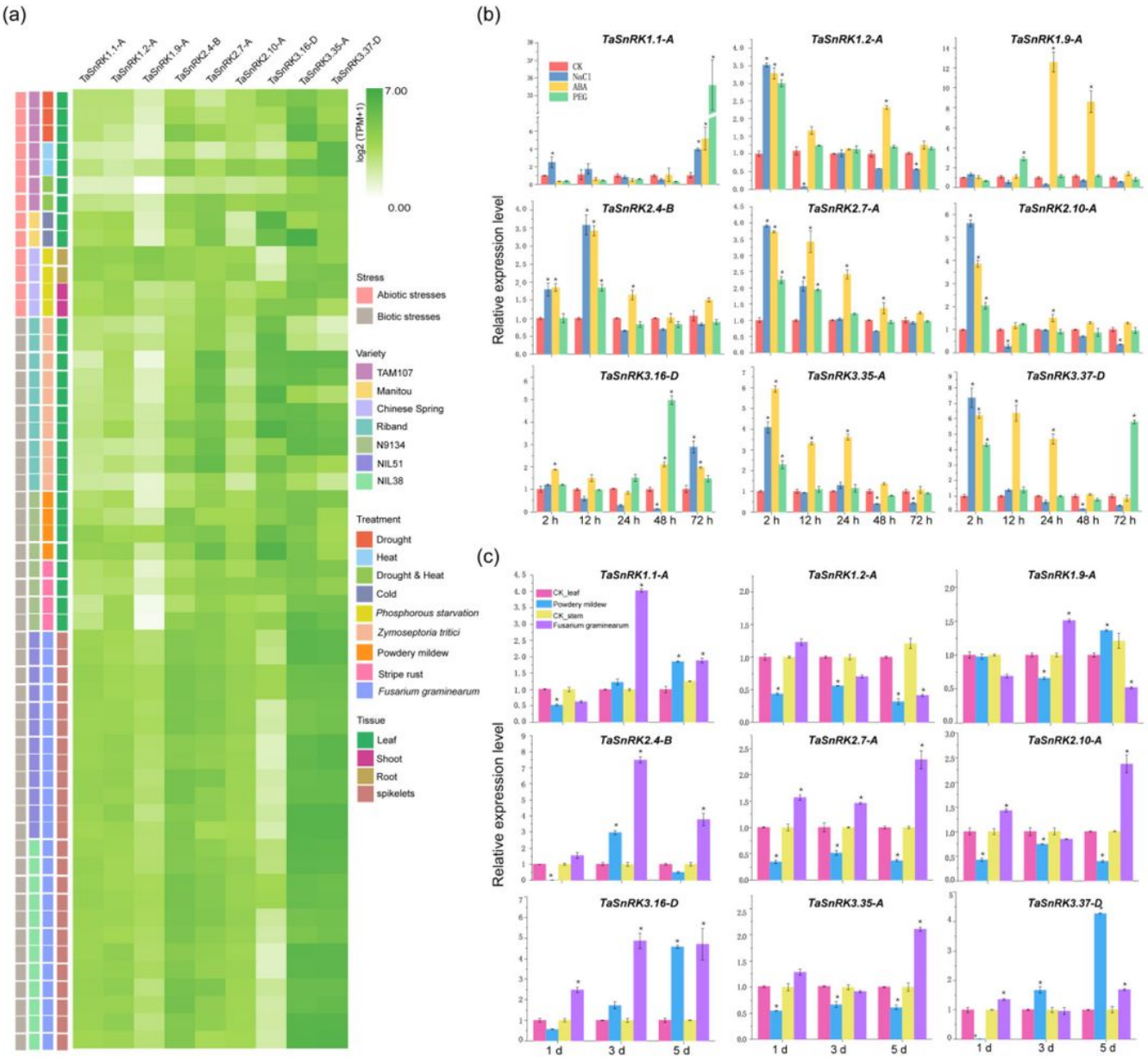

Figure 8

Expression patterns of nine selected TaSnRK genes under abiotic and biotic stresses. (a): Expression of the nine TaSnRK genes under multiple abiotic stresses involving PEG-6000 stress, cold stress, drought stress,

heat stress, drought and heat combined stress, and phosphorous starvation (SRA numbers: PRJNA257938, PRJNA253535, PRJNA306536, and PRJDB2496), and biotic stress involving Zymoseptoria tritici, powdery mildew, stripe rust, and Fusarium graminearum (SRA numbers: PRJEB8798, PRJNA243835, and PRJEB12358). Detailed information is listed in Table S8 and S10. (b): Expression of the nine TaSnRK genes under abiotic stresses including NaCl, ABA, and PEG. (c): Expression of the nine TaSnRK genes under powdery mildew and Fusarium graminearum. The relative expressions are shown in part (b), and (c) were determined by qRT-PCR with 2-△△ct method. Values are mean ± SD of three replications, and each replication included two technical replications. “*” indicates significant differences in comparison with the control at $P < 0.05$.

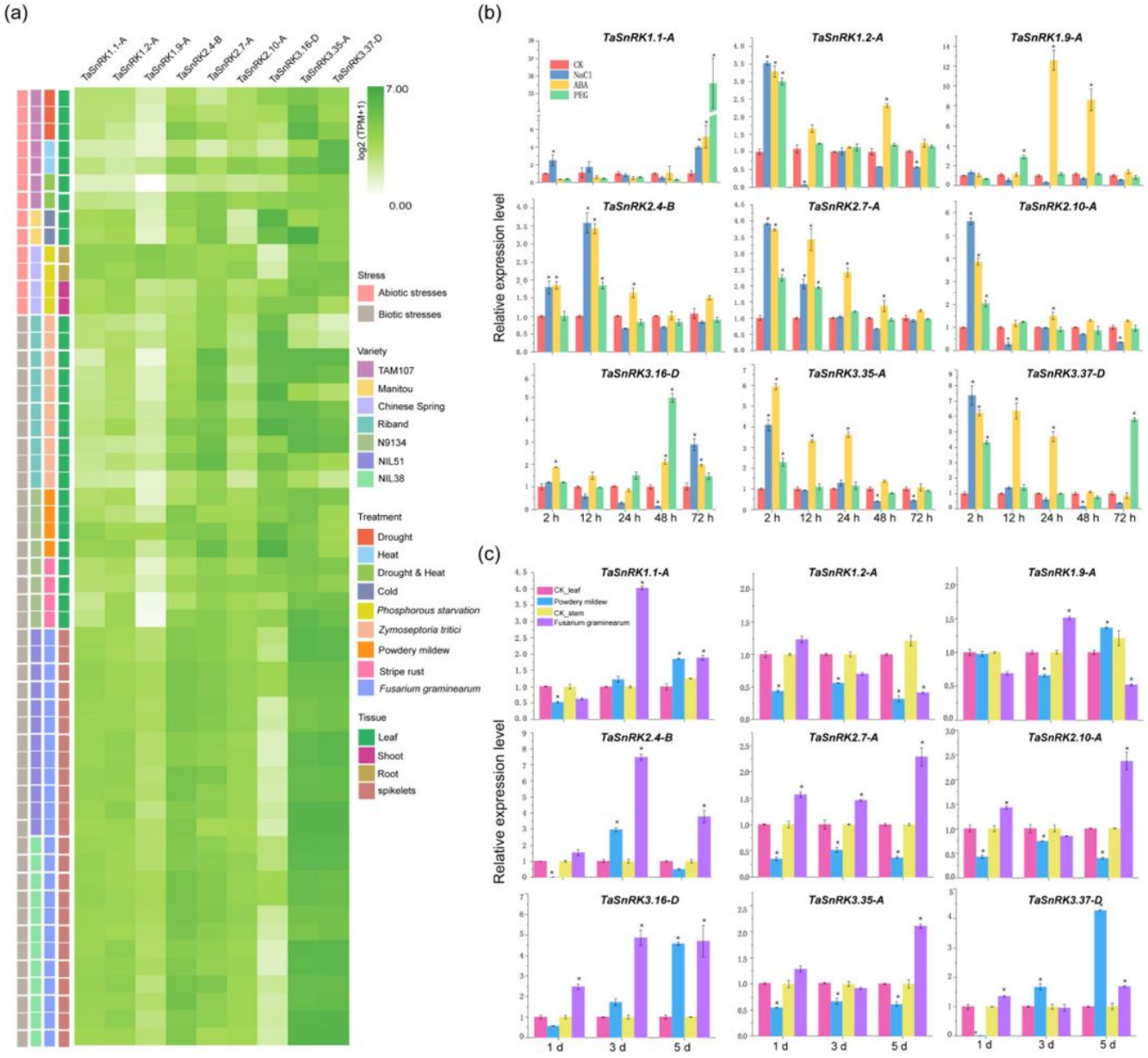

Figure 8

Expression patterns of nine selected TaSnRK genes under abiotic and biotic stresses. (a): Expression of the nine TaSnRK genes under multiple abiotic stresses involving PEG-6000 stress, cold stress, drought stress, heat stress, drought and heat combined stress, and phosphorous starvation (SRA numbers: PRJNA257938, PRJNA253535, PRJNA306536, and PRJDB2496), and biotic stress involving Zymoseptoria tritici, powdery mildew, stripe rust, and Fusarium graminearum (SRA numbers: PRJEB8798, PRJNA243835, and PRJEB12358). Detailed information is listed in Table S8 and S10. (b): Expression of the nine TaSnRK genes under abiotic stresses including NaCl, ABA, and PEG. (c): Expression of the nine TaSnRK genes under powdery mildew and Fusarium graminearum. The relative expressions are shown in part (b), and (c) were determined by qRT-PCR with 2-△△ct method. Values are mean ± SD of three replications, and each replication included two technical replications. “*” indicates significant differences in comparison with the control at P < 0.05.

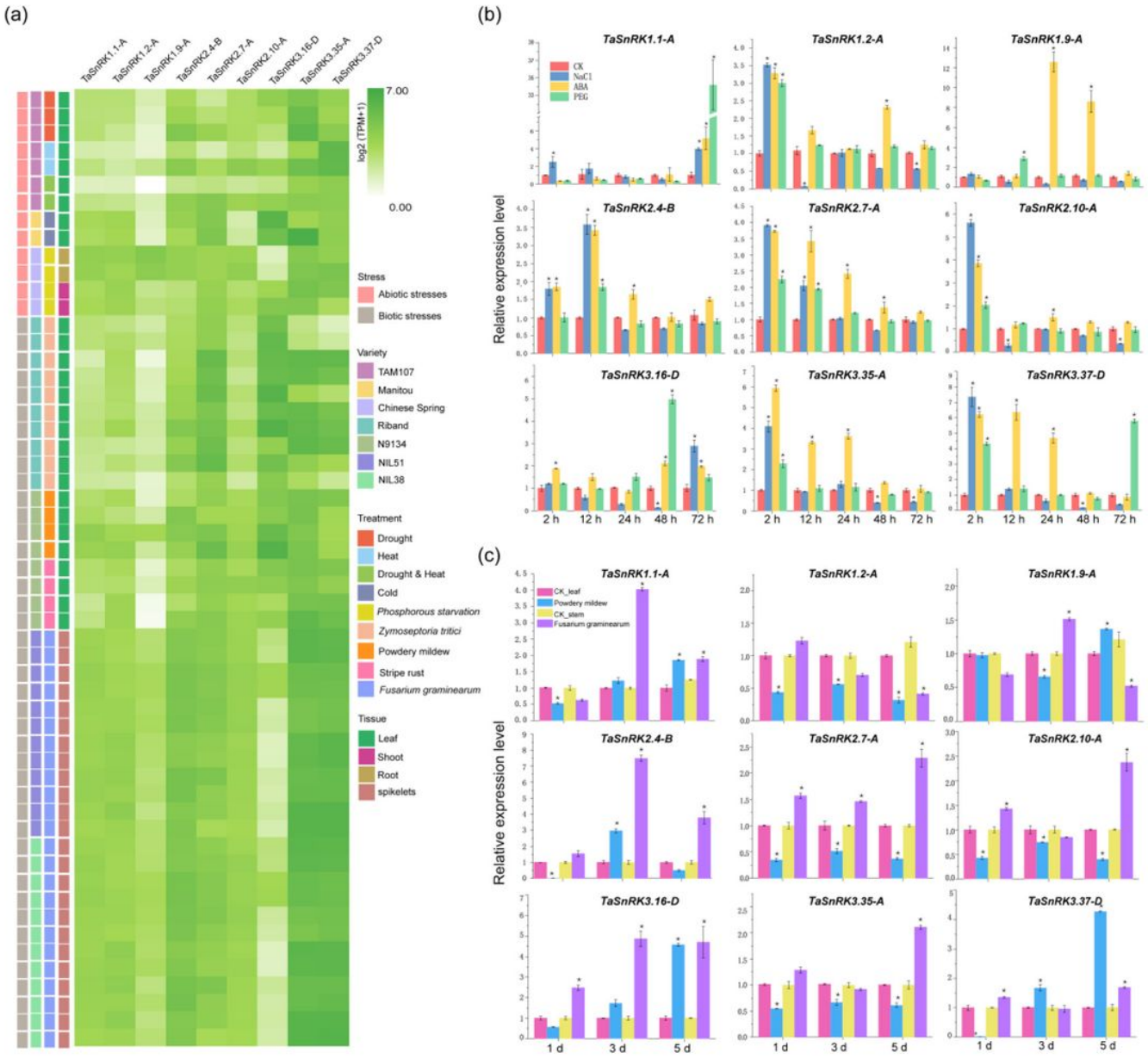

Figure 8

Expression patterns of nine selected TaSnRK genes under abiotic and biotic stresses. (a): Expression of the nine TaSnRK genes under multiple abiotic stresses involving PEG-6000 stress, cold stress, drought stress, heat stress, drought and heat combined stress, and phosphorous starvation (SRA numbers: PRJNA257938, PRJNA253535, PRJNA306536, and PRJDB2496), and biotic stress involving Zymoseptoria tritici, powdery mildew, stripe rust, and Fusarium graminearum (SRA numbers: PRJEB8798, PRJNA243835, and PRJEB12358). Detailed information is listed in Table S8 and S10. (b): Expression of the nine TaSnRK genes under abiotic stresses including NaCl, ABA, and PEG. (c): Expression of the nine TaSnRK genes under powdery mildew and Fusarium graminearum. The relative expressions are shown in part (b), and (c) were determined by qRT-PCR with 2-△△ct method. Values are mean ± SD of three replications, and each replication included two technical replications. “*” indicates significant differences in comparison with the control at P < 0.05.

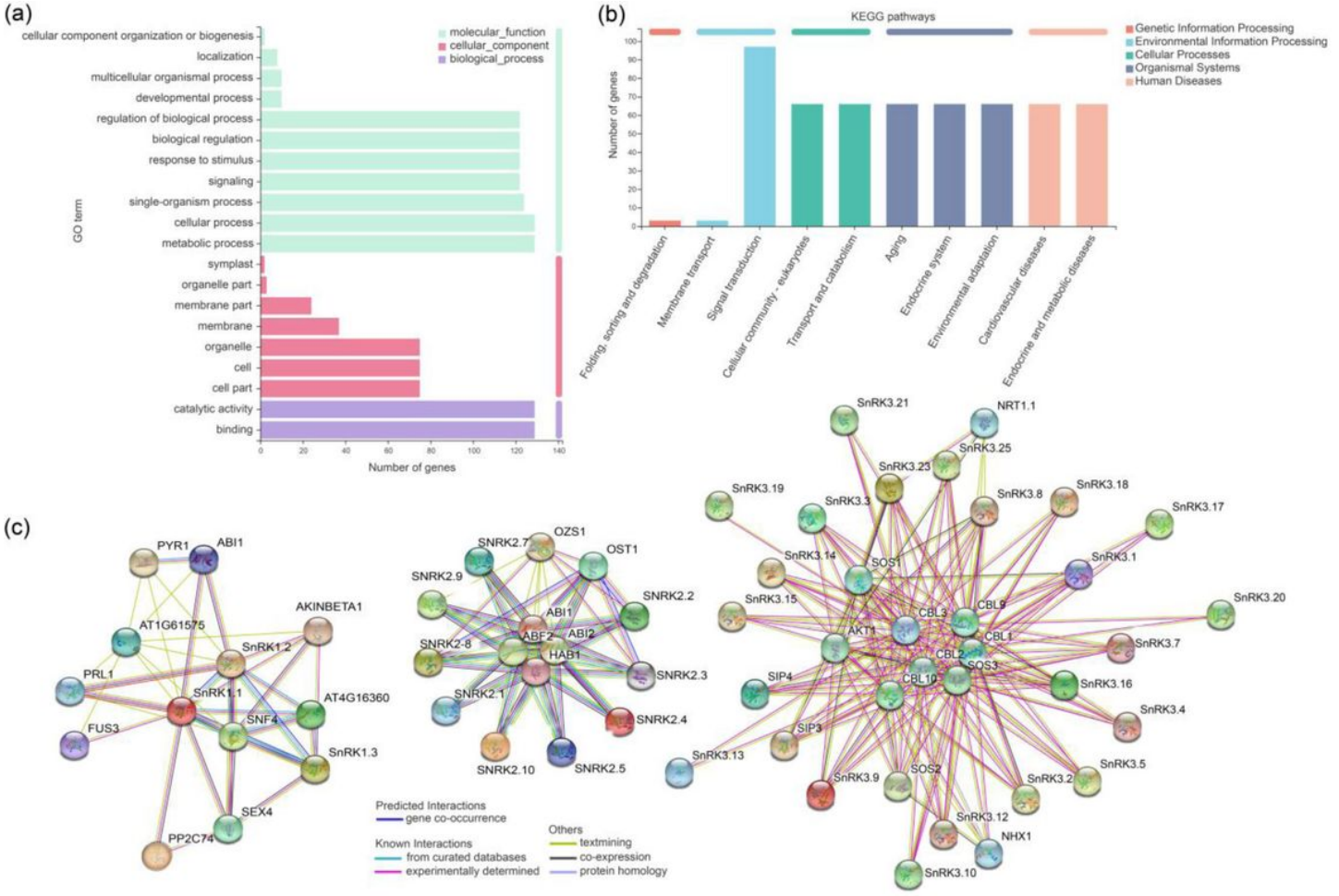

Figure 9

Functional annotation analysis of TaSnRK genes. (a): GO classification based on 149 TaSnRK genes annotation. GO terms were summarized in three main categories, including molecular function (gree), cellular components (red), and biological processes (purple). (b): KEGG pathway classification based on 149 TaSnRKs annotation. KEGG terms were summarized in five main categories, pink for genetic information processing, azure for environmental information processing, green for cellular processes, light gray for

organismal systems, and light orange for human diseases. (c): Interaction network of AtSnRK proteins and related proteins. From left to right are subfamilies SnRK1, SnRK2, SnRK3. The line's colors indicated the relationship of the interaction between the two proteins, of which sky blue and rose red indicated known interactions from curated databases and experimentally determined respectively. The blue line indicated predicted interactions from gene co-occurrence. Other interactions, like textmining, co-expression, and protein homology, indicated by peak green, black, and bluish violet line, respectively.

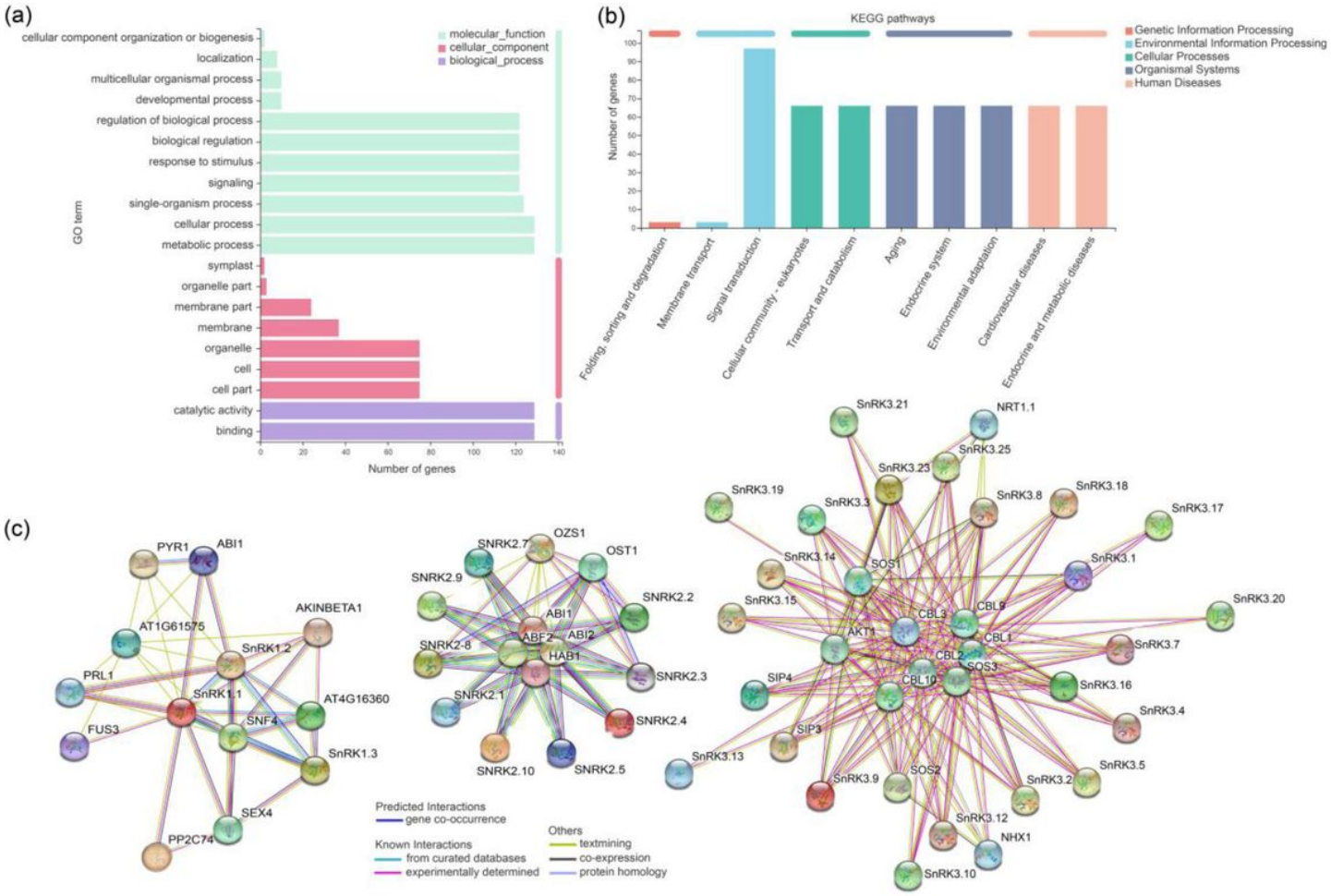

Figure 9

Functional annotation analysis of TaSnRK genes. (a): GO classification based on 149 TaSnRK genes annotation. GO terms were summarized in three main categories, including molecular function (gree), cellular components (red), and biological processes (purple). (b): KEGG pathway classification based on 149 TaSnRKs annotation. KEGG terms were summarized in five main categories, pink for genetic information processing, azure for environmental information processing, green for cellular processes, light gray for organismal systems, and light orange for human diseases. (c): Interaction network of AtSnRK proteins and related proteins. From left to right are subfamilies SnRK1, SnRK2, SnRK3. The line's colors indicated the relationship of the interaction between the two proteins, of which sky blue and rose red indicated known interactions from curated databases and experimentally determined respectively. The blue line indicated predicted interactions from gene co-occurrence. Other interactions, like textmining, co-expression, and protein homology, indicated by peak green, black, and bluish violet line, respectively.

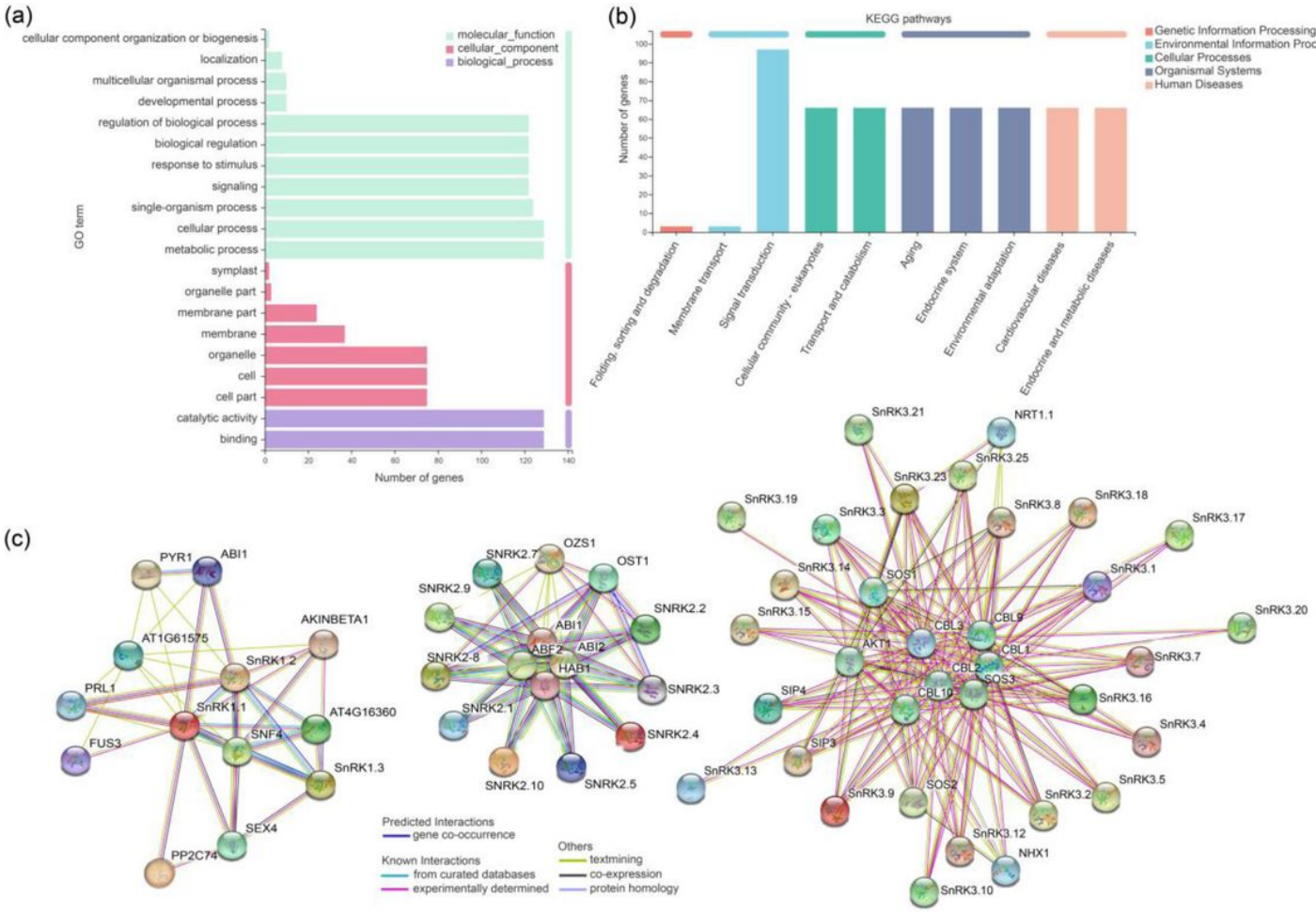

Figure 9

Functional annotation analysis of TaSnRK genes. (a): GO classification based on 149 TaSnRK genes annotation. GO terms were summarized in three main categories, including molecular function (gree), cellular components (red), and biological processes (purple). (b): KEGG pathway classification based on 149 TaSnRKs annotation. KEGG terms were summarized in five main categories, pink for genetic information processing, azure for environmental information processing, green for cellular processes, light gray for organismal systems, and light orange for human diseases. (c): Interaction network of AtSnRK proteins and related proteins. From left to right are subfamilies SnRK1, SnRK2, SnRK3. The line's colors indicated the relationship of the interaction between the two proteins, of which sky blue and rose red indicated known interactions from curated databases and experimentally determined respectively. The blue line indicated predicted interactions from gene co-occurrence. Other interactions, like textmining, co-expression, and protein homology, indicated by peak green, black, and bluish violet line, respectively.

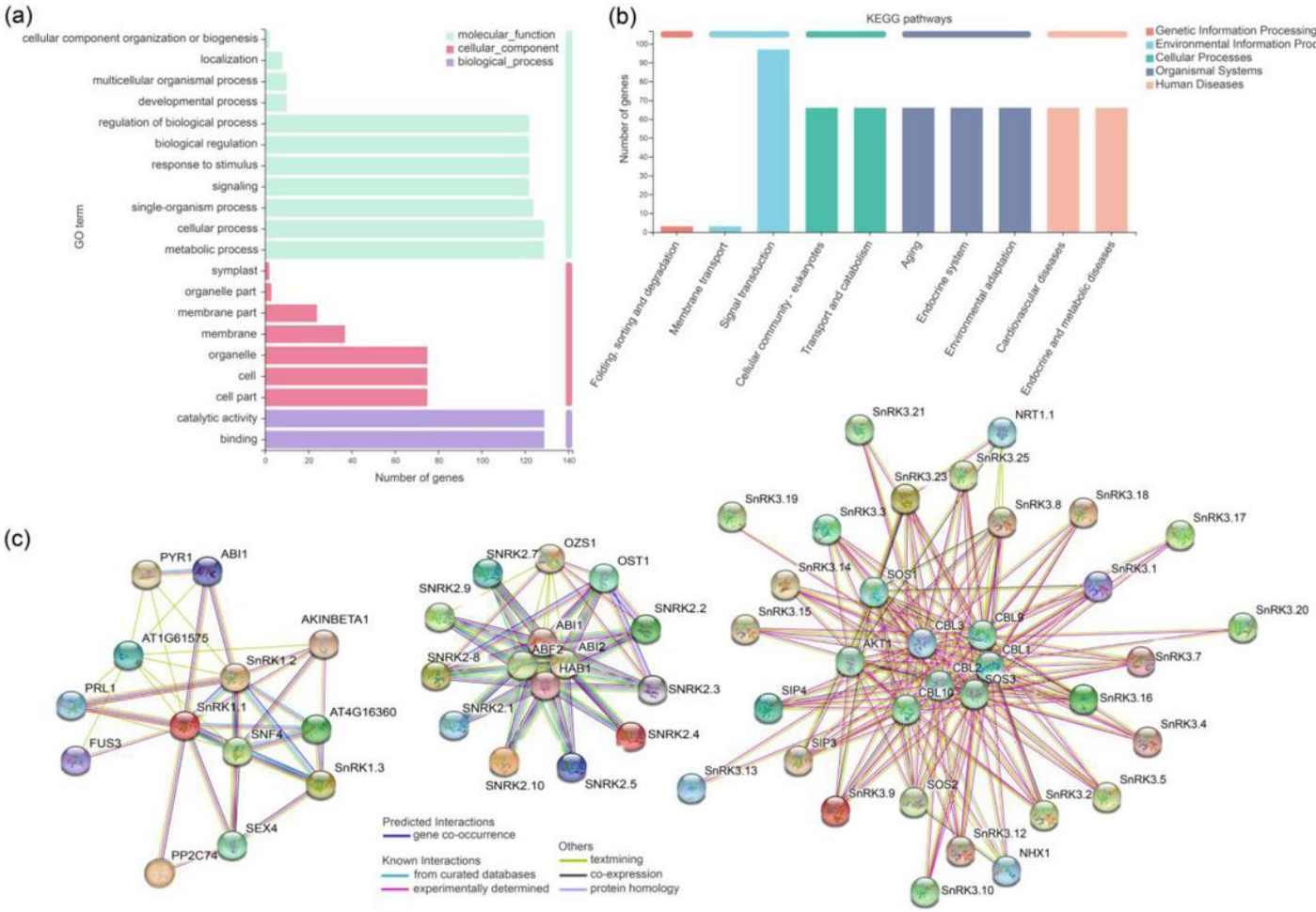

Figure 9

Functional annotation analysis of TaSnRK genes. (a): GO classification based on 149 TaSnRK genes annotation. GO terms were summarized in three main categories, including molecular function (gree), cellular components (red), and biological processes (purple). (b): KEGG pathway classification based on 149 TaSnRKs annotation. KEGG terms were summarized in five main categories, pink for genetic information processing, azure for environmental information processing, green for cellular processes, light gray for organismal systems, and light orange for human diseases. (c): Interaction network of AtSnRK proteins and related proteins. From left to right are subfamilies SnRK1, SnRK2, SnRK3. The line's colors indicated the relationship of the interaction between the two proteins, of which sky blue and rose red indicated known interactions from curated databases and experimentally determined respectively. The blue line indicated predicted interactions from gene co-occurrence. Other interactions, like textmining, co-expression, and protein homology, indicated by peak green, black, and bluish violet line, respectively.

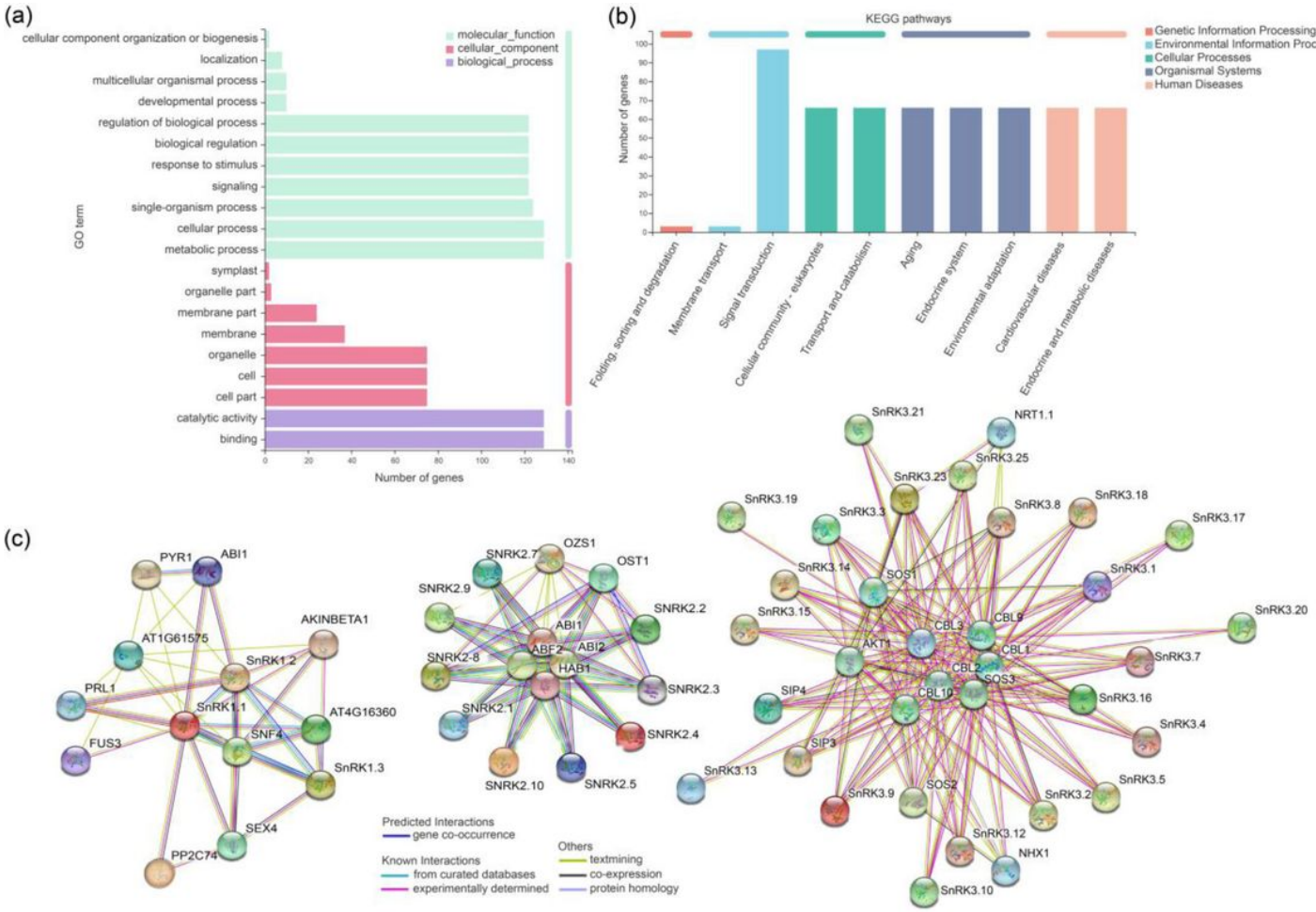

Figure 9

Functional annotation analysis of TaSnRK genes. (a): GO classification based on 149 TaSnRK genes annotation. GO terms were summarized in three main categories, including molecular function (gree), cellular components (red), and biological processes (purple). (b): KEGG pathway classification based on 149 TaSnRKs annotation. KEGG terms were summarized in five main categories, pink for genetic information processing, azure for environmental information processing, green for cellular processes, light gray for organismal systems, and light orange for human diseases. (c): Interaction network of AtSnRK proteins and related proteins. From left to right are subfamilies SnRK1, SnRK2, SnRK3. The line's colors indicated the relationship of the interaction between the two proteins, of which sky blue and rose red indicated known interactions from curated databases and experimentally determined respectively. The blue line indicated predicted interactions from gene co-occurrence. Other interactions, like textmining, co-expression, and protein homology, indicated by peak green, black, and bluish violet line, respectively.

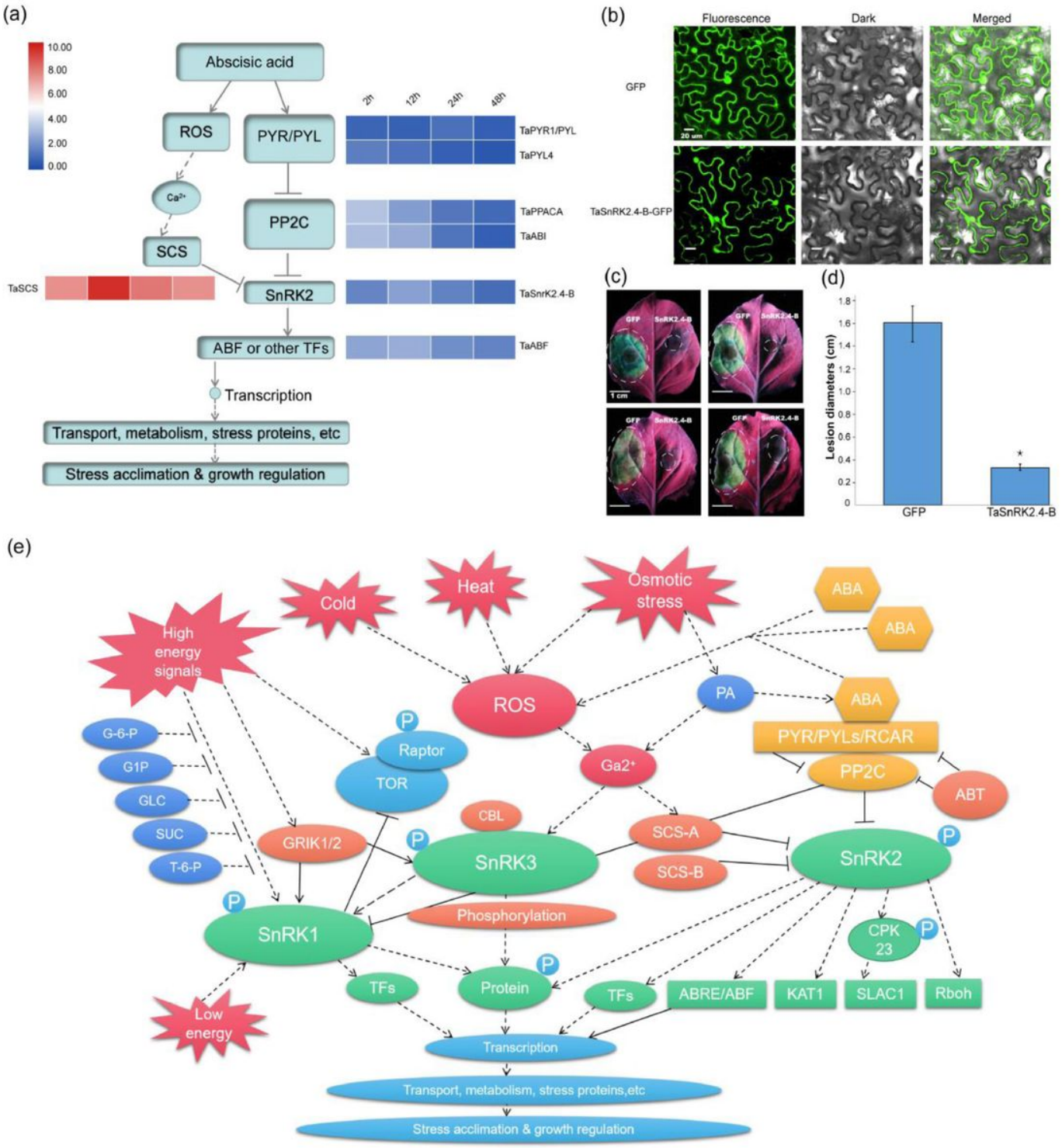

Figure 10

Functional verification of gene TaSnRK2.4-B. (a): Expression level detected by qRT-PCR of wheat genes involving ABA pathway. (b): TaSnRK2.4-B was constructed into plasmid with fusions of GFP. Panels from left to right refer to Fluorescence, Dark, and Merged images, respectively. Scale bars = 20 μm. (c): Photograph under ultraviolet lights. The white circles showed the infected areas of P. infestans, and “GFP” referred to the free GFP. (d): Lesion diameter of control (GFP) and TaSnRK2.4-B. The “*” on the bar indicated significant differences determined using Duncan’s test ($P < 0.05$). (e): The Role model of SnRK2 in plant response to

osmotic stress have previously been reported in plant species [1,4,6-7,10-11,24-25,42,46-47,54,60]. Connections represent positive (arrow) and negative (block) regulation. Black solid indicates direct regulation/interaction and dashed line indicates indirect regulation.

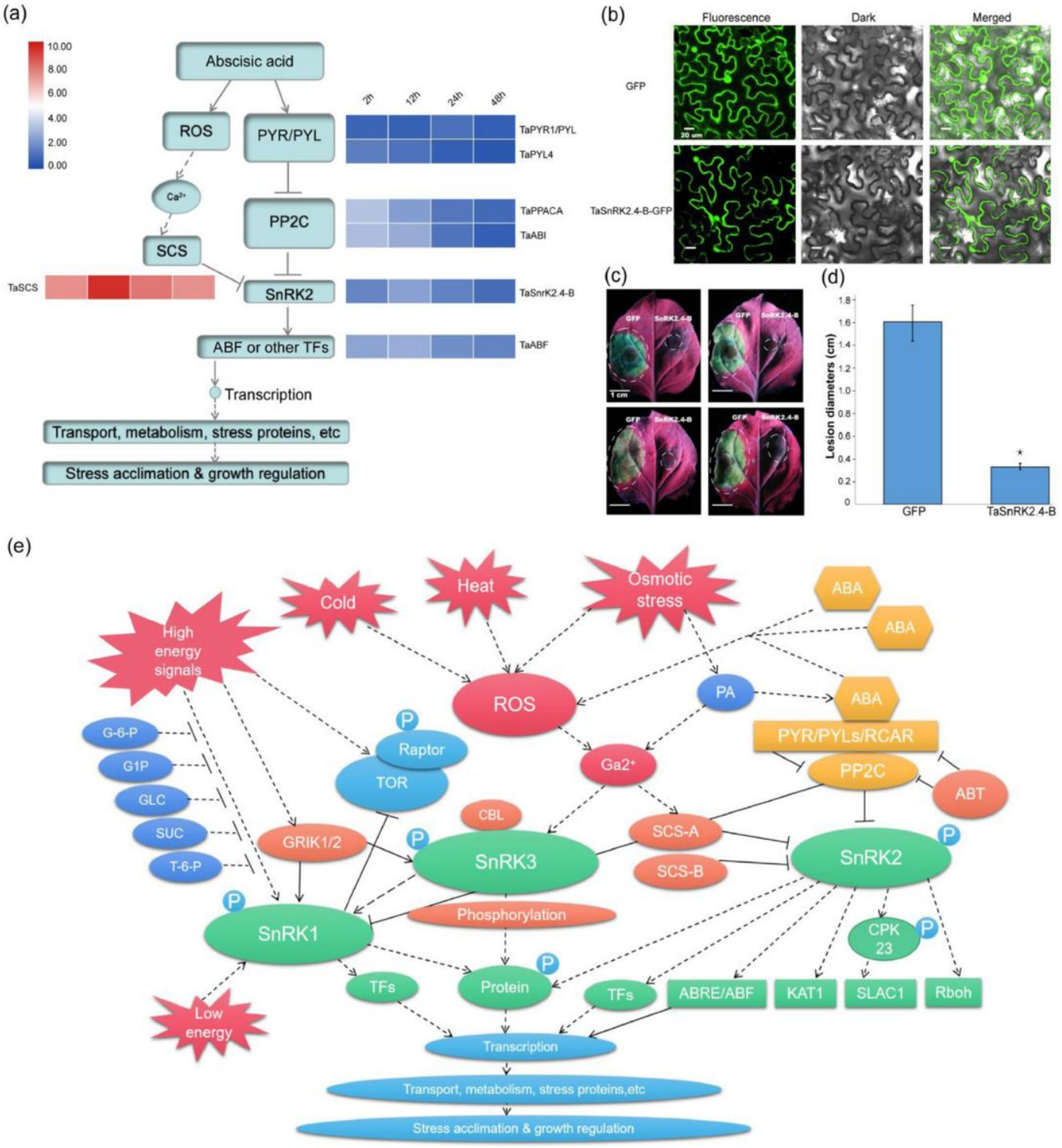

Figure 10

Functional verification of gene TaSnRK2.4-B. (a): Expression level detected by qRT-PCR of wheat genes involving ABA pathway. (b): TaSnRK2.4-B was constructed into plasmid with fusions of GFP. Panels from left to right refer to Fluorescence, Dark, and Merged images, respectively. Scale bars = 20 μm. (c): Photograph

under ultraviolet lights. The white circles showed the infected areas of P. infestans, and “GFP” referred to the free GFP. (d): Lesion diameter of control (GFP) and TaSnRK2.4-B. The “*” on the bar indicated significant differences determined using Duncan’s test ($P < 0.05$). (e): The Role model of SnRK2 in plant response to osmotic stress have previously been reported in plant species [1,4,6-7,10-11,24-25,42,46-47,54,60]. Connections represent positive (arrow) and negative (block) regulation. Black solid indicates direct regulation/interaction and dashed line indicates indirect regulation.

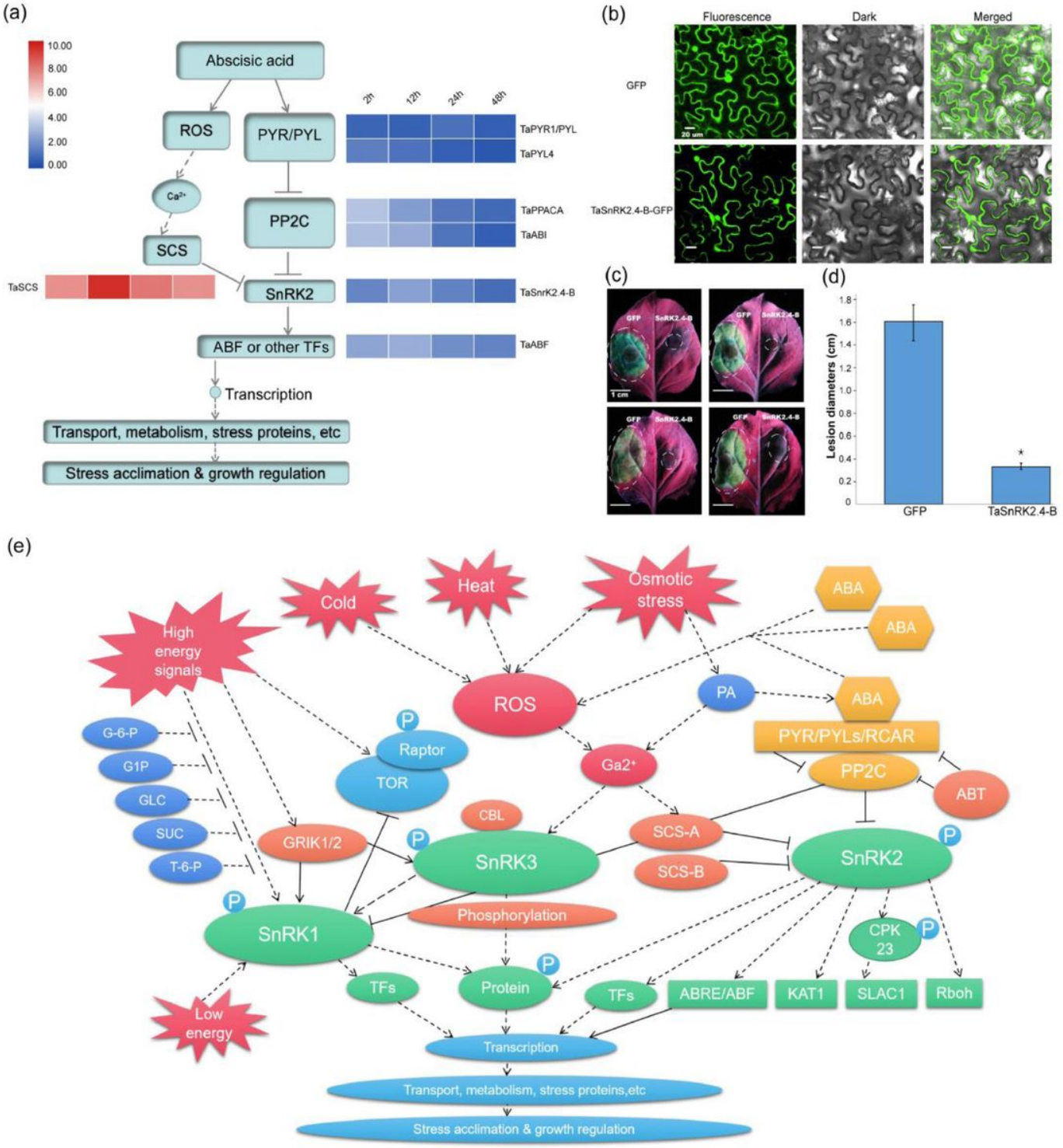

Figure 10

Functional verification of gene TaSnRK2.4-B. (a): Expression level detected by qRT-PCR of wheat genes involving ABA pathway. (b): TaSnRK2.4-B was constructed into plasmid with fusions of GFP. Panels from left to right refer to Fluorescence, Dark, and Merged images, respectively. Scale bars = 20 μm. (c): Photograph under ultraviolet lights. The white circles showed the infected areas of P. infestans, and “GFP” referred to the free GFP. (d): Lesion diameter of control (GFP) and TaSnRK2.4-B. The “*” on the bar indicated significant differences determined using Duncan’s test ($P < 0.05$). (e): The Role model of SnRK2 in plant response to osmotic stress have previously been reported in plant species [1,4,6-7,10-11,24-25,42,46-47,54,60]. Connections represent positive (arrow) and negative (block) regulation. Black solid indicates direct regulation/interaction and dashed line indicates indirect regulation.

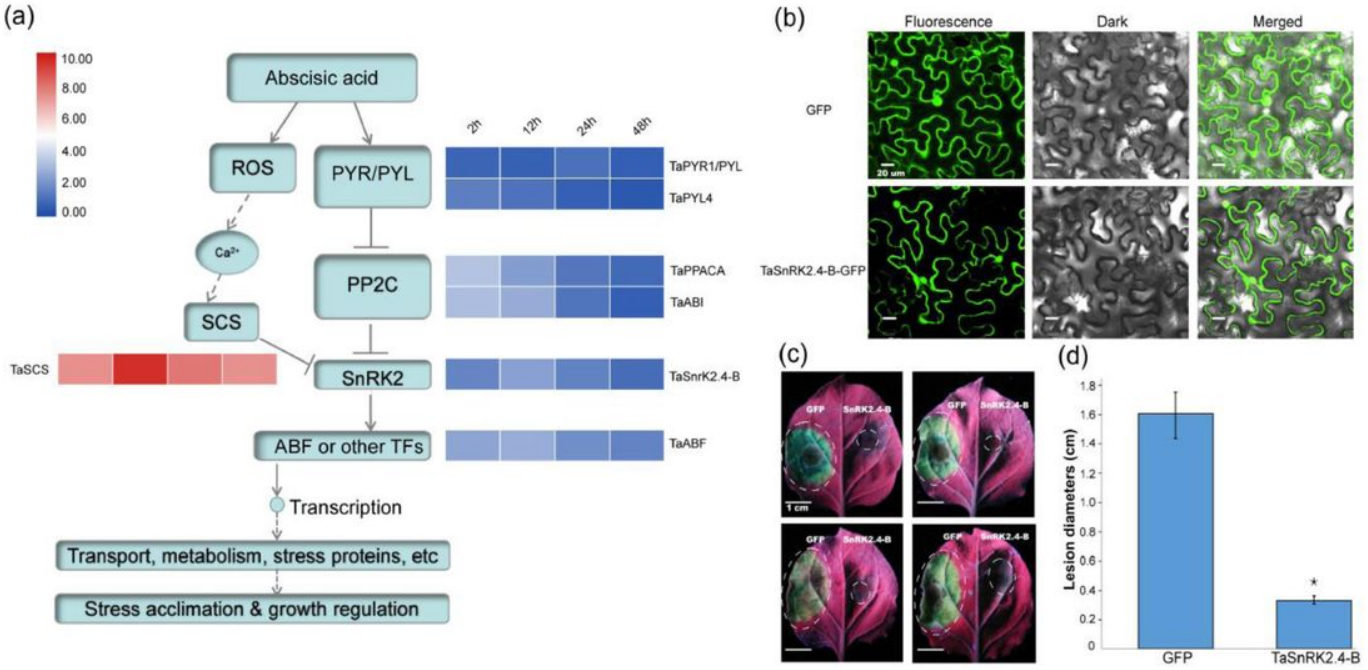

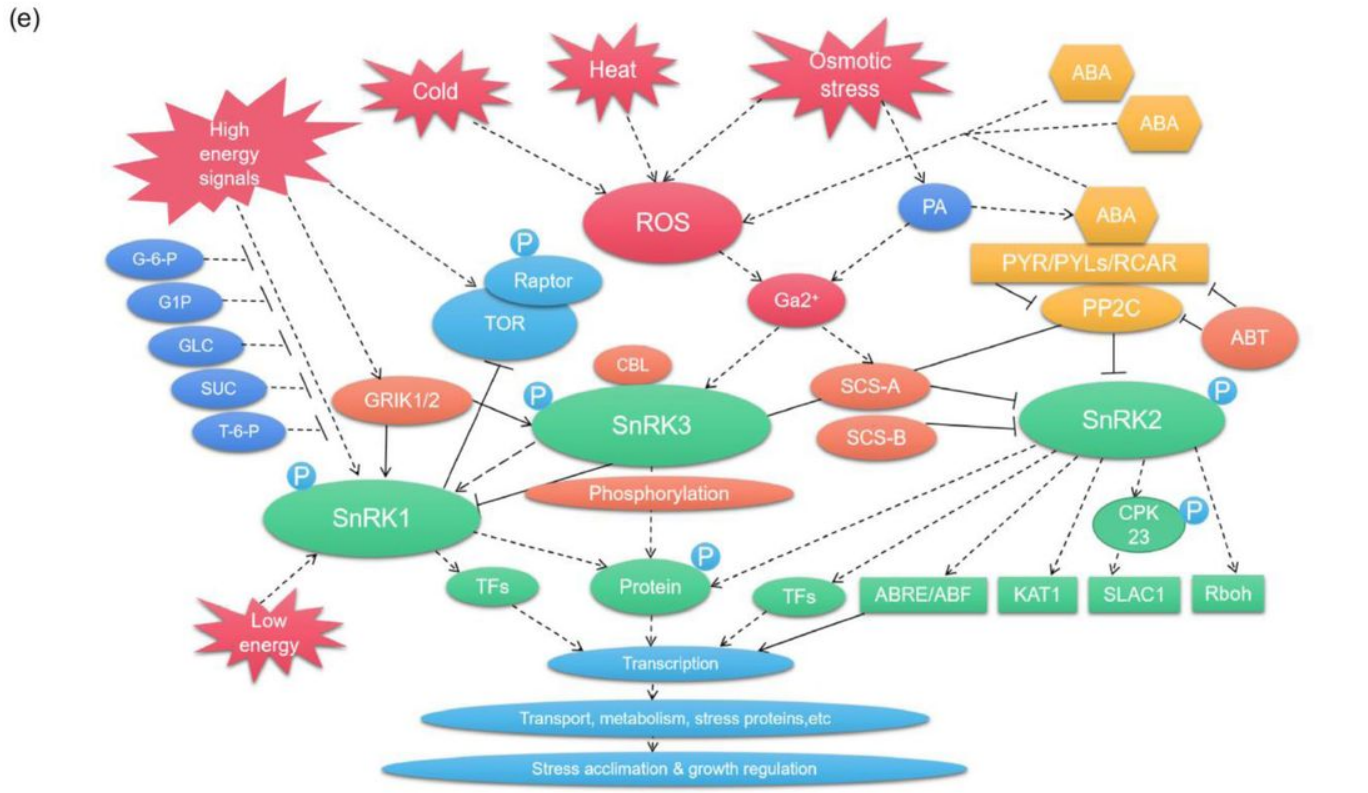

Figure 10

Functional verification of gene TaSnRK2.4-B. (a): Expression level detected by qRT-PCR of wheat genes involving ABA pathway. (b): TaSnRK2.4-B was constructed into plasmid with fusions of GFP. Panels from left to right refer to Fluorescence, Dark, and Merged images, respectively. Scale bars = 20 μm. (c): Photograph under ultraviolet lights. The white circles showed the infected areas of P. infestans, and “GFP” referred to the free GFP. (d): Lesion diameter of control (GFP) and TaSnRK2.4-B. The “*” on the bar indicated significant differences determined using Duncan’s test ($P < 0.05$). (e): The Role model of SnRK2 in plant response to osmotic stress have previously been reported in plant species [1,4,6-7,10-11,24-25,42,46-47,54,60]. Connections represent positive (arrow) and negative (block) regulation. Black solid indicates direct regulation/interaction and dashed line indicates indirect regulation.

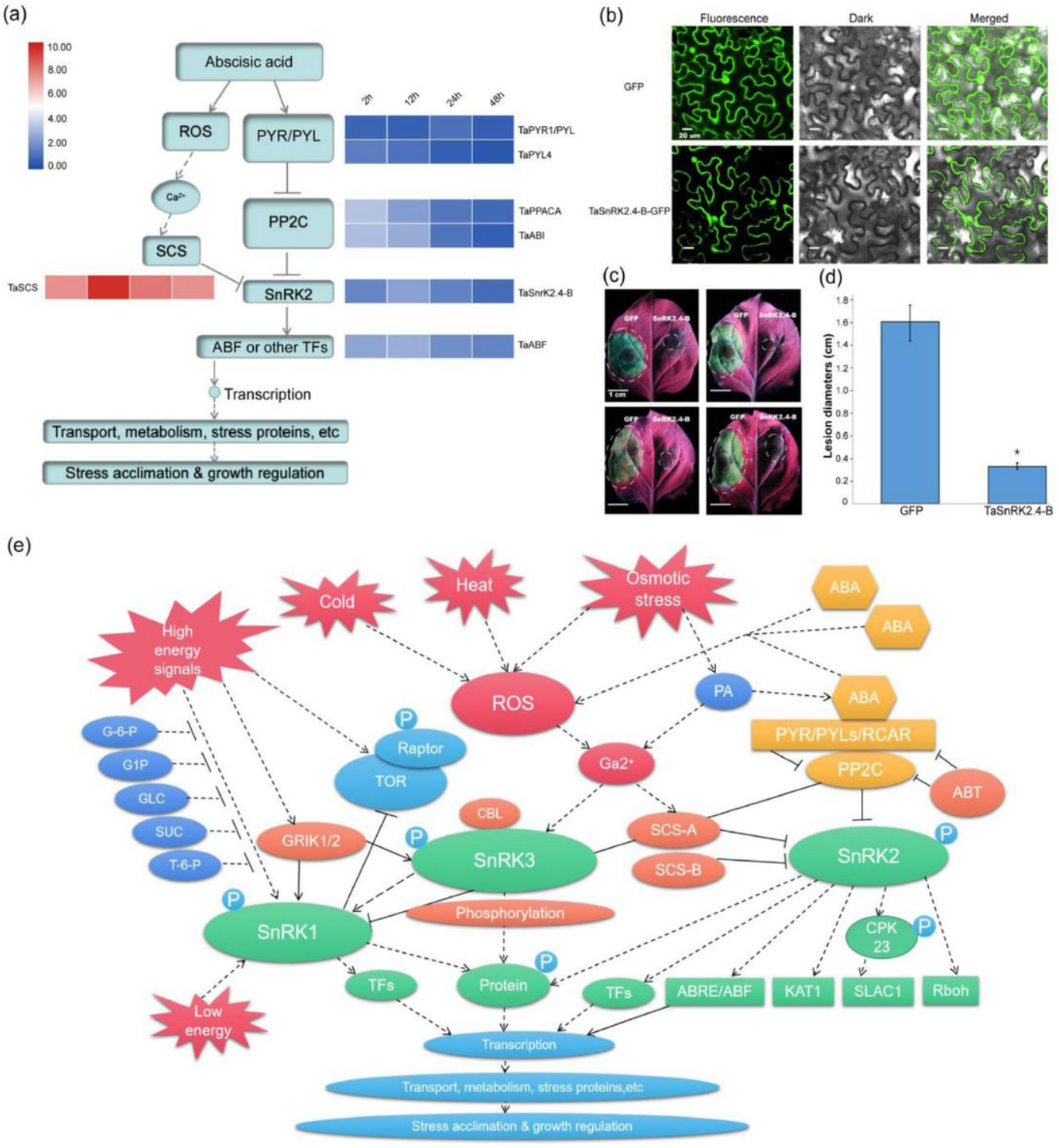

Figure 10

Functional verification of gene TaSnRK2.4-B. (a): Expression level detected by qRT-PCR of wheat genes involving ABA pathway. (b): TaSnRK2.4-B was constructed into plasmid with fusions of GFP. Panels from left to right refer to Fluorescence, Dark, and Merged images, respectively. Scale bars = 20 μm. (c): Photograph under ultraviolet lights. The white circles showed the infected areas of P. infestans, and “GFP” referred to the free GFP. (d): Lesion diameter of control (GFP) and TaSnRK2.4-B. The “*” on the bar indicated significant differences determined using Duncan’s test ($P < 0.05$). (e): The Role model of SnRK2 in plant response to

osmotic stress have previously been reported in plant species [1,4,6-7,10-11,24-25,42,46-47,54,60]. Connections represent positive (arrow) and negative (block) regulation. Black solid indicates direct regulation/interaction and dashed line indicates indirect regulation.

Supplementary Files

This is a list of supplementary files associated with this preprint. Click to download.

- FigureS1.tif
- FigureS1.tif
- FigureS1.tif
- FigureS1.tif
- FigureS1.tif
- FigureS2.tif
- FigureS2.tif
- FigureS2.tif
- FigureS2.tif
- FigureS2.tif
- FigureS2.tif
- FigureS3.tif
- FigureS3.tif
- FigureS3.tif
- FigureS3.tif
- FigureS3.tif
- FigureS3.tif
- FigureS4.tif
- FigureS4.tif
- FigureS4.tif
- FigureS4.tif
- FigureS4.tif
- FigureS5.tif
- FigureS5.tif
- FigureS5.tif
- FigureS5.tif
- FigureS5.tif
- FigureS6.tif
- FigureS6.tif
- FigureS6.tif
- FigureS6.tif

- FigureS6.tif
- FigureS7.tif
- FigureS7.tif
- FigureS7.tif
- FigureS7.tif
- FigureS7.tif
- FigureS8.tif
- FigureS8.tif
- FigureS8.tif
- FigureS8.tif
- FigureS8.tif
- TableS1.xls
- TableS1.xls
- TableS1.xls
- TableS1.xls
- TableS1.xls
- TableS10.xls
- TableS10.xls
- TableS10.xls
- TableS10.xls
- TableS10.xls
- TableS11.xls
- TableS11.xls
- TableS11.xls
- TableS11.xls
- TableS11.xls
- TableS12.xls
- TableS12.xls
- TableS12.xls
- TableS12.xls
- TableS12.xls
- TableS2.xls
- TableS2.xls
- TableS2.xls
- TableS2.xls

- TableS2.xls
- TableS3.xls
- TableS3.xls
- TableS3.xls
- TableS3.xls
- TableS3.xls
- TableS4.xls
- TableS4.xls
- TableS4.xls
- TableS4.xls
- TableS4.xls
- TableS5.xls
- TableS5.xls
- TableS5.xls
- TableS5.xls
- TableS5.xls
- TableS6.xls
- TableS6.xls
- TableS6.xls
- TableS6.xls
- TableS6.xls
- TableS7.xls
- TableS7.xls
- TableS7.xls
- TableS7.xls
- TableS7.xls
- TableS8.xls
- TableS8.xls
- TableS8.xls
- TableS8.xls
- TableS8.xls
- TableS9.xls
- TableS9.xls
- TableS9.xls
- TableS9.xls

- TableS9.xls